

10. LATE CRETACEOUS–QUATERNARY BIOMAGNETOSTRATIGRAPHY OF ODP SITES 1168, 1170, 1171, AND 1172, TASMANIAN GATEWAY¹

C.E. Stickley,² H. Brinkhuis,³ K.L. McGonigal,⁴
G.C.H. Chaproniere,⁵ M. Fuller,⁶ D.C. Kelly,⁷ D. Nürnberg,⁸
H.A. Pfuhl,⁹ S.A. Schellenberg,¹⁰ J. Schoenfeld,⁸ N. Suzuki,¹¹
Y. Touchard,¹² W. Wei,¹³ G.L. Williams,¹⁴ J. Lara,⁴ and S.A. Stant⁴

ABSTRACT

Late Cretaceous (Maastrichtian)–Quaternary summary biostratigraphies are presented for Ocean Drilling Program (ODP) Leg 189 Sites 1168 (West Tasmanian Margin), 1170 and 1171 (South Tasman Rise), and 1172 (East Tasman Plateau). The age models are calibrated to magnetostratigraphy and integrate both calcareous (planktonic foraminifers and nannofossils) and siliceous (diatoms and radiolarians) microfossil groups with organic walled microfossils (organic walled dinoflagellate cysts, or dinocysts). We also incorporate benthic oxygen isotope stratigraphies into the upper Quaternary parts of the age models for further control. The purpose of this paper is to provide a summary age-depth model for all deep-penetrating sites of Leg 189 incorporating updated shipboard biostratigraphic data with new information obtained during the 3 yr since the cruise. In this respect we provide a report of work to November 2003, not a final synthesis of the biomagnetostratigraphy of Leg 189, yet we present the most complete integrated age model for these sites at this time.

Detailed information of the stratigraphy of individual fossil groups, paleomagnetism, and isotope data are presented elsewhere. Ongoing efforts aim toward further integration of age information for Leg 189 sites

¹Stickley, C.E., Brinkhuis, H., McGonigal, K.L., Chaproniere, G.C.H., Fuller, M., Kelly, D.C., Nürnberg, D., Pfuhl, H.A., Schellenberg, S.A., Schoenfeld, J., Suzuki, N., Touchard, Y., Wei, W., Williams, G.L., Lara, J., and Stant, S.A., 2004. Late Cretaceous–Quaternary biomagnetostratigraphy of ODP Sites 1168, 1170, 1171, and 1172, Tasmanian Gateway. In Exxon, N.F., Kennett, J.P., and Malone, M.J. (Eds.), *Proc.*

ODP, Sci. Results, 189, 1–57 [Online]. Available from World Wide Web: <http://www-odp.tamu.edu/publications/189_SR/VOLUME/CHAPTERS/111.PDF>. [Cited YYYY-MM-DD]

²Lamont-Doherty Earth Observatory, Palisades NY 10964, USA. Current address: School of Earth, Ocean and Planetary Sciences, PO Box 914, Cardiff University, Cardiff, CF10 3YE, United Kingdom.

cathy@earth.cf.ac.uk

³Botanical Palaeoecology, Laboratory of Palaeobotany and Palynology, Utrecht University, CD-3584 Utrecht, The Netherlands.

⁴Department of Geological Sciences, Florida State University, Tallahassee FL 32306, USA.

⁵Department of Geology, The Australian National University, Canberra ACT 0200, Australia.

⁶Hawaii Institute of Geophysics and Planetology, University of Hawaii at Manoa, Honolulu HI 96822, USA.

⁷Department of Geology and Geophysics, University of Wisconsin–Madison, Madison WI 53706, USA.

⁸GEOMAR Research Center for Marine Geosciences, D-24148 Kiel, Germany.

⁹Max Planck Institute for Biogeochemistry, 07745 Jena, Germany.

¹⁰Department of Geological Sciences, San Diego State University, San Diego CA 92182, USA.

¹¹Institute of Geology and Paleontology, Tohoku University, Sendai 980-8578, Japan.

¹²CEREGE, Europôle Méditerranéen de l’Arbois BP80, F-13545 Aix en Provence Cedex 4, France.

¹³Scripps Institution of Oceanography, University of California, San Diego, La Jolla CA 92093, USA.

¹⁴Geological Survey of Canada (Atlantic), Bedford Institute of Oceanography, Dartmouth NS B2Y 4A2, Canada.

and will include an attempt to correlate zonation schemes for all the major microfossil groups and detailed correlation between all sites.

INTRODUCTION

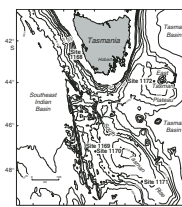
Five sites (Sites 1168–1172) were drilled in water depths of 2463–3568 m during Ocean Drilling Program (ODP) Leg 189 in the Tasmanian Gateway in March–May 2000 (Fig. F1). In all, 4539 m of Late Cretaceous to Quaternary marine sediments were recovered, with an overall recovery of 89%. The sediments of Leg 189 essentially record the Antarctic Cenozoic evolution from “Greenhouse” to “Icehouse” (see Exxon, Kennett, Malone, et al., 2001). Postcruise work is presented in this volume and notably in Exxon et al. (in press). The biomagnetostratigraphic age models for the four deep sites (Sites 1168, 1170, 1171, and 1172) are presented in this paper. Difficulties in drilling at Site 1169 resulted in a high amount of core disturbance, causing unreliable age assignment. Drilling was aborted beyond one advanced piston corer/extended core barrel (APC/XCB) hole, and no further postcruise attempt has been made to refine the shipboard age model (Shipboard Scientific Party, 2001c) for this site.

The relatively shallow region off Tasmania is one of the few places where well-preserved and almost complete marine Cenozoic carbonate-rich sequences can be drilled in present-day latitudes of 40°–50°S and paleolatitudes of up to 70°S. The broad geological history of all the sites is comparable, although important differences exist east to west and north to south (e.g., Exxon, Kennett, Malone, et al., 2001; Brinkhuis, Munstermann, et al., this volume; Brinkhuis, Sengers, et al., this volume; Huber et al., submitted [N1]; McGonigal, in press; Pfuhl et al., in press; Pfuhl and McCave, this volume; Stant et al., this volume; Stickley et al., submitted [N2]). The wide range of lithologies recovered during Leg 189 (Exxon, Kennett, Malone, et al., 2001) are almost completely fossiliferous throughout the Cretaceous to Quaternary; they contain a wealth and diversity of microfossils (e.g., diatoms, nannofossils, ostracodes, planktonic and benthic foraminifers, radiolarians, and silicoflagellates) and palynomorphs (dinocysts, acritarchs, spores, and pollen) in varying abundances and associations, providing ample opportunity to develop correlations between groups. The main groups are used here to derive age models for the four deep-penetrating sites. These are the most complete integrated biomagnetostratigraphic data for Leg 189 to March 2003. This is not intended as a final synthesis, however, and ongoing work on individual fossil groups is still refining some intervals.

Microfossil Groups at Leg 189 Sites and Their Application to the Age Models

Five microfossil groups of age significance are present in Leg 189 sediments in varying abundances. These comprise a calcareous grouping (nannofossils and planktonic foraminifers), a siliceous grouping (diatoms and radiolarians), and palynomorphs (notably organic walled dinoflagellate cysts or dinocysts, spores, and pollen). Other groups (e.g., benthic foraminifers, ostracodes, silicoflagellates, and ebridians) are present in varying abundance through selected stratigraphic intervals (see Exxon, Kennett, Malone, et al., 2001) but are not used here for age assignment.

F1. Leg 189 drill sites, p. 26.



The stratigraphic distribution of the main microfossil groups through the drilled sequences changes markedly with depositional environment/lithology. The calcareous groups are most abundant in the pelagic calcareous oozes of the Oligocene–Quaternary (**Stant et al.**, this volume; **McGonigal and Wei**, this volume; McGonigal, in press; **Wei et al.**, this volume), whereas palynomorphs are the dominant group in the shallow-water siliciclastic sediments of the Maastrichtian and Paleogene (**Brinkhuis, Munstermann, et al.**, this volume; **Brinkhuis, Sengers, et al.**, this volume). However, palynomorphs and calcareous groups are largely abundant throughout the drilled sequences at Site 1168. In addition, well-preserved dinocysts are present in the Quaternary intervals of Sites 1168–1172, making these occurrences the southernmost Quaternary dinocysts records to date. Diatoms are commonly abundant in sediments of late Eocene age and younger at all sites (except Site 1168), with pyritized specimens frequently occurring in the Maastrichtian–middle Eocene intervals. Radiolarians are abundant at Site 1171 from the upper Eocene and at Site 1170 from the Oligocene. At Site 1172 they are common only in the Eocene and Miocene intervals. At Site 1168 diatoms and radiolarians are preserved only in two short intervals in the mid-Oligocene and upper Miocene, and therefore are not useful for age assignment at this site. Benthic foraminifers are present throughout the drilled intervals of all sites except for the upper Eocene glauconitic sands. They give an indication of paleobathymetric history through the sequences (see Exon, Kennett, Malone, et al., 2001).

Extensive postcruise high-resolution calcareous nannofossil stratigraphic work has been undertaken through the Neogene and relevant Paleogene sections, instigating refinement of the initial age models presented in Exon, Kennett, Malone, et al. (2001). The present paper summarizes the latest nannofossil stratigraphies in our integrated age models, and the reader is referred to **Stant et al.** (this volume), **McGonigal and Wei** (this volume), McGonigal (in press), and **Wei et al.** (this volume) for further details. The zonal schemes of Martini (1971), Gartner (1977), and Okada and Bukry (1980) were employed with some modifications. Previous southwest Pacific studies have shown these standard zonations are not always applicable in higher latitudes because of the absence or rarity of index species (Edwards and Perch-Nielsen, 1975). Biomagnetostratigraphic correlations at several Southern Hemisphere high-latitude sites have shown considerably different ages (Wei and Wise, 1992) relative to those compiled from the mid-latitudes by Berggren et al. (1995a, 1995b). Correlation with magnetostratigraphy was essential for constraint of the nannofossil bioevents. The resulting nannofossil biostratigraphy has produced some very useful subantarctic temperate biostratigraphic records. In particular, the Oligocene to Pliocene interval is among the most detailed of Southern Ocean sites at similar latitudes. This sequence will serve as an important reference section for the Southern Hemisphere.

The planktonic foraminiferal cool subtropical (temperate) biostratigraphic scheme of Jenkins (1985, 1993a, 1993b) and the Antarctic schemes of Stott and Kennett (1990) and Berggren et al. (1995a, 1995b) formed the basis for the zonal scheme used during Leg 189 (see Exon, Kennett, Malone, et al., 2001). Because of the southern location of Australia during the Paleogene, the subantarctic zonal scheme (Stott and Kennett, 1990; Berggren et al., 1995a, 1995b) was used in place of the traditional temperate scheme (Jenkins, 1985, 1993a, 1993b). This temperate scheme was appropriate for the upper Paleogene and Neogene. The low-diversity planktonic foraminiferal assemblages of the Eocene

are generally very well preserved, but their abundances are low. The shipboard foraminiferal biostratigraphy is integrated into the age model here. Further work on refining this is ongoing and so far has concentrated on Site 1168 only.

Oligocene to Quaternary holoplanktonic diatoms are abundant at all sites drilled during Leg 189 (except Site 1168) and form an important constituent of the age models for this interval, particularly at Sites 1170 and 1171. Application of existing circum-Antarctic biostratigraphic schemes (Gersonde and Burckle, 1990; Baldauf and Barron, 1991; Harwood and Maruyama, 1992; Gersonde and Bárcena, 1998; Gersonde et al., 1998; Zielinski and Gersonde, 2002; Florindo et al., 2003; Roberts et al., in press) has proved useful for these southern sites. The modifications adopted during ODP Leg 177 (Shipboard Scientific Party, 1999a) and Leg 181 (Shipboard Scientific Party, 1999b) are retained here. For instance the *Thalassiosira insigna*-*Thalassiosira vulnifica* Zone of Harwood and Maruyama (1992) is replaced by the *T. insigna* Zone (Shipboard Scientific Party, 1999b). This change was made because of the probable diachroneity of the first occurrence (FO) of *T. vulnifica*. In addition, the basal age of the *Fragilariopsis reinholdii* Zone, defined by the FO of the nominate taxon, is placed at ~8.1 Ma within Chron C4. This datum is close to that of the equatorial Pacific zonation (Barron, 1992). In addition to southern high-latitude diatoms, warm and temperate species were also encountered during Leg 189. Therefore, additional stratigraphic ranges have been added following the compilation of Barron (1992). The resulting diatom stratigraphy is in generally good agreement with that for the nanofossils for the majority of intervals. Further integration of siliceous and calcareous groups for the subantarctic Oligocene–Quaternary looks encouraging from these initial findings. In addition, higher-resolution diatom biostratigraphy is being undertaken on Leg 189 sediments. Abundant neritic and offshore diatoms of the upper Eocene and lower Oligocene are, in conjunction with dinocysts, proving useful for reconstructing the timing and paleoenvironment of the Eocene–Oligocene (E–O) transition at Sites 1170–1172 (e.g., Stickley et al., submitted [N2]).

Radiolarians are well represented at all Leg 189 sites (except Site 1168) with varying diversity through the sequences. The subantarctic radiolarian biostratigraphic sequence from the middle Eocene through Pleistocene is unique because no useful radiolarian zones for temperate regions of the Southern Hemisphere have been published. These data will provide an important new radiolarian zonation and the potential for correlation between tropical and Antarctic biostratigraphies despite a near absence of tropical and cold-water age-diagnostic species in the Tasmanian region. The radiolarian age assignments used in this age model are (tentatively) based on existing Antarctic and subtropical zonal schemes (e.g., Abelmann, 1990, 1992; Caulet, 1991; Chen, 1975; Hollis, 1993; Lazarus, 1992; Nishimura, 1987; Takemura, 1992; Takemura and Ling, 1997) and modifications of tropical zones (Sanfilippo and Nigrini, 1998). The shipboard radiolarian biostratigraphy, with some deletions, is integrated into the age model here. Further work on refining the radiolarian biostratigraphy is ongoing, and so far has concentrated on the Eocene of Site 1172.

Palynomorphs are extremely abundant in the Paleogene and Cretaceous intervals of Leg 189 sediments and are providing the first well-calibrated Paleogene dinocyst record of the Southern Hemisphere (see Brinkhuis, Munstermann, et al., this volume; Brinkhuis, Sengers, et al., this volume; Sluijs et al., this volume; Williams et al., this vol-

ume). A significant number of studies concentrating on Upper Cretaceous to middle Eocene dinocysts from the broad Antarctic realm or Southern Ocean are available, notably from southeast Australia, New Zealand, the Ross Shelf, and Seymour Island as well as several Deep Sea Drilling Project/ODP sites (see overviews in, e.g., Askin, 1988a, 1988b; Wilson, 1988; Wrenn and Hart, 1988; Mao and Mohr, 1995; Truswell, 1997; Hannah et al., 1997; Levy and Harwood, 2000). These studies have documented Southern Ocean Paleogene dinocyst distribution and taxonomy in great detail. However, previous studies concentrating on the E-O transition in the region are but few (e.g., Edbrooke et al., 1998). Moreover, meaningful chronostratigraphic calibration of Paleogene dinocyst events is, typically, largely absent.

Combined dinocyst and diatom stratigraphies in some of the critical boundary intervals has allowed an integrated age model and environmental analysis of the Eocene/Oligocene (E/O) boundary (Sluijs et al., this volume; Stickley et al., submitted [N2]) and the Cretaceous/Tertiary (K/T) boundary (Schellenberg et al., in press) transitions, for example, as well as reconstruction of environmental periodicities and circulation patterns in the Eocene (Huber et al., submitted [N1]; Röhl et al., in press b). In addition, drilling has yielded excellent material to study the variability of dinocyst morphology, notably within the *Vozzhennikovia*, *Deflandrea*, and *Enneadocysta* groups. Postcruise work has focused on dinocyst successions from Sites 1168 (Eocene–Quaternary) and 1172 (Maastrichtian–Oligocene and Quaternary) (Brinkhuis, Munstermann, et al., this volume; Brinkhuis, Sengers, et al., this volume). Age assignment of events for Sites 1168, 1170, and 1171 is derived by correlation to the dinocyst stratigraphy of Site 1172, which is closely calibrated to the magnetostratigraphy of that site. The dinocyst stratigraphy of the Eocene and lowermost Oligocene intervals of Sites 1170 and 1171 are virtually unchanged from the shipboard data, but are summarized here. For further details on the dinocyst scheme for all four deep-penetrating sites as well as site-to-site correlations incorporating early Oligocene diatom events see Sluijs et al. (this volume).

Magnetostratigraphy

Shipboard paleomagnetic and rock magnetic investigations included routine measurements of natural remanent magnetization (NRM). Both were measured before and after alternating-field demagnetization to 20 mT. Low-field magnetic susceptibility measurements were made with the multisensor track. NRMs and a limited set of rock magnetic observations were made on discrete samples. A nonmagnetic APC core barrel assembly was used for alternate cores in selected holes and the magnetic overprints in core recovered with this assembly were compared with those obtained with standard assemblies. Where magnetic cleaning successfully isolated the characteristic remnant magnetization, paleomagnetic inclinations were used to define magnetic polarity zones. On some occasions, it was possible to recover a satisfactory magnetic stratigraphy even when the inclination was of a single polarity because of a persistent overprint. On such occasions, there were indications of the magnetic stratigraphy in the intensity and associated minor differences in the inclination. To recover the magnetostratigraphy, the z-component alone was used. The z-component was biased in one direction but showed a clear alternating signal superposed upon this. By removing the bias, the magnetization with alternating sign, which carries the magnetostratigraphic signal, is made clearer. Postcruise inter-

pretations of the magnetic polarity stratigraphy, with constraints from the biostratigraphic data, are presented here. The revised timescale of Cande and Kent (1995), as presented in Berggren et al. (1995a, 1995b), was used as a reference for the ages of Cenozoic polarity chronos.

Despite the high carbonate content of sediments recovered through much of the drilled sequences, especially at Sites 1170 and 1171, the generation of a sufficient magnetostratigraphy for useful age-depth reconstruction was possible. Magnetostratigraphic interpretation of the paleomagnetic record at all sites has been possible through most of the sections. Although the quality of the magnetic record deteriorated in older intervals, a relatively complete magnetostratigraphy was achieved, particularly across the E/O boundary. At Site 1168, however, the magnetostratigraphic record has been difficult to establish because of a weak magnetic signal. We present data from only the more strongly magnetized sections of this site. In addition, at Site 1171, the interpretation of the Eocene inclination record was problematic, which led to the development of an approach based upon the sign of the z-component. This approach generated distinctive magnetostratigraphic boundaries, whereas they were almost totally obscured in the inclination record. Further details on the magnetostratigraphy of Site 1168 and Site 1172 are presented in Fuller and Touchard (in press).

High-Resolution Quaternary Isotope and Reflectance (L^*) Stratigraphy

The chronology from the benthic oxygen isotope records of Holes 1168A, 1170A, and 1172A, as reported in Nürnberg et al. (in press), are integrated into the biomagnetostratigraphic age models for comparison and further age control for the Quaternary intervals (Tables T1, T2, T4; Figs. F2–F13). In Holes 1168A and 1170A stable oxygen isotope measurements were made on 1–7 tests of foraminifers: *Cibicidoides wuellerstorfi*, *Cibicidoides mundulus*, *Uvigerina pygmea* (Hole 1170A only), and *Uvigerina peregrina* (Hole 1168A only). The >250- μm size fraction was used to eliminate biases caused by any downslope-displaced smaller tests. For Hole 1172A, oxygen isotope analyses were conducted on 1–3 tests of single benthic foraminiferal species of the genus *Cibicidoides*. All tests were ultrasonically cleaned in distilled water prior to analysis. The chronostratigraphy is determined by graphic correlation of the benthic oxygen isotope curves with the stacked standard records. The marine oxygen isotope stages (MIS) were recognized using the nomenclature proposed by Prell et al. (1986) and Tiedemann et al. (1994). The record of Martinson et al. (1987) was used as reference curve for the youngest isotope excursions back to Event 8.5. The SPECMAP stack (Imbrie et al., 1984) was used from Event 8.5 to 13.2, and the orbitally tuned benthic isotope record of ODP Site 677 was used as a reference curve for older isotope events (Shackleton et al., 1990). The base of the Holocene plateau (9.7 ka) was recognized in Holes 1168A, 1170A, and 1172A. Initial correlations in Hole 1170A were made with the magnetostratigraphic data. In Hole 1168A the FO of *Emiliana huxleyi* and the last occurrence (LO) of *Calcidiscus macintyrei* datums were used for initial correlation. Following these initial correlations datums were tied to the standard records. Correlations were performed with the AnalySeries software (version 1.1) (Paillard et al., 1996). For Hole 1172A, prominent maxima and minima in the oxygen isotope record were correlated to the reference oxygen isotope record of Shackleton et al. (1990) (ODP Site 677 timescale calibration). The age model was verified by comparing it to

the oxygen isotope records of Holes 1168A and 1170A. See Nürnberg et al. (in press) for further details of Leg 189 Quaternary benthic oxygen isotope analyses and results.

The reflectance (lightness [L^*]) record, measuring color variations, for Hole 1171A (see Shipboard Scientific Party, 2001e) is used for the high-resolution Quaternary chronology presented in Table T3 and Figures F8 and F10, because an oxygen isotope record is not yet available. A chronology is determined from an inter-Site correlation of the Hole 1171A L^* record with those from Holes 1170A and 1172A. This detailed correlation allows the transfer of age control points and, thus, the establishment of a stratigraphic framework for Hole 1171A. See Nürnberg et al. (in press) for further information on the use and reasoning behind reflectance data for stratigraphic purposes and, specifically, for the Hole 1171A Quaternary reflectance stratigraphy record and establishment of a chronology.

MATERIALS AND METHODS

Detailed lithologic descriptions of the materials used are presented in Shipboard Scientific Party (2001b, 2001d, 2001e, 2001f). For processing and counting techniques of individual fossil groups see the overview in Shipboard Scientific Party (2001a). The stratigraphic positions of planktonic foraminiferal, radiolarian, and dinocyst bioevents in these age models are based on analyses of all core catcher samples (resolution ~9 m) or selected core catcher samples for palynology, whereas calcareous nannofossil stratigraphy is derived from analyses of two samples per section (resolution ~75 cm) for the Quaternary, and at least one sample per section (resolution ~1.5 m) for the Miocene. Diatom stratigraphy is based on analyses of all core catcher samples for the Neogene and Quaternary sections and of two to three samples per section (resolution ~50–75 cm) for the Paleogene intervals.

All depths are presented in meters below seafloor (mbsf) and are taken from the JANUS database (www-odp.tamu.edu/database). Correlation of datums observed in overlapping holes allowed refinement of the depth error (in meters) for those datums. Offsets in mbsf between overlapping holes for a particular site are not considered significant at this resolution, except for that between Holes 1171C and 1171D, where the offset is >3 m. Therefore, except for Site 1171, where depths for Hole 1171D are adjusted to correlate with overlapping parts of Hole 1171C, all age-depth data are presented “by hole” for a particular site. Refer to Shipboard Scientific Party (2001b, 2001d, 2001e, 2001f) for information on hole depth offsets and meters composite depth (mcd). Median depths (in mbsf) within the depth error of an event datum are used for simplicity, except where an obvious succession of events calls for otherwise. We acknowledge that by this methodology the FO events may be forced too shallow and the LO events too deep; therefore, depth errors for biostratigraphic datums are noted in Tables T1–T4. In some cases, due to the relatively low resolution of most of the biotic data, it is difficult to distinguish hiatus(es) from condensed sections. Further work is helping to refine these ambiguous intervals.

Amount of core disturbance including flow-in is noted and taken into account in these age models (Figs. F2–F13). In intervals where core disturbance is greatest (e.g., Cores 189-1170A-7H to 14H) and the resulting biostratigraphy is too chaotic to declare an unequivocal solution, we present the *most likely* scenario by (1) using the most robust

and consistent datums (across Leg 189 sites and the Southern Ocean in general) and (2) loosely comparing the resulting sedimentation rate with those from nearby sites in the Southern Ocean that have established age models (e.g., isotopic or biostratigraphic). In such uncertain intervals we also present an alternative age model. Although isotopic work (for example) may help refine some uncertainties, the time frame of highly disturbed intervals may prove difficult to improve any further than is presented here. The geochronological timescale and epochal boundary definitions described in Berggren et al. (1995a, 1995b) are used throughout this report.

AGE MODEL AND SEDIMENTATION RATES

Site 1168

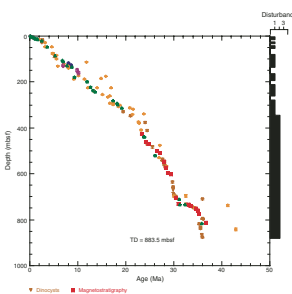
Site 1168 is located in middle bathyal water depths (2463 m) on the western Tasmanian margin 70 km from the coast (Fig. F1) and north of the present-day Subtropical Front. Three holes were drilled to a total depth of 883.5 mbsf: Hole 1168A (APC/XCB), Hole 1168B (APC), and Hole 1168C (APC/XCB). Biotic and magnetostratigraphic datums from Hole 1168A only indicate a (upper middle?) upper Eocene to upper Quaternary sequence (Table T1; Figs. F2, F3, F4). The sequence is divided into five lithostratigraphic units (Shipboard Scientific Party, 2001b). Unit V, 121.5 m of organic-rich siltstones and claystones, is overlain by 13.4 m (Unit IV) of uppermost Eocene–lowermost Oligocene glauconitic siltstones and organic-rich claystones with varying carbonate content. Above this is Unit III, 88.6 m of siliciclastic sediments of early Oligocene age. Above Unit III lies 400 m of lower Oligocene–middle Miocene nannofossil chalks and claystones of varying silt content (Unit II). The stratigraphically highest unit (Unit I) comprises 260 m of foraminiferal and nannofossil oozes and chalks of middle Miocene to late Quaternary age. See Shipboard Scientific Party (2001b) for detailed lithologic descriptions. Microfossil and magnetostratigraphic data of age significance for Site 1168 are listed in Table T1 and depicted in Figures F2, F3, and F4.

Paleogene (Late Eocene to Oligocene)

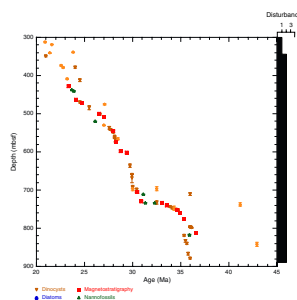
The age model for the Paleogene intervals of Site 1168 is based on several dinocyst, foraminiferal, and nannofossil events from Hole 1168A correlated only to the magnetostratigraphy (Table T1). The base of Hole 1168A (base Core 189-1168A-95X; 883.5 mbsf) is not dated but a level close to the bottom of the hole (base Core 189-1168A-94X; 880.3 mbsf) is assigned an age of middle to late Eocene (~35–36 Ma) based on the occurrence of several dinocyst marker events (see also Brinkhuis, Munstermann et al., this volume), the LO of the nannofossil *Reticulofenestra reticulata* (35.9 Ma), and magnetostratigraphic evidence (Table T1). However, the FO of the planktonic foraminifer *Globigeropsis index* indicates an age at least as old as middle Eocene near the bottom of Hole 1168A (42.9 Ma; ~843 mbsf). Further work will help resolve this dispute, but we currently favor the dinocyst-nannofossil evidence on the majority of data points allowing good age control for these intervals and problems with foraminiferal data higher in the hole. Additionally, the middle/upper Eocene (Bartonian/Priabonian) boundary is difficult to place following such foraminiferal evidence. The preservation of

T1. Age-depth data, Site 1168, p. 39.

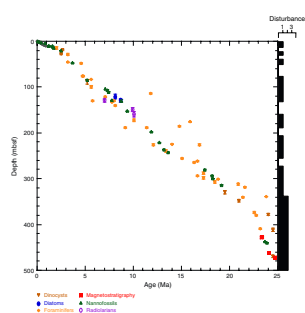
F2. Age-depth plot, Site 1168, p. 27.



F3. Age-depth plot, Site 1168, Paleogene, p. 28.



F4. Age-depth plot, Site 1168, Neogene and Quaternary, p. 29.



>130 m of sediments of exclusively late Eocene age, therefore, indicates rapid deposition at this time. Some of the absolute ages of the dinocyst datums in the bottom of the hole may need slight revision; we indicate all the data in the primary age model, however, to highlight the stratigraphic position of these datums.

The stratigraphic position of the E/O (Priabonian/Rupelian) boundary (sensu GSSP; 33.7 Ma) is difficult to place due to lack of calcareous markers. However, we approximate its position at just below ~740 mbsf by the onset of Chron C13n (33.535 Ma) (Table T1). The Oligocene interval at Site 1168 is greatly expanded compared to the other Leg 189 sites. Here, a relatively complete ~320-m-thick sequence is well dated by dinocyst, nannofossil, planktonic foraminiferal, and magnetostratigraphic datums. The planktonic foraminiferal datums FO of *Chiloguembelina cubensis* (41.2 Ma; 738 mbsf), FO of *Guembelitria triseriata* (32.5 Ma; ~697 mbsf), and LO of *Globigerina labiacrassata* (27.1 Ma; ~475 mbsf) occur too high in the sequence (or are assigned too old an age) for reasonable resolution with the rest of the data set, however. Revision of the ranges of these species at this site is necessary. A short (~1 m.y.) mid-early Oligocene hiatus is suggested at ~733 mbsf by the dinocyst datum LO of *Enneadocysta partridgei* (32.5 Ma) and the nannofossil datums LO of *Isthmolithus recurvus* (32.3 Ma) and LO of *Reticulofenestra umbilicus* (31.3 Ma). Early Oligocene hiatuses are also recognized at the other Leg 189 sites (see below, and Stickley et al., submitted [N2]), but those at Site 1172 (for example) are much longer in duration (and more frequent) than that at Site 1168. The lower/upper Oligocene (Rupelian/Chattian) boundary (28.5 Ma) is approximated by the onset of Subchron C10n.2n (28.7 Ma) at ~592 mbsf, indicating ~150 m of sediment of late Oligocene age above this level. The resulting age model gives an average sedimentation rate of ~6 cm/k.y. for the late Eocene, falling to ~3 cm/k.y. in the early and late Oligocene.

Neogene (Miocene to Pliocene) and Quaternary

Age determination for the Neogene intervals of Site 1168 is primarily based on integrated nannofossil and planktonic foraminiferal events with a few diatom and radiolarian datums (Table T1). Marine isotope stages are recognized in the benthic oxygen isotope signal back to MIS 24 (920 ka), which we incorporate into the Quaternary biostratigraphy. Unfortunately, the paleomagnetic signal is too weak to determine a robust magnetostratigraphy in the Neogene and Quaternary intervals (although we present these data in Table T1 as an alternative). For further discussion of the paleomagnetic record of Site 1168 see Touchard and Fuller (in press).

The Oligocene/Miocene (O/M; Chattian/Aquitanian) boundary (23.8 Ma) is approximated at 440 mbsf by the LO of nannofossil *Reticulofenestra bisecta bisecta* (23.9 Ma) and magnetostratigraphy (Table T1). We retain the Berggren et al. (1995a, 1995b) absolute age for the boundary (23.8 Ma) for reasons discussed above. The O/M boundary itself appears to be relatively expanded compared to other sites of Leg 189, regardless of which age is used.

The chronology of the ~355 m of sediment above the O/M boundary in Hole 1168A is somewhat problematic. There is no dispute that this interval (~84–440 mbsf) is entirely Miocene in age, yet biodatums disagree on the subdivision of its chronology (Table T1); further work should help resolve these disagreements, but currently we favor the nannofossil data because of their smaller depth error. The FO of the

planktonic foraminifer *Praeorbulina curva* (16.3 Ma) approximates the lower/middle Miocene (Burdigalian/Langhian) boundary (16.4 Ma) at ~265 mbsf. The biodatums agree relatively well for the middle Miocene interval (~198–265 mbsf), except three planktonic foraminiferal events that are either stratigraphically too shallow in the sequence (longer range?) or assigned too old an age for this site. The middle/upper Miocene (Serravallian/Tortonian) boundary (11.2 Ma) is approximated at ~198 mbsf by the LO of the nannofossil *Cyclcargolithus floridanus* (11.9 Ma). A late Miocene age is assigned to the interval ~84–198 mbsf at Site 1168, the Miocene/Pliocene (Messinian/Zanclean) boundary (5.3 Ma), being approximated by the nannofossil datum LO of *Triquetrorhabdulus rugosus* (5.23 Ma) and the dinocyst datum LO of *Reticulatosphaera actinocoronata* (5.2 Ma) at ~84 mbsf; however, dispute exists on the subchronology of this interval (see Table T1). The nannofossil data are favored because of their smaller depth error.

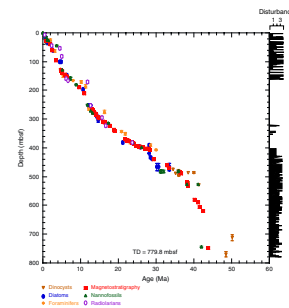
The interval ~15–84 mbsf is assigned a Pliocene age based on dinocyst, foraminiferal, and nannofossil evidence and appears to be relatively complete at Site 1168. The lower/upper Pliocene (Zanclean/Piacenzian) boundary (3.58 Ma) is placed at ~42.7 mbsf at the onset of Subchron C2An.3n (Table T1; Figs. F2, F4). The nannofossil datum FO of *Gephyrocapsa caribbeanica* (1.72 Ma) approximates the Pliocene/Pleistocene boundary (1.77 Ma) at ~15 mbsf. The chronology above this level is resolved at high resolution by a robust benthic oxygen isotope stratigraphy and several nannofossil datums. The nannofossil data and the oxygen isotope stratigraphy are in generally good agreement at this site (Table T1). A short hiatus (~300 k.y.) commencing at ~1.6 Ma is suggested by nannofossil data at ~10.8 mbsf. The isotope stratigraphy suggests that just the top 5 cm of Hole 1168A is Holocene in age. The resulting age model gives an average linear sedimentation rate through the early Miocene of ~2 cm/k.y., decreasing to a ~1.6 cm/k.y. throughout from the middle Miocene onward.

Site 1170

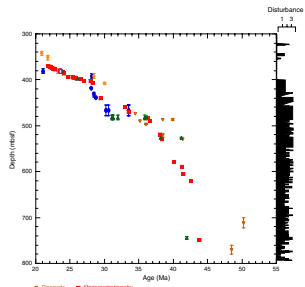
Site 1170 is located in deep water (2704 m) on the flat western part of the South Tasman Rise (STR), 400 km south of Tasmania (Fig. F1). The site lies within present-day northern subantarctic surface waters, ~150 km south of the Subtropical Front and well north of the Subantarctic Front. Four holes were drilled to a total depth of 780 mbsf: Hole 1170A (APC/XCB), Holes 1170B and 1170C (APC), and Hole 1170D (rotary core barrel [RCB]). Biotic and magnetostratigraphic datums from Holes 1170A, 1170B, and 1170D indicate a middle Eocene to upper Quaternary sequence at Site 1170 (Table T2; Figs. F5, F6, F7). The sequence is divided into five lithostratigraphic units (Shipboard Scientific Party, 2001d), the oldest of which (Unit V) comprises silty claystones of middle and late Eocene age, overlain by 25 m of glauconite-rich clayey siltstone deposited during the latest Eocene to earliest Oligocene (Unit IV). Unit IV is overlain by 472 m of deepwater pelagic nannofossil chalk and ooze of early Oligocene through Quaternary age (Units III–I) containing abundant siliceous microfossils. See Shipboard Scientific Party (2001d) for detailed lithologic descriptions. Microfossil and magnetostratigraphic data of age significance for Site 1170 are listed in Table T2 and depicted in Figures F5, F6, and F7.

T2. Age-depth data, Site 1170, p. 44.

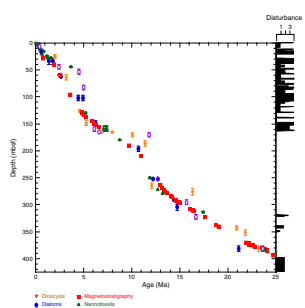
F5. Age-depth plot, Site 1170, p. 30.



F6. Age-depth plot, Site 1170, Paleogene, p. 31.



F7. Age-depth plot, Site 1170, Neogene and Quaternary, p. 32.



Paleogene (Middle Eocene to Oligocene)

The age model for the Paleogene intervals of Site 1170 is based on several dinocyst (Eocene), diatom (Oligocene), and nannofossil (Eocene and Oligocene) events correlated to the magnetostratigraphy (Table T2). The base of Hole 1170D (base Core 189-1170D-38R; ~780 mbsf) is dated at ~48.5 Ma (earliest middle Eocene) based on the first abundant occurrence (FAO) of the dinocyst *E. partridgei*, which is tied to Subchron C21r at Site 1172 (Brinkhuis, Sengers, et al., this volume). A greater number of dinocyst events than nannofossil events are recorded in the Eocene (despite better sampling resolution for nannofossils), allowing relatively good age constraint for these intervals.

In general, there are some disagreements between the dinocyst stratigraphy and magnetostratigraphy vs. the nannofossil stratigraphy in the middle Eocene. For example, a questionable hiatus at ~527 mbsf (Subunit VA; Hole 1170D) may be indicated by the co-occurrence of two nannofossil datums—the LO of *Chiasmolithus solitus* (38.2 Ma) and the FO of *Reticulofenestra reticulata* (41.2 Ma)—as well as dinocyst datum FO of *Hemiplacophora semilunifera* (41.4 Ma). Such a hiatus, however, appears to be in conflict with the magnetostratigraphy. Further work is needed to clarify this problem; however, we follow the magnetostratigraphic data in this age model (i.e., no middle Eocene hiatus) but also retain the position of the LO of *C. solitus* datum (only), based on the position of magnetochrons. The positions of the Eocene stage boundaries are impossible to determine from the present data, however.

The dinocyst and nannofossil data appear to be in good agreement in the upper Eocene at the current resolution, and a relatively expanded upper Eocene section (compared to Site 1172, for example) is recognized. The E/O boundary (*sensu* GSSP; the Priabonian/Rupelian boundary at 33.7 Ma) is difficult to determine on the given information because several important high-latitude E/O boundary markers are missing at this site (e.g., the LO of *Reticulofenestra oamaruensis* and the LO of *Subbotina brevis*). However, we approximate its position at ~472 mbsf by using combined dinocyst and diatom datums in Hole 1170D (cf. Sluijs et al., this volume). A series of short hiatuses over the E–O transition and early Oligocene are possibly recognized, but these are difficult to isolate on the relatively low resolution data available. Further details on the dinocyst and diatom stratigraphy at the E–O transition are presented in Sluijs et al. (this volume) and Stickley et al. (submitted [N2]).

Age control for the Oligocene interval is based largely on diatom events, magnetostratigraphy, and a nannofossil event, which are all in excellent agreement. The combined data suggest that most of the lower Oligocene is missing, whereas the upper Oligocene is relatively complete. The diatom datum FO of *Coscinodiscus lewisi* var. *levis* (28.5 Ma) marks the lower/upper Oligocene (Rupelian/Chattian) boundary at ~432 mbsf (Hole 1170D). The stratigraphic positions of planktonic foraminiferal datums LO of *Subbotina angiporoides* (30 Ma) and FO of *Chiloguembelina cubensis* (28.5 Ma) are in disagreement with the nannofossil and diatom stratigraphy for the Oligocene. Taken in isolation they suggest, in contrast to the current interpretation, that more of the lower Oligocene is preserved and that much of the upper Oligocene is missing. The LO of *C. cubensis* would suggest the Rupelian/Chattian boundary to occur 40 m higher at ~392 mbsf (Hole 1170A). However, these foraminiferal data are based on poor-resolution shipboard core catcher samples. Thus as ongoing foraminiferal studies are being under-

taken to resolve this issue, the diatom-nannofossil-magnetostratigraphic interpretation is favored based on postcruise analysis at better resolution (~30–80 cm depth error). In particular, the tightly constrained stratigraphic positions of robust nannofossil datum LO of *Chiasmolithus altus* (26.1 Ma; ~397 mbsf in Hole 1170A) and diatom datums FO of *Rocella vigilans* var. B sensu Harwood and Maruyama (1992) (28.1 Ma; ~418 mbsf in Hole 1170A), FO of *Rocella gelida* (25.8 Ma; ~396.7 mbsf in Hole 1170A), and LO of *Rocella vigilans* var. B (25.5 Ma; ~395.6 mbsf in Hole 1170A) are difficult to refute. A distinct stratigraphic gap exists between the ranges of *R. vigilans* var. A sensu Harwood and Maruyama (1992) and *R. vigilans* var. B over the Rupelian/Chattian boundary (Table T2). This phenomenon has also been reported on the Kerguelen Plateau (Harwood and Maruyama, 1992, Roberts et al., 2003). At Site 1170, this gap is ~20 m.

The resulting age model gives an average sedimentation rate through the middle Eocene of ~2.4 cm/k.y. In the late Eocene sedimentation rates fall to 1.1 cm/k.y. on average, falling still further to ~75 mm/k.y. in the early Oligocene, returning to ~1.1 cm/k.y. in the late Oligocene.

Neogene (Miocene to Pliocene) and Quaternary

Age determination for the Neogene and Pleistocene intervals of Site 1170 are based on integrated diatom, nannofossil, planktonic foraminifer, and a few radiolarian events tied to the magnetostratigraphy. Marine isotope stages are recognized in the benthic oxygen isotope signal back to MIS 18.2 (722 ka), which we incorporate into the biostratigraphic age model. Although the age model for the Neogene intervals is resolved at a higher resolution than for the Paleogene, generally the chronology for this time period remains problematic because of a high amount of core disturbance, particularly around the (presumed position of the) Miocene/Pliocene (Messinian/Zanclean) boundary (5.3 Ma). We present the most likely age model based on the strategy outlined in “Materials and Methods,” p. 7.

The Oligocene/Miocene (Chattian/Aquitanian) boundary (23.8 Ma) is marked by a hiatus (or series of hiatuses/condensed sections) of ~1 m.y. centered around 380–383 mbsf (Hole 1170A) based on seven biomagnetostratigraphic events including the (apparent) onset and termination of subchron C6Cn.2n (23.8 and 23.6 Ma, respectively) and the LO of *Reticulofenestra bisecta* s. str. (23.9 Ma), all occurring within an interval of 90 cm (382.0–382.9 mbsf; Hole 1170A). The recognition of the Mi-1 event from the oxygen isotope record of Hole 1170A (see Pfuhl and McCave, this volume; Pfuhl et al., in press) may dispute this short hiatus or condensed section, however. Evidence would suggest that much of the lower and middle Miocene is relatively complete at Site 1170 with no major hiatuses recorded, although higher-resolution work may confirm a possible ~1-m.y. hiatus around the upper lower Miocene to lower/middle Miocene (Burdigalian/Langhian) boundary (16.4 Ma) approximated by the close stratigraphic placement of the FO of *Calcidiscus premacintyrei* (17.4 Ma) and the onset of Subchron C5Cn.1n (16.3 Ma) at ~310.5 mbsf (Hole 1170A). This nannofossil datum is tightly constrained by a ~10-cm error (partly forced by the position of the chron). An expanded section is suggested for the interval around the middle/upper Miocene (Serravallian/Tortonian) boundary (11.2 Ma), indicated by nannofossil, diatom, and magnetostratigraphic data: the nannofossil datum LO of *C. floridanus* (11.9 Ma) is placed at ~249 mbsf (Hole 1170A) with an error of 75 cm, the onset of Subchron C5n.2n

(10.9 Ma) is recognized 40 m higher at 210 mbsf (Hole 1170B), and the diatom datum LO of *Denticulopsis dimorpha* (10.7 Ma) is seen at ~196 mbsf (Hole 1170A). Based on this information, the average linear sedimentation rate across this boundary is ~4.5 cm/k.y.

Nannofossil and radiolarian evidence supports a hiatus at ~158 mbsf (Hole 1170A) spanning 7.4–6.1 Ma. This hiatus is based on the concurrent FOs of *Amaurolithus primus* (7.4 Ma) and *Amaurolithus delicatus* (7.3 Ma), the first two amauroliths in a well-documented evolutionary lineage (Raffi et al., 1998). The top of the *Reticulofenestra pseudoumbilica* paracme event (7.1 Ma) (Backman and Raffi, 1997) is also tentatively placed at the same depth. At Site 1168 these three events are separated by ~10 m. However, because of core disturbance problems, an error of 5.1 m is associated with these events at Site 1170. On account of the disturbed nature of the cores in the late Miocene, nannofossil samples within disturbed core intervals (based on examination of core photos) were not included in the final determination of events. The radiolarian datum LO of *Amphymenium challengerae* (6.1 Ma) marks the termination of the hiatus. It is possible the hiatus may have started 600 k.y. earlier (at 8 Ma) if the planktonic foraminiferal datum LO of *Paragloborotalia continuosa* (8 Ma) (~165 mbsf, Hole 1170A) is taken into consideration with the above datums. If this is accepted, then the hiatus is placed at ~163 mbsf (Hole 1170A) to incorporate the six biodatums above it (Table T2).

Amauroliths are robust, dissolution-resistant nannofossils that are consistently present, though rare to few, at all Leg 189 sites. The *R. pseudoumbilica* paracme is well documented and appears isochronous (e.g., Backman and Raffi, 1997). The onset and termination of this paracme event were determined semiquantitatively. The classic zero appearance of this species, as noted by Backman and Raffi (1997), was not observed at the Leg 189 sites (cool-temperate in nature). However, a clear decrease in *R. pseudoumbilica* and its cooler-water form *R. gelida* (not shown in Table T2) is quite marked and concomitant (see McGonigal and Wei, this volume; McGonigal, in press).

The Miocene/Pliocene boundary (5.3 Ma) is constrained by nannofossil evidence at ~130 mbsf (Hole 1170A) based on the LO of *T. rugosus* (5.23 Ma), indicating >250 m of sediment of Miocene age at Site 1170. The Pliocene and Quaternary intervals are dated confidently on several robust and supportive nannofossil and diatom datums (Table T2). These intervals have the most potential for a high-resolution, integrated nannofossil-diatom Southern Ocean stratigraphy for the Pliocene–Pleistocene. In addition, one foraminiferal datum, one radiolarian datum, and three magnetostratigraphic datums complete the age model for these younger intervals. Of particular note is the position of the base of the Olduvai Chron (C2n; 1.95 Ma), which is undisputed at 39.7 mbsf (Hole 1170A). The chronology above this level is resolved at high resolution by a robust benthic oxygen isotope stratigraphy, several nannofossil datums, and one diatom datum. The nannofossil data, diatom data, and the oxygen isotope stratigraphy are in generally good agreement at this site (Table T2). The acme of the nannofossil *E. huxleyi* has age significance and suggests that the top ~80 cm of Hole 1170A is younger than 85 ka, whereas the isotope stratigraphy suggests that the top 20 cm of Hole 1170A is Holocene in age.

The resulting age model gives an average linear sedimentation rate through the early Miocene of ~1 cm/k.y., increasing to, on average, ~1.4 cm/k.y. in the middle and late Miocene. Pliocene–Pleistocene sedimentation rates are ~2.5 cm/k.y. on average.

Site 1171

Site 1171 is located in lower bathyal water depths of ~2150 m on a gentle southwesterly slope on the southernmost STR, ~550 km south of Tasmania and 270 km southeast of Site 1170. At 48°S, Site 1171 lies in subantarctic waters between the Subtropical Convergence to the north and the Subantarctic Front to the south. Four holes were drilled to a total depth of 959 mbsf: Holes 1171A and 1171B (APC), Hole 1171C (APC/XCB), and Hole 1171D (RCB). Biotic and magnetostratigraphic datums from Holes 1171A–1171D indicate a lower Eocene to upper Quaternary sequence at Site 1171 (Table T3; Figs. F8, F9, F10). There is a 3.6 m offset in mbsf between Holes 1171C and 1171D. This offset is large with regard to the resolution of our data. Therefore, in this report we correct for the offset in order to successfully correlate the age data between overlapping parts of these holes by increasing the mbsf level (archived in the ODP database) by 3.6 m for Hole 1171D. This offset is incorrectly reported in Shipboard Scientific Party (2001e) as occurring the other way around (i.e., Hole 1171D offset too deeply). The error is recognized here from postcruise diatom data (occurring in both Holes 1171C and 1171D) and lithologic descriptions (Shipboard Scientific Party, 2001e). **Sluijs et al.** (this volume) demonstrate the offset further by comparison of magnetic susceptibility records from Holes 1171C and 1171D.

The sequence was divided into six lithostratigraphic units and a number of subunits Shipboard Scientific Party (2001e). The older sequence consists broadly of ~616 m of silty claystone of earliest Eocene to late Eocene age (lithostratigraphic Units VI and V) overlain by 67 m of diatom-bearing claystone of late Eocene age (lithostratigraphic Unit IV) and 6 m of glauconitic siltstone deposited during the latest Eocene (Unit III). Unit III is overlain by 67 m of deepwater nannofossil chalk and ooze of early Oligocene to early Miocene age (Unit II); limestone and siliceous limestone beds are in the base of the Oligocene section. Unit I consists of 234 m of deepwater foraminiferal-bearing nannofossil ooze and chalk of early Miocene to Holocene age. See Shipboard Scientific Party (2001e) for detailed lithologic descriptions. Microfossil and magnetostratigraphic data of age significance for Site 1171 are listed in Table T3 and depicted in Figures F8, F9, and F10.

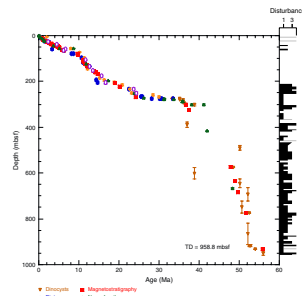
Paleogene (Lower Eocene to Oligocene)

The age model for the Paleogene interval of Site 1171 is based on several dinocyst (Eocene and earliest Oligocene), diatom (Oligocene), and nannofossil (Eocene and Oligocene) events correlated to the magnetostratigraphy (from Site 1172) (Table T3). A greater number of dinocyst events than nannofossil events are recorded in the Eocene, allowing relatively good age constraint for these intervals. The base of Hole 1171D (base of Core 189-1171D-75R; ~959 mbsf corrected depth) is tentatively dated at <54 Ma (i.e. Subchron C24r or younger) (earliest Eocene) based on the dinocysts (cf. Röhl et al., in press a).

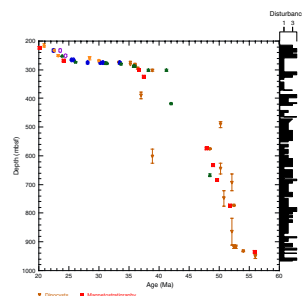
The lower/middle Eocene (Ypresian/Lutetian) boundary (~49 Ma) is placed at the termination of Chron C22n at ~634 mbsf (Hole 1171D corrected depth). As for Site 1170, nannofossil data suggest a hiatus spanning the interval 41.2–38.2 Ma (at ~302 mbsf; Unit IV, Hole 1171D corrected depth), which is in disagreement with dinocyst and magnetostratigraphic data. We are unable to speculate any further on this given the available information but we dismiss such a middle Eocene hiatus

T3. Age-depth data, Site 1171, p. 49.

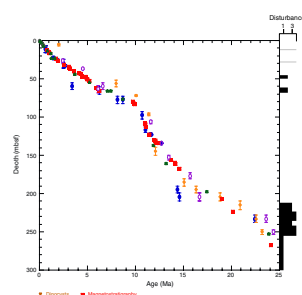
F8. Age-depth plot, Site 1171, p. 33.



F9. Age-depth plot, Site 1171, Paleogene, p. 34.



F10. Age-depth plot, Site 1171, Neogene and Quaternary, p. 35.



(1) on the basis of similar problems at Site 1170 but, more importantly, (2) on the given (tightly constrained) placement of nannofossil datum FO of *R. umbilicus* (42 Ma) at ~416 mbsf (depth error 1.5 m) (Hole 1171D corrected depth), which would create a doubtfully high sedimentation rate (of >14 cm/k.y.) should the hiatus exist. Further work is being undertaken to clarify this issue. As for Site 1170, the upper Eocene is relatively expanded at Site 1171 (compared to Site 1172). The middle/upper Eocene (Bartonian/Priabonian) boundary (37 Ma) is difficult to position on the current information although the termination of Subchron C17n.1n (36.6 Ma) at ~302 mbsf (Hole 1171D corrected depth) approximates it.

The E/O boundary (Priabonian/Rupelian; 33.7 Ma) appears to be tightly constrained by the nannofossil datum LO of *R. oamaruensis* (33.7 Ma) at ~279 mbsf (Hole 1171D corrected depth; 70-cm depth error). A series of short hiatuses (cf. Sites 1170 and 1172) over the entire lower Oligocene interval and possibly some of the upper Oligocene are suggested by complementary data from diatom, dinocyst ([Sluijs et al., this volume](#)), and nannofossil datums. These datums are tightly constrained stratigraphically (e.g., the LO of *C. altus* [26.1 Ma] at ~273 mbsf [Hole 1171D corrected depth] with an error of just 9 cm). The age model indicates that ~25 m of Oligocene-age sediment is preserved at Site 1171 compared to almost 90 m at Site 1170. The relatively thin Oligocene section means many important datums are either not observed at this sampling resolution or are missing altogether. For example, the stratigraphic gap between the distinct diatom datums LO of *R. vigilans* var. A and FO of *R. vigilans* var. B, which at Site 1170 was clearly observed (see above), is difficult to resolve at Site 1171. Unfortunately, the paleomagnetic record in the critical (carbonate) Oligocene intervals is very poor and cannot be used to help constrain this age information, yet integrated dinocyst and diatom datums provide a reasonable age assessment ([Sluijs et al., this volume](#)).

The Paleogene age model gives an average sedimentation rate of ~4.5 cm/k.y. for the early Eocene, falling to ~2–2.6 cm/k.y. in the middle Eocene, and rising to ~3.4–7 cm/k.y. (depending on the position of the middle/late Eocene [Bartonian/Priabonian] boundary). The high amount of nondeposition through the Oligocene gives rise to a very low sedimentation rate of ~2 mm/k.y. for this Epoch.

Neogene (Miocene and Pliocene) and Quaternary

Age determinations for the Neogene and Pleistocene intervals of Site 1171 are based on integrated diatom, nannofossil, planktonic foraminiferal, and a few radiolarian events tied to the magnetostratigraphy. The Neogene intervals are resolved at a higher resolution than for the Paleogene intervals, and unlike Site 1170, the stratigraphy is relatively straightforward. The resultant age model for the Miocene and younger sections shows relatively a good integration of siliceous and calcareous microfossil groups.

As for Site 1170, the Oligocene/Miocene (Chattian/Aquitanian) boundary (23.8 Ma) at Site 1171 is marked by a hiatus of ~1 m.y. at ~253 mbsf (Hole 1171C) based on nannofossil, foraminiferal, and radiolarian evidence. Of particular note is the placement of the LO of the *R. bisecta* s. str. (23.9 Ma) datum at this horizon within a depth error of just 30 cm. The age model suggests >200 m of relatively complete Miocene section at Site 1171 except for a condensed interval over the lower/middle Miocene (Burdigalian/Langhian) boundary (16.4 Ma) at

~197–198 mbsf (Hole 1171C) and a hiatus at ~65 mbsf (Hole 1171A) spanning the interval 7.8–6.3 Ma based on nannofossil data (Table T3). The middle Miocene appears to be relatively complete at Site 1171 with the middle/upper Miocene (Serravallian/Tortonian) boundary (11.2 Ma) placed within the interval 113–123 mbsf (Hole 1171C) on diatom and magnetostratigraphic data. This boundary interval appears to be expanded but not as greatly as that at Site 1170.

The Pliocene and Pleistocene intervals are well dated on several robust and supportive nannofossil and diatom datums (Table T3). As for Site 1170, there is a lot of potential for a high-resolution, integrated nannofossil-diatom Southern Ocean stratigraphy in these intervals. The resulting biostratigraphy appears to be corroborated by a detailed magnetostratigraphy and by a single foraminiferal and radiolarian datum. The Miocene/Pliocene (Messinian/Zanclean) (5.3 Ma) boundary is approximated at ~55 mbsf (Hole 117A) on the position of the nannofossil datum LO of *T. rugosus* (5.23 Ma). Also of note is the recognition of the lower/upper Pliocene (Zanclean/Piacenzian) boundary at the onset of the Gauss Chron (C2An.3n; 3.58 Ma) at 40.4 mbsf (Hole 1171C) and the Pliocene/Pleistocene (Gelasian/Calabrian) boundary at the termination of the Olduvai Chron (1.77 Ma) at 24 mbsf (Hole 1171C). The age model above this level is resolved at high resolution by a chronology derived from correlation of the Hole 1171A L* record with those from Holes 1170A and 1172A (see “Materials and Methods,” p. 7) and several diatom and nannofossil datums. The nannofossil data, diatom data, and L* stratigraphy are in excellent agreement at this site (Table T3). The acme of nannofossil *E. huxleyi* suggests that the top ~50 cm of Hole 1171A is younger than 85 ka, whereas the L* stratigraphy suggests that the top 25 cm of Hole 1171A is Holocene in age.

The resulting age model gives an average linear sedimentation rate through the early Miocene of ~0.9 cm/k.y., increasing to ~1.4 cm/k.y. (average) in the middle Miocene, and ~2.5 cm/k.y. (average) in the late Miocene. Pliocene–Pleistocene sedimentation rates are a little over ~1 cm/k.y. on average (0.9 cm/k.y. in the Pliocene rising to ~1.4 cm/k.y. in the Pleistocene).

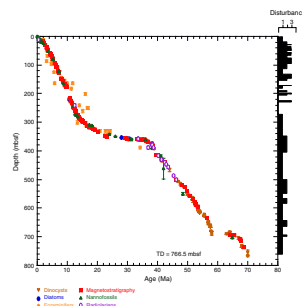
Site 1172

Site 1172 is located in a water depth of ~2620 m on the flat western side of the East Tasman Plateau (Fig. F1) in cool subtropical water just north of the present-day Subtropical Front. Four holes were drilled to a total depth of 766.5 mbsf: Hole 1172A (APC/XCB), Holes 1172B and 1172C (APC), and Hole 1172D (RCB). Biotic and magnetostratigraphic datums from Holes 1172A and 1172D indicate a lower Maastrichtian (Upper Cretaceous) to upper Quaternary sequence at Site 1172 (Table T4; Figs. F11, F12, F13). The sequence is divided into four lithostratigraphic units (Shipboard Scientific Party, 2001f), the oldest of which (Unit IV) comprises ~263 m of silty organic-rich claystones of Maastrichtian to early Eocene age. Overlying this is ~142 m of middle–upper Eocene diatomaceous organic-rich claystones (Unit III). Unit II is thin (~5 m) but is formed of a complex sequence of glauconitic claystones and siltstones of latest Eocene to earliest Oligocene age. The youngest unit (Unit I) is ~356 m of calcareous nannofossil and foraminiferal ooze. See Shipboard Scientific Party (2001f) for detailed lithologic descriptions.

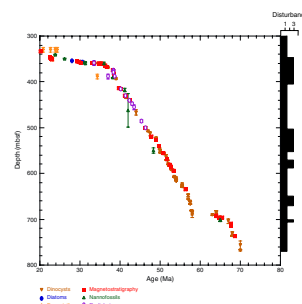
Microfossil and magnetostratigraphic data of age significance for Site 1172 are listed in Table T4 and depicted in Figures F11, F12, and F13.

F4. Age-depth data, Site 1172, p. 57.

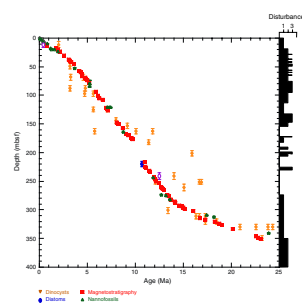
F11. Age-depth plot, Site 1172, p. 36.



F12. Age-depth plot, Site 1172, Maastrichtian and Paleogene, p. 37.



F13. Age-depth plot, Site 1172, Neogene and Quaternary, p. 38.



There is a small offset of ~1 m in absolute mbsf between Hole 1172A and 1172D (age data recognized in both holes are ~1 m deeper by mbsf in Hole 1172D). This offset is not adjusted for in Table T4 (i.e., data are presented “by hole”). See Shipboard Scientific Party (2001f) for general information.

Late Cretaceous and Paleogene (Maastrichtian to Oligocene)

Some of the most successful deep drilling of Leg 189 occurred at Site 1172. For example, recovery included an almost complete K/T interval (see also Schellenberg et al., in press), a possible Paleocene/Eocene boundary interval (see also Röhl et al., in press a), and a complete E/O boundary interval (see also Stickley et al., submitted [N2]). The age model for the Maastrichtian interval is based mainly on dinocyst events with two nannofossil events. The Paleocene and lower Eocene intervals of Site 1172 are dated solely by dinocyst datums tied to a robust magnetostratigraphy (Table T4). Dinocyst and magnetostratigraphic data also provide the basis of the age model for the middle upper Eocene intervals with a few nannofossil and radiolarian datums and one planktonic foraminiferal datum. The upper Eocene/lower Oligocene boundary interval is dated entirely by dinocysts and diatoms tied to the magnetostratigraphy. This site provides the best opportunity of all the deep sites of Leg 189 for studying this critical boundary interval. In the Oligocene, diatoms, nannofossils, and planktonic foraminifers provide the age information, tied to the magnetostratigraphy.

The base of Hole 1172D (base of Core 189-1172D-31R; ~766.5 mbsf) is dated at 70 Ma (early Maastrichtian) based on the FAO of the dinocyst genus *Manumiella*. The K/T boundary (65 Ma) occurs at 695.99 mbsf on lithologic, dinocyst, diatom (pyritized), and magnetostratigraphic evidence. A hiatus of ~800 k.y. marks the boundary itself, with all of Chron C29r and possibly parts of Chrons C29n and C30n missing. Schellenberg et al. (in press) provide details on the age model and paleoenvironmental interpretation of the K/T boundary at Site 1172. Just over 70 m of Maastrichtian-age sediments were recovered at this site.

Geochemical and palynological data from Röhl et al. (in press a) and Brinkhuis, Sengers, et al., (this volume) suggest the Paleocene/Eocene Thermal Maximum (PETM) (~55 Ma) occurs at ~620 mbsf in Hole 1172D. See the discussion in Röhl et al. (in press a) on the Paleocene/Eocene (P/E) transition and PETM at Site 1172. Brinkhuis, Sengers, et al. (this volume) provide further information on the dinocyst successions through the Paleocene and Paleocene–Eocene (P–E) transition. The resulting age model suggests that ~76 m of sediment of Paleocene age is recovered at Site 1172.

The lower/middle Eocene (Ypresian/Lutetian) boundary (~49 Ma) is marked by the termination of Chron C22n at 526.4 mbsf (Hole 1172D), suggesting that nearly 94 m of relatively complete lower Eocene sediments were recovered at Site 1172. In addition, the bottom of Hole 1172A is dated to the early Eocene. The middle/upper Eocene (Bartonian/Priabonian) boundary (37 Ma) is difficult to place in these sediments because of the commencement of notable condensation at this time (Röhl et al., in press b; Stickley et al., submitted [N2]). However, it is approximated at ~368 mbsf (within Core 189-1172A-40X) by dinocyst datums FAO of *Spinidinium macmurdoense* (36.9 Ma) and FO of *Sto-*

veracysta ornata (36.95 Ma), suggesting that >158 m of middle Eocene sediments are preserved at Site 1172.

The upper Eocene and E/O boundary intervals are condensed into ~10 m of sediment; however, the stratigraphy is resolved at high resolution by several dinocyst and diatom datums with a robust magnetostratigraphy. The exact position of the E/O boundary sensu Berggren et al. (1995a, 1995b) (Priabonian/Rupelian; 33.7 Ma) is difficult to place because of the lack of marker calcareous microfossils, yet its position is approximated to ~33.5 Ma (cf. Oi-1a event of, e.g., Zachos et al., 1996) at 358.9 mbsf (Hole 1172A) by several lines of evidence (e.g., the termination of Chron C13n and the diatom datums LO of *Distephanosira architecturalis* and LO of *Hemiaulus characteristicus*). The E/O boundary to lower Oligocene sequence is interrupted by a series of short hiatuses associated with the initiation of deepwater current action in the Tasmanian Gateway. For detailed information on the upper Eocene through lower Oligocene age model and paleoenvironmental interpretation see Stickley et al. (submitted [N2]).

Just a little more than 18 m of sediments of Oligocene age are preserved at Site 1172. Diatoms and magnetostratigraphy (with one nannofossil and one planktonic foraminiferal datum) effectively provide the age control for the lower Oligocene, whereas nannofossils and magnetostratigraphy resolve the upper Oligocene chronology. For such a condensed sequence, age control is resolved at moderate–high resolution. The lower/upper Oligocene (Rupelian/Chattian) boundary (28.5 Ma) is approximated at ~354 mbsf (Hole 1172A) by the diatom datum LO of *Rocella vigilans* var. A (29 Ma). However, there is some dispute over the position of the Oligocene/Miocene (O/M) (Chattian/Aquitanian) boundary (23.8 Ma), and therefore over the thickness of the upper Oligocene. Nannofossil evidence approximates the O/M boundary to ~340 mbsf (Hole 1172A) by the LO of *R. bisecta* s. str. (23.9 Ma), giving a thickness of ~14 m for sediments of late Oligocene age, whereas the planktonic foraminiferal datum LO of *Turborotalia euapertura* (23.8 Ma) would place the boundary at ~330 mbsf (Hole 1172A) within a foraminifer-only based late Oligocene to early Miocene hiatus. The latter scenario would give ~24 m of upper Oligocene sediments. We favor the nannofossil evidence (and therefore uncertainty regarding such a hiatus) for the placement of the O/M boundary on their smaller depth error (Table T4).

The resulting age model gives an average sedimentation rate of 1.4 cm/k.y. for the Maastrichtian, falling to <1 cm/k.y. in the Paleocene. Sedimentation rates steadily fall from 1.6 cm/k.y., through 1.3 cm/k.y., to 3 mm/k.y. for the early, middle, and late Eocene, respectively, and by the Oligocene rates had fallen to just 2 mm/k.y. on average.

Neogene (Miocene to Pliocene) and Quaternary

Age determination for the Neogene and Quaternary intervals of Site 1172 are based mainly on integrated nannofossil and planktonic foraminiferal datums tied to the magnetostratigraphy, with a few radiolarian and diatom datums (Table T4). A benthic oxygen isotope stratigraphy back to ~600 ka, as reported in Nürnberg et al. (in press), is incorporated into the age model.

Parts of the chronology within the Miocene interval are problematic, with planktonic foraminiferal data giving slightly different age information than the nannofossil data (Table T4). We favor the nannofossil datums in these problematic intervals on account of their robustness at

the other sites of Leg 189 and their small depth error compared to the foraminiferal datums. It is out of the scope of this paper to speculate on the causes for these differences, although it appears many of the discrepancies could be resolved by higher-resolution foraminiferal stratigraphic work. The magnetostratigraphy may also need some revision in light of this. However, we present the most likely scenario at this time. Further, oxygen isotope stratigraphy will greatly aid age assessment through these problematic intervals.

We approximate the lower/middle Miocene (Burdigalian/Langhian) boundary (16.4 Ma) at ~308 mbsf (Hole 1172A) with (coincidentally) the placement of a hiatuses determined from nannofossil and foraminiferal evidence. This possible hiatus (or condensed interval) lasts ~1.1 m.y. and is defined by the FO of *C. premacintyreai* (17.4 Ma), the LO of *Catapsydrax dissimilis* (17.3 Ma), the FO of *Globorotalia miozea* (16.7 Ma), and the FO of *Praeorbulina curva* (16.3 Ma). The resulting age model suggests >33 m of sediment of early Miocene age. The middle/upper Miocene (Serravallian/Tortonian) boundary (11.2 Ma) is unresolved. The nannofossil datum LO of *C. floridanus* (11.9 Ma) approximates this boundary at ~244 mbsf, suggesting nearly 64 m of middle Miocene sediment, whereas magnetostratigraphic data places the boundary 14 m higher in Hole 1172A (Table T4), giving ~50 m of middle Miocene sediment. Resolution of the subchronology of the middle Miocene varies depending which microfossil group is followed; however, for reasons stated above we favor the nannofossil biostratigraphy and magnetostratigraphy through this interval despite a greater number of observed planktonic foraminiferal datums. The Miocene/Pliocene (Messinian/Zanclean) boundary (5.3 Ma) is placed within a short hiatus at ~79 mbsf at the position of nannofossil datums LO of *Discoaster quinqueramus* (5.53 Ma) and LO of *T. rugosus* (5.23 Ma), suggesting nearly 165 m of sediment of late Miocene age. As at Site 1170, core disturbance across this interval results in an error of ~6 m in the depth assignment of these events. Foraminiferal evidence places this boundary deeper in Hole 1172A (at ~96 mbsf), but we reject this information for reasons stated above and because several other foraminiferal datums in the upper Miocene interval give inconsistent and puzzling information (see Table T4). We conclude that age assignments for some of the planktonic foraminiferal datums require revision for Site 1172, and perhaps the generation of an entirely new zonation scheme for this part of the Southern Ocean.

Nannofossil datums and magnetostratigraphy provide good age control for the Pliocene interval. The onset of Subchron C2An.3n (Gauss) (3.58 Ma) is recognized at ~46 mbsf (Hole 1172A), allowing the placement of the lower/upper Pliocene (Zanclean/Piacenzian) boundary at this level. In Hole 1172A, the Pliocene/Pleistocene boundary (1.77 Ma) is placed either at the termination of Chron C2n (Olduvai) at ~17 mbsf, or at ~20 mbsf on nannofossil evidence (Table T4). This gives a thickness of ~59–62 m for sediments of Pliocene age at Site 1172. Further work is required to resolve this dispute. The chronology above 17 mbsf is resolved at high resolution by a robust benthic oxygen isotope stratigraphy and several nannofossil datums. The nannofossil data and the oxygen isotope stratigraphy are in excellent agreement at the current resolution (Table T4). A short hiatus spanning ~1.6–1.3 Ma, defined by nannofossils, is recognized at ~19 mbsf (Hole 1172A). The isotope stratigraphy suggests that the top 13 cm of Hole 1172A is Holocene in age.

The resulting age model gives an average sedimentation rate through the early Miocene of ~0.5 cm/k.y., increasing to ~1.2 cm/k.y. in the

middle Miocene, and ~2.5 cm/k.y. in the late Miocene. Pliocene–Pleistocene sedimentation rates are ~1.5 cm/k.y. on average.

Revisions

Areas for improvement, particularly where only shipboard data are available, include revision of the planktonic foraminiferal data for Sites 1168, 1170, and 1171, the radiolarian data for all sites, the diatom data for the Neogene and Quaternary sections of Sites 1170–1172, and the dinocyst data for the Paleogene of Sites 1170 and 1171. The magnetostratigraphic interpretation also needs some revision in parts of each site, particularly in intervals where core was the most disturbed.

ACKNOWLEDGMENTS

This research used samples and data provided by the Ocean Drilling Program (ODP). ODP is sponsored by the U.S. National Science Foundation (NSF) and participating countries under management of Joint Oceanographic Institutions (JOI) Inc. Funding for this research was provided by the Natural Environment Research Council (NERC)/UK-ODP to CES and HAP, and by USSAC funds to KLM, who used laboratory facilities provided by NSF grant no. DPP 94-22893. HB thanks NWO, the Netherlands Organization for Scientific Research. We are particularly grateful to reviewers John A. Barron, Sherwood W. Wise Jr., and co-editor James P. Kennett for their thorough reviews of this paper and suggestions for its improvement. We also thank co-editor Mitch Malone and Lorri Peters of the ODP publications team for their meticulous editorial help on an earlier version of this paper. The Time Team wishes to thank the other members of the Leg 189 Science Party for general support.

REFERENCES

- Abelmann, A., 1990. Oligocene to middle Miocene radiolarian stratigraphy of southern high latitudes from Leg 113, Sites 689–690, Maud Rise. In Barker, P.F., Kennett, J.P., et al., *Proc. ODP, Sci. Results*, 113: College Station, TX (Ocean Drilling Program), 675–708.
- Abelmann, A., 1992. Early to middle Miocene radiolarian stratigraphy of the Kerguelen Plateau, Leg 120. In Wise, S.W., Jr., Schlich, R., et al., *Proc. ODP, Sci. Results*, 120: College Station, TX (Ocean Drilling Program), 757–783.
- Askin, R.A., 1988a. Campanian to Paleocene palynological succession of Seymour and adjacent islands, northeastern Antarctic Peninsula. In Feldmann, R.M., and Woodburne, M.O. (Eds.), *Geology and Paleontology of Seymour Island, Antarctic Peninsula*. Mem.—Geol. Soc. Am., 169:131–153.
- Askin, R.A., 1988b. The palynological record across the Cretaceous/Tertiary transition on Seymour Island, Antarctica. In Feldmann, R.M., and Woodburne, M.O. (Eds.), *Geology and Paleontology of Seymour Island, Antarctic Peninsula*. Mem.—Geol. Soc. Am., 169:155–162.
- Backman, J., and Raffi, I., 1997. Calibration of Miocene nannofossil events to orbitally tuned cyclostratigraphies from Ceara Rise. In Shackleton, N.J., Curry, W.B., Richter, C., and Bralower, T.J. (Eds.), *Proc. ODP, Sci. Results*, 154: College Station, TX (Ocean Drilling Program), 83–99.
- Baldauf, J.G., and Barron, J.A., 1991. Diatom biostratigraphy: Kerguelen Plateau and Prydz Bay regions of the Southern Ocean. In Barron, J., Larsen, B., et al., *Proc. ODP, Sci. Results*, 119: College Station, TX (Ocean Drilling Program), 547–598.
- Barron, J.A., 1992. Neogene diatom datum levels in the equatorial and North Pacific. In Ishizaki, K., and Saito, T. (Eds.), *The Centenary of Japanese Micropaleontology*: Tokyo (Terra Sci. Publ.), 413–425.
- Berggren, W.A., Hilgen, F.J., Langereis, C.G., Kent, D.V., Obradovich, J.D., Raffi, I., Raymo, M.E., and Shackleton, N.J., 1995a. Late Neogene chronology: new perspectives in high-resolution stratigraphy. *Geol. Soc. Am. Bull.*, 107:1272–1287.
- Berggren, W.A., Kent, D.V., Swisher, C.C., III, and Aubry, M.-P., 1995b. A revised Cenozoic geochronology and chronostratigraphy. In Berggren, W.A., Kent, D.V., Aubry, M.-P., and Hardenbol, J. (Eds.), *Geochronology, Time Scales and Global Stratigraphic Correlation*. Spec. Publ.—SEPM (Soc. Sediment. Geol.), 54:129–212.
- Cande, S.C., and Kent, D.V., 1995. Revised calibration of the geomagnetic polarity timescale for the Late Cretaceous and Cenozoic. *J. Geophys. Res.*, 100:6093–6095.
- Caulet, J.-P., 1991. Radiolarians from the Kerguelen Plateau, Leg 119. In Barron, J., Larsen, B., et al., *Proc. ODP, Sci. Results*, 119: College Station, TX (Ocean Drilling Program), 513–546.
- Chen, P.-H., 1975. Antarctic radiolaria. In Hayes, D.E., Frakes, L.A., et al., *Init. Repts. DSDP*, 28: Washington (U.S. Govt. Printing Office), 437–513.
- Edbrooke, S.W., Crouch, E.M., Morgans, H.E.G., and Sykes, R., 1998. Late Eocene–Oligocene Te Kuiti Group at Mount Roskill, Auckland, New Zealand. *N. Z. J. Geol. Geophys.*, 41:85–93.
- Edwards, A.R., and Perch-Nielsen, K., 1975. Calcareous nannofossils from the southern southwest Pacific, DSDP Leg 29. In Kennett, J.P., Houtz, R.E., et al., *Init. Repts. DSDP*, 29: Washington (U.S. Govt. Printing Office), 469–539.
- Exon, N.F., Kennett, J.P., and Malone, M.J. (Eds.), in press. *Cenozoic Palaeoceanography and Tectonics in the Expanding Tasmanian Seaway*. Geophys. Monogr.
- Exon, N.F., Kennett, J.P., Malone, M.J., et al., 2001. *Proc. ODP, Init. Repts.*, 189 [CD-ROM]. Available from: Ocean Drilling Program, Texas A&M University, College Station TX 77845-9547, USA.
- Florindo, F., Bohaty, S.M., Erwin, P.S., Richter, C., Roberts, A.P., Whalen, P.A., and Whitehead, J.M., 2003. Magnetobiostratigraphic chronology and palaeoenviron-

- mental history of Cenozoic sequences from ODP Sites 1165 and 1166, Prydz Bay, Antarctica. *Palaeogeogr., Palaeoclimatol., Palaeoecol.*, 198:69–100.
- Fuller, M., and Touchard, Y., in press. On the magnetostratigraphy of the East Tasman Plateau, timing of the opening of the Tasmanian Gateway and paleoenvironmental changes: results from ODP Leg 189 Site 1172. In Exon, N.F., Kennett, J.P., and Malone, M.J. (Eds.), *Cenozoic Palaeoceanography and Tectonics in the Expanding Tasmanian Seaway*. Geophys. Monogr.
- Gartner, S., 1977. Calcareous nannofossil biostratigraphy and revised zonation of the Pleistocene. *Mar. Micropaleontol.*, 2:1–25.
- Gersonde, R., and Bárcena, M.A., 1998. Revision of the Late Pliocene–Pleistocene diatom biostratigraphy for the northern belt of the Southern Ocean. *Micropaleontology*, 44:84–98.
- Gersonde, R., and Burckle, L.H., 1990. Neogene diatom biostratigraphy of ODP Leg 113, Weddell Sea (Antarctic Ocean). In Barker, P.F., Kennett, J.P., et al., *Proc. ODP, Sci. Results*, 113: College Station, TX (Ocean Drilling Program), 761–789.
- Gersonde, R., Spiess, V., Flores, J.A., Hagan, R., and Kuhn, G., 1998. The sediments of Gunnerus Ridge and Kainan Maru Seamount (Indian sector of the Southern Ocean). *Deep-Sea Res.*, 45:1515–1540.
- Harwood, D.M., and Maruyama, T., 1992. Middle Eocene to Pleistocene diatom biostratigraphy of Southern Ocean sediments from the Kerguelen Plateau, Leg 120. In Wise, S.W., Jr., Schlich, R., et al., *Proc. ODP, Sci. Results*, 120: College Station, TX (Ocean Drilling Program), 683–733.
- Hannah, M.J., Cita, M.B., Coccioni, R., and Monechi, S., 1997. The Eocene/Oligocene boundary at 70° South, McMurdo Sound, Antarctica. *Terra Antart.*, 4:79–87.
- Hollis, C.J., 1993. Latest Cretaceous to late Paleocene radiolarian biostratigraphy: a new zonation from the New Zealand region. *Mar. Micropaleontol.*, 21:295–327.
- Imbrie, J., Hays, J.D., Martinson, D.G., McIntyre, A., Mix, A.C., Morley, J.J., Pisias, N.G., Prell, W.L., and Shackleton, N.J., 1984. The orbital theory of Pleistocene climate: support from a revised chronology of the marine $\delta^{18}\text{O}$ record. In Berger, A., Imbrie, J., Hays, J., Kukla, G., and Saltzman, B. (Eds.), *Milankovitch and Climate* (Pt. 1): Hingham, MA (D. Riedel Publ. Co.), 269–305.
- Jenkins, D.G., 1985. Southern mid-latitude Paleocene to Holocene planktic foraminifera. In Bolli, H.M., Saunders, J.B., and Perch-Nielsen, K. (Eds.), *Plankton Stratigraphy*: Cambridge (Cambridge Univ. Press), 263–282.
- Jenkins, D.G., 1993a. Cenozoic southern mid- and high-latitude biostratigraphy and chronostratigraphy based on planktonic foraminifera. In Kennett, J.P., and Warnke, D.A. (Eds.), *The Antarctic Paleoenvironment: a Perspective on Global Change*. Antarct. Res. Ser., 60:125–144.
- Jenkins, D.G., 1993b. The evolution of the Cenozoic Southern high- and mid-latitude planktonic foraminiferal faunas. In Kennett, J.P., and Warnke, D.A. (Eds.), *The Antarctic Paleoenvironment: a Perspective on Global Change*. Antarct. Res. Ser., 60:175–194.
- Lazarus, D., 1992. Antarctic Neogene radiolarians from the Kerguelen Plateau, Legs 119 and 120. In Wise, S.W., Jr., Schlich, R., et al., *Proc. ODP, Sci. Results*, 120: College Station, TX (Ocean Drilling Program), 785–809.
- Levy, R.H., and Harwood, D.M., 2000. Tertiary marine palynomorphs from the McMurdo Sound erratics, Antarctica. In Stilwell, J.D., and Feldmann, R.M. (Eds.), *Paleobiology and Paleoenvironments of Eocene Rocks, McMurdo Sound, East Antarctica*. Antarct. Res. Ser., 76:183–242.
- Mao, S., and Mohr, B.A.R., 1995. Middle Eocene dinocysts from Bruce Bank (Scotia Sea, Antarctica) and their palaeoenvironmental and palaeogeographic implications. *Rev. Palaeobot. Palynol.*, 86:235–263.
- Martini, E., 1971. Standard Tertiary and Quaternary calcareous nannoplankton zonation. In Farinacci, A. (Ed.), *Proc. 2nd Int. Conf. Planktonic Microfossils Roma*: Rome (Ed. Tecnosci.), 2:739–785.

- Martinson, D.G., Pisias, N.G., Hays, J.D., Imbrie, J., Moore, T.C., Jr., and Shackleton, N.J., 1987. Age dating and the orbital theory of the ice ages: development of a high-resolution 0 to 300,000-year chronostratigraphy. *Quat. Res.*, 27:1–29.
- McGonigal, K.L., in press. Quantitative Miocene calcareous nannofossil biostratigraphy from the Tasmanian Gateway. In Exon, N.F., Kennett, J.P., and Malone, M.J. (Eds.), *Cenozoic Palaeoceanography and Tectonics in the Expanding Tasmanian Seaway*. Geophys. Monogr.
- Nishimura, A., 1987. Cenozoic radiolaria in the western North Atlantic, Site 603, Leg 93 of the Deep Sea Drilling Project. In van Hinte, J.E., Wise, S.W., Jr., et al., *Init. Repts. DSDP*, 93 (Pt. 2): Washington (U.S. Govt. Printing Office), 713–737.
- Nürnberg, D., Brughmans, N., Schönfeld, J., Ninnemann, U., and Dullo, U., in press. Paleo-export production, terrigenous flux, and sea-surface temperatures around Tasmania—implications for glacial/inglacial changes in the Subtropical Convergence Zone (ODP Leg 189). In Exon, N.F., Kennett, J.P., and Malone, M.J. (Eds.), *Cenozoic Palaeoceanography and Tectonics in the Expanding Tasmanian Seaway*. Geophys. Monogr.
- Okada, H., and Bukry, D., 1980. Supplementary modification and introduction of code numbers to the low-latitude coccolith biostratigraphic zonation (Bukry, 1973; 1975). *Mar. Micropaleontol.*, 5:321–325.
- Paillard, D., Labeyrie, L., and Yiou, P., 1996. Macintosh program performs time-series analysis. *Eos, Trans. Am. Geophys. Union*, 77:379.
- Pfuhl, H.A., McCave, I.N., Schellenberg, S.A., and Ferretti, P., in press. Changes in Southern Ocean circulation in late Oligocene to early Miocene time. In Exon, N.F., Kennett, J.P., and Malone, M.J. (Eds.), *Cenozoic Palaeoceanography and Tectonics in the Expanding Tasmanian Seaway*. Am. Geophys. Union, Geophys. Monogr.
- Prell, W.L., Imbrie, J., Martinson, D.G., Morley, J.J., Pisias, N.G., Shackleton, N.J., and Streeter, H.F., 1986. Graphic correlation of oxygen isotope stratigraphy: application to the late Quaternary. *Paleoceanography*, 1:137–162.
- Raffi, I., Backman, J., and Rio, D., 1998. Evolutionary trends of calcareous nannofossils in the late Neogene. *Mar. Micropaleontol.*, 35:17–41.
- Roberts, A.P., Bicknell, S.J., Byatt, J., Bohaty, S.M., Florindo, F., and Harwood, D.M., 2003. Magnetostratigraphic calibration of Southern Ocean diatom datums from the Eocene–Oligocene of Kerguelen Plateau (Ocean Drilling Program Sites 744 and 748). *Palaeogeogr., Palaeoclimatol., Palaeoecol.*, 198:145–168.
- Röhl, U., Brinkhuis, H., Sluijs, A., and Fuller, M., in press a. On the search for the Paleocene/Eocene boundary in the Southern Ocean: exploring ODP Leg 189 Holes 1171D and 1172D, Tasman Sea. In Exon, N.F., Kennett, J.P., and Malone, M.J. (Eds.), *Cenozoic Palaeoceanography and Tectonics in the Expanding Tasmanian Seaway*. Geophys. Monogr.
- Röhl, U., Brinkhuis, H., Stickley, C.E., Fuller, M., Schellenberg, S.A., Wefer, G., and Williams, G.L., in press b. Sea level and astronomically induced environmental changes in middle and late Eocene sediments from the east Tasman Plateau. In Exon, N.F., Kennett, J.P., and Malone, M.J. (Eds.), *Cenozoic Palaeoceanography and Tectonics in the Expanding Tasmanian Seaway*. Geophys. Monogr.
- Sanfilippo, A., and Nigrini, C., 1998. Code numbers for Cenozoic low latitude radiolarian biostratigraphic zones and GPTS conversion tables. *Mar. Micropaleontol.*, 33:109–156.
- Schellenberg, S.A., Brinkhuis, H., Stickley, C.E., Fuller, M., Kyte, F.T., and Williams, G.L., in press. The Cretaceous/Paleogene transition on the east Tasman Plateau, southwestern Pacific. In Exon, N.F., Kennett, J.P., and Malone, M.J. (Eds.), *Cenozoic Palaeoceanography and Tectonics in the Expanding Tasmanian Seaway*. Geophys. Monogr.
- Shackleton, N.J., Berger, A., and Peltier, W.A., 1990. An alternative astronomical calibration of the lower Pleistocene timescale based on ODP Site 677. *Trans. R. Soc. Edinburgh: Earth Sci.*, 81:251–261.

- Shipboard Scientific Party, 1999a. Explanatory notes. In Gersonde, R., Hodell, D.A., Blum, P., et al., *Proc. ODP, Init. Repts.*, 177, 1–57 [CD-ROM]. Available from: Ocean Drilling Program, Texas A&M University, College Station, TX 77845-9547, U.S.A.
- Shipboard Scientific Party, 1999b. Explanatory notes. In Carter, R.M., McCave, I.N., Richter, C., Carter, L., et al., *Proc. ODP, Init. Repts.*, 181, 1–65. [CD-ROM]. Available from: Ocean Drilling Program, Texas A&M University, College Station, TX 77845-9547, U.S.A.
- Shipboard Scientific Party, 2001a. Explanatory notes. In Exxon, N.F., Kennett, J.P., Malone, M.J., et al., *Proc. ODP, Init. Repts.*, 189, 1–59 [CD-ROM]. Available from: Ocean Drilling Program, Texas A&M University, College Station TX 77845-9547, USA.
- Shipboard Scientific Party, 2001b. Site 1168. In Exxon, N.F., Kennett, J.P., Malone, M.J., et al., *Proc. ODP, Init. Repts.*, 189, 1–170 [CD-ROM]. Available from: Ocean Drilling Program, Texas A&M University, College Station TX 77845-9547, USA.
- Shipboard Scientific Party, 2001c. Site 1169. In Exxon, N.F., Kennett, J.P., Malone, M.J., et al., *Proc. ODP, Init. Repts.*, 189, 1–64 [CD-ROM]. Available from: Ocean Drilling Program, Texas A&M University, College Station TX 77845-9547, USA.
- Shipboard Scientific Party, 2001d. Site 1170. In Exxon, N.F., Kennett, J.P., Malone, M.J., et al., *Proc. ODP, Init. Repts.*, 189, 1–167 [CD-ROM]. Available from: Ocean Drilling Program, Texas A&M University, College Station TX 77845-9547, USA.
- Shipboard Scientific Party, 2001e. Site 1171. In Exxon, N.F., Kennett, J.P., Malone, M.J., et al., *Proc. ODP, Init. Repts.*, 189, 1–176 [CD-ROM]. Available from: Ocean Drilling Program, Texas A&M University, College Station TX 77845-9547, USA.
- Shipboard Scientific Party, 2001f. Site 1172. In Exxon, N.F., Kennett, J.P., Malone, M.J., et al., *Proc. ODP, Init. Repts.*, 189, 1–149 [CD-ROM]. Available from: Ocean Drilling Program, Texas A&M University, College Station TX 77845-9547, USA.
- Stott, L.D., and Kennett, J.P., 1990. Antarctic Paleogene planktonic foraminifer biostratigraphy: ODP Leg 113, Sites 689 and 690. In Barker, P.F., Kennett, J.P., et al., *Proc. ODP, Sci. Results*, 113: College Station, TX (Ocean Drilling Program), 549–569.
- Takemura, A., 1992. Radiolarian Paleogene biostratigraphy in the southern Indian Ocean, Leg 120. In Wise, S.W., Jr., Shlitch, R., et al., *Proc. ODP, Sci. Results*, 120: College Station, TX (Ocean Drilling Program), 735–756.
- Takemura, A., and Ling, H.Y., 1997. Eocene and Oligocene radiolarian biostratigraphy from the Southern Ocean: correlation of ODP Legs 114 (Atlantic Ocean) and 120 (Indian Ocean). *Mar. Micropaleontol.*, 30:97–116.
- Tiedemann, R., Sarnthein, M., and Shackleton, N.J., 1994. Astronomic timescale for the Pliocene Atlantic $\delta^{18}\text{O}$ and dust flux records of Ocean Drilling Program Site 659. *Paleoceanography*, 9:619–638.
- Touchard, Y., and Fuller, M., in press. Magnetostratigraphy of the late Eocene–Oligocene record at Hole 1168A, Leg 189: opening of the Tasmanian Gateway. In Exxon, N.F., Kennett, J.P., and Malone, M.J. (Eds.), *Cenozoic Palaeoceanography and Tectonics in the Expanding Tasmanian Seaway*. Geophys. Monogr.
- Truswell, E.M., 1997. Palynomorph assemblages from marine Eocene sediments on the West Tasmanian continental margin and the South Tasman Rise. *Aust. J. Earth Sci.*, 44:633–654.
- Wei, W., and Wise, S.W., Jr., 1992. Eocene–Oligocene calcareous nannofossil magnetostratigraphy of the Southern Ocean. *Newsl. Stratigr.*, 26:119–132.
- Wilson, G.J., 1988. Paleocene and Eocene dinoflagellate cysts from Waipawa, Hawkes Bay, New Zealand. *N. Z. Geol. Surv. Bull.*, 57:1–96.
- Wrenn, J.H., and Hart, G.F., 1988. Paleogene dinoflagellate cyst biostratigraphy of Seymour Island, Antarctica. *Mem.—Geol. Soc. Am.*, 169:321–447.
- Zachos, J.C., Quinn, R.M., and Salamy, K., 1996. High resolution (10^4 yr) deep-sea foraminiferal stable isotope records of the Eocene–Oligocene climate transition. *Paleoceanography*, 11:251–266.
- Zielinski, U., and Gersonde, R., 2002. Plio–Pleistocene diatom biostratigraphy from ODP Leg 177, Atlantic sector of the Southern Ocean. *Mar. Micropaleontol.*, 45:225–268.

CHAPTER NOTES

- N1. Huber, M., Brinkhuis, H., Stickley, C.E., Döös, K., Sluijs, A., Warnaar, J., Schellenberg, S.A., and Williams, G.L., submitted. Eocene circulation of the Southern Ocean: was Antarctica kept warm by subtropical waters? *Paleoceanography*.
- N2. Stickley, C.E., Brinkhuis, H., Schellenberg, S.A., Sluijs, A., Röhl, U., Fuller, M., Grauert, M., Huber, M., Warnaar, J., and Williams, G.L., submitted. Timing and nature of the deepening of the Tasmanian Gateway. *Paleoceanography*.

Figure F1. Location of Leg 189 drill sites.

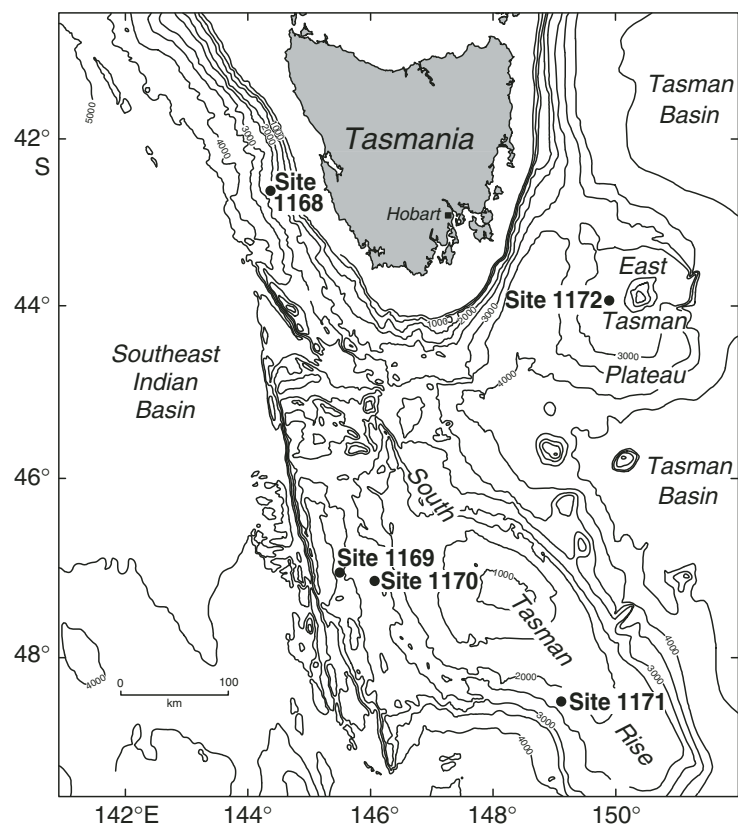


Figure F2. Age-depth plot, Site 1168. Core disturbance is shown in the right-hand column on an arbitrary scale of 1–4 (4 being the most disturbed intervals). All datums indicated in Table T1, p. 39, Table T2, p. 44, Table T3, p. 49, and Table T4, p. 57, (including alternative datums) are plotted to show scatter. TD = total depth.

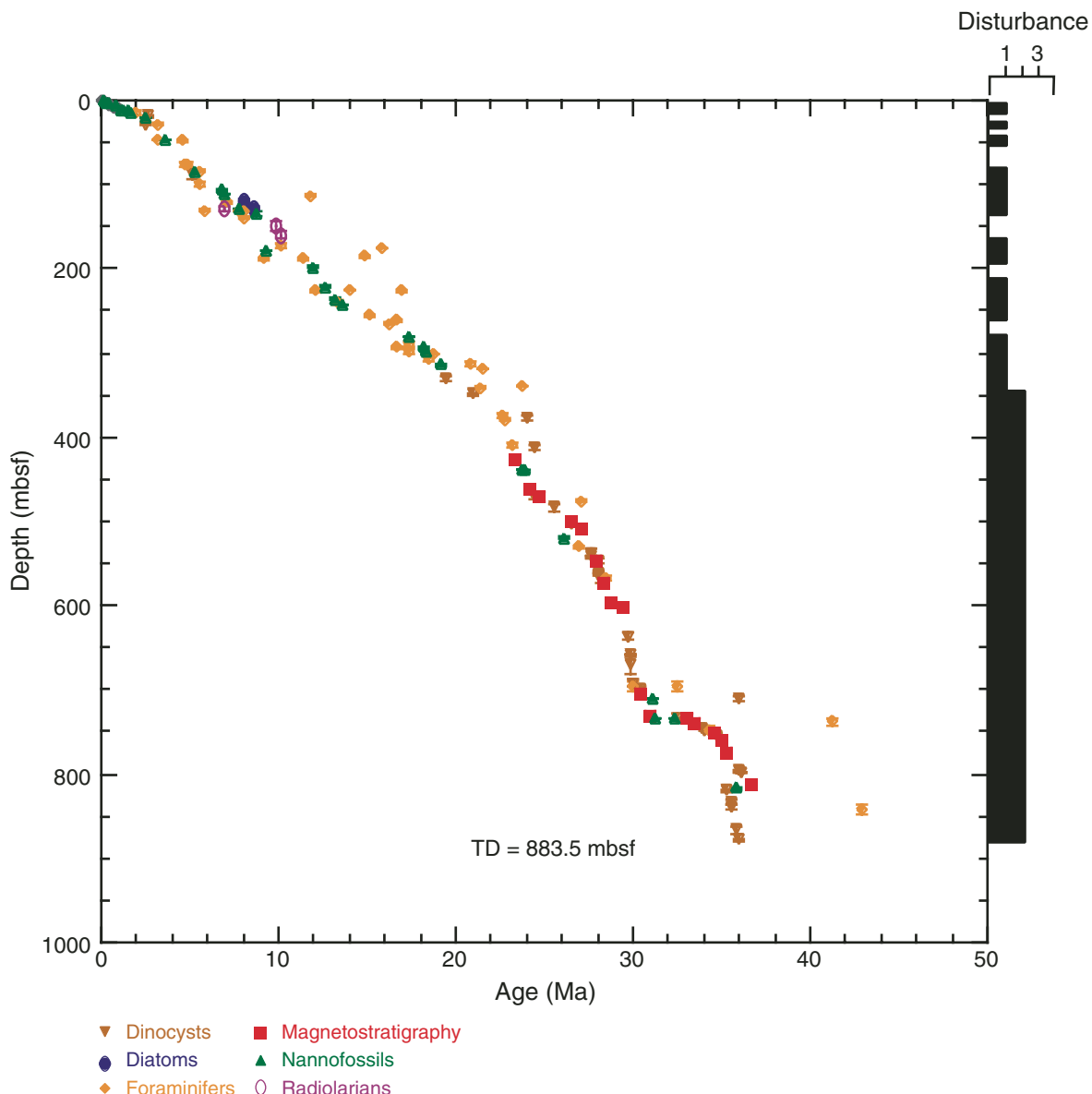


Figure F3. Age-depth plot, Site 1168, Paleogene. Core disturbance is shown in the right-hand column on an arbitrary scale of 1–4 (4 being the most disturbed intervals). All datums indicated in Table T1, p. 39, Table T2, p. 44, Table T3, p. 49, and Table T4, p. 57, (including alternative datums) are plotted to show scatter.

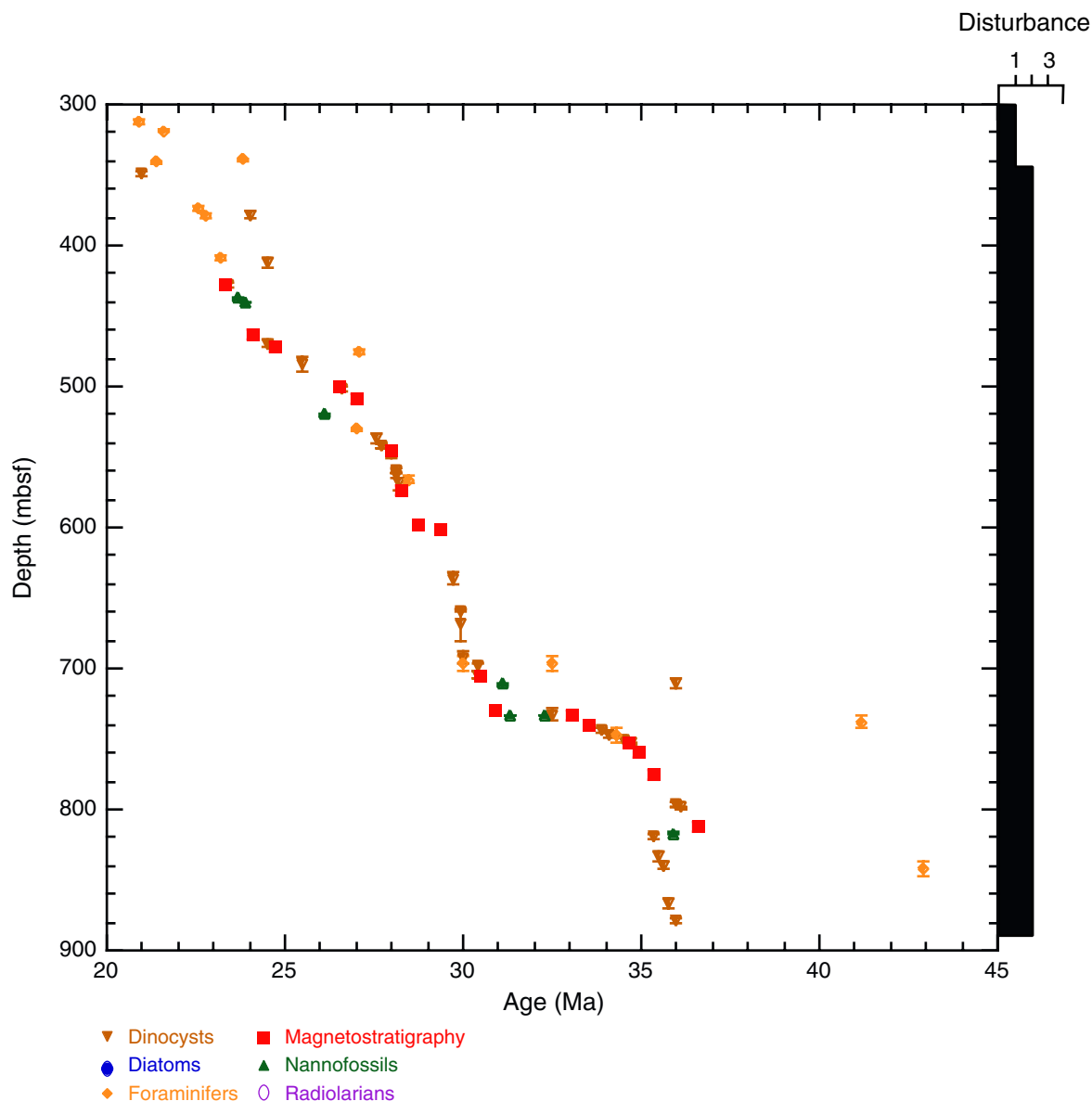


Figure F4. Age-depth plot, Site 1168, Neogene and Quaternary. Core disturbance is shown in the right-hand column on an arbitrary scale of 1–4 (4 being the most disturbed intervals). All datums indicated in Table T1, p. 39, Table T2, p. 44, Table T3, p. 49, and Table T4, p. 57, (including alternative datums) are plotted to show scatter.

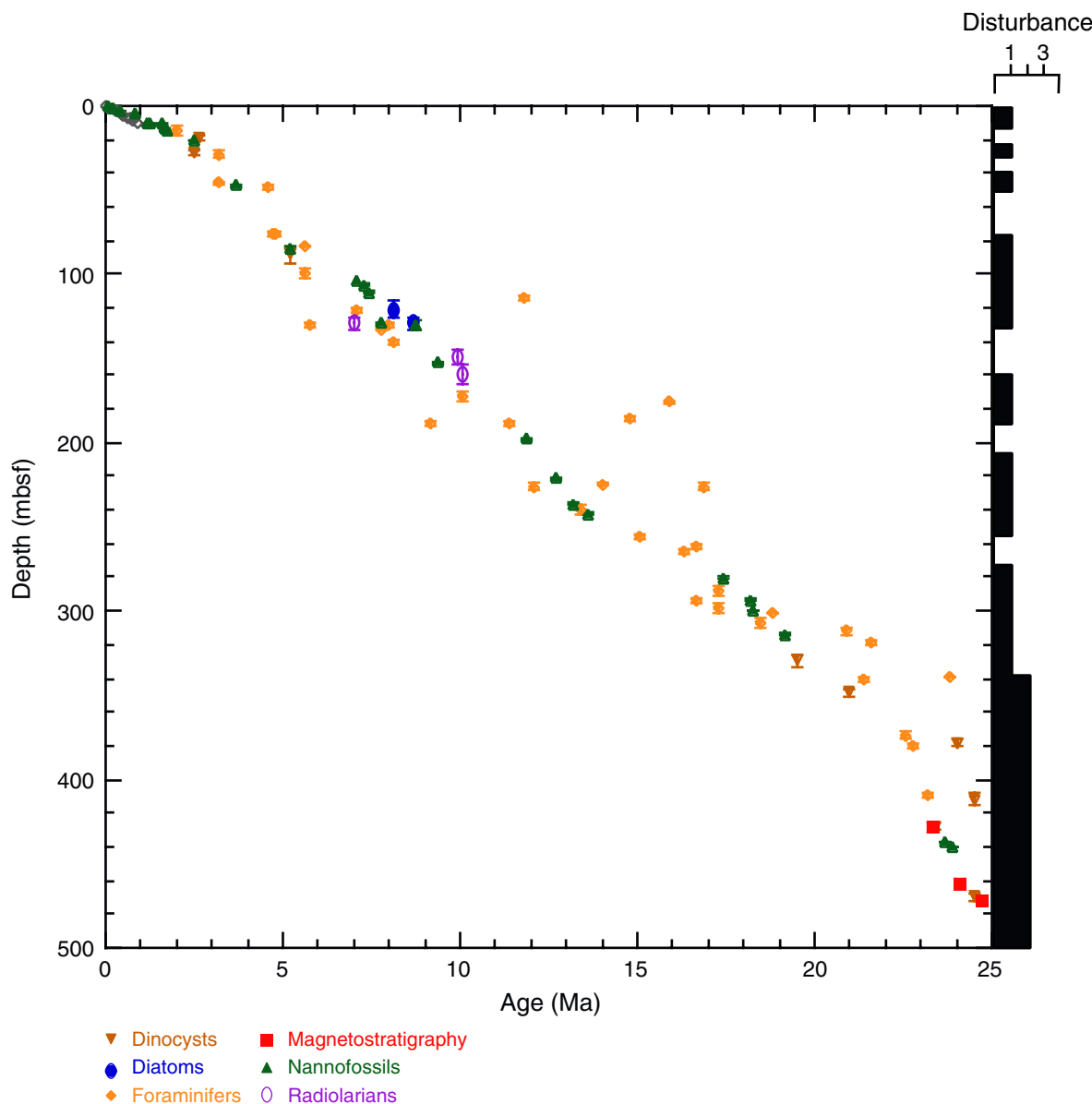


Figure F5. Age-depth plot, Site 1170. Core disturbance is shown in the right-hand column on an arbitrary scale of 1–4 (4 being the most disturbed intervals). All datums indicated in Table T1, p. 39, Table T2, p. 44, Table T3, p. 49, and Table T4, p. 57, (including alternative datums) are plotted to show scatter. TD = total depth.

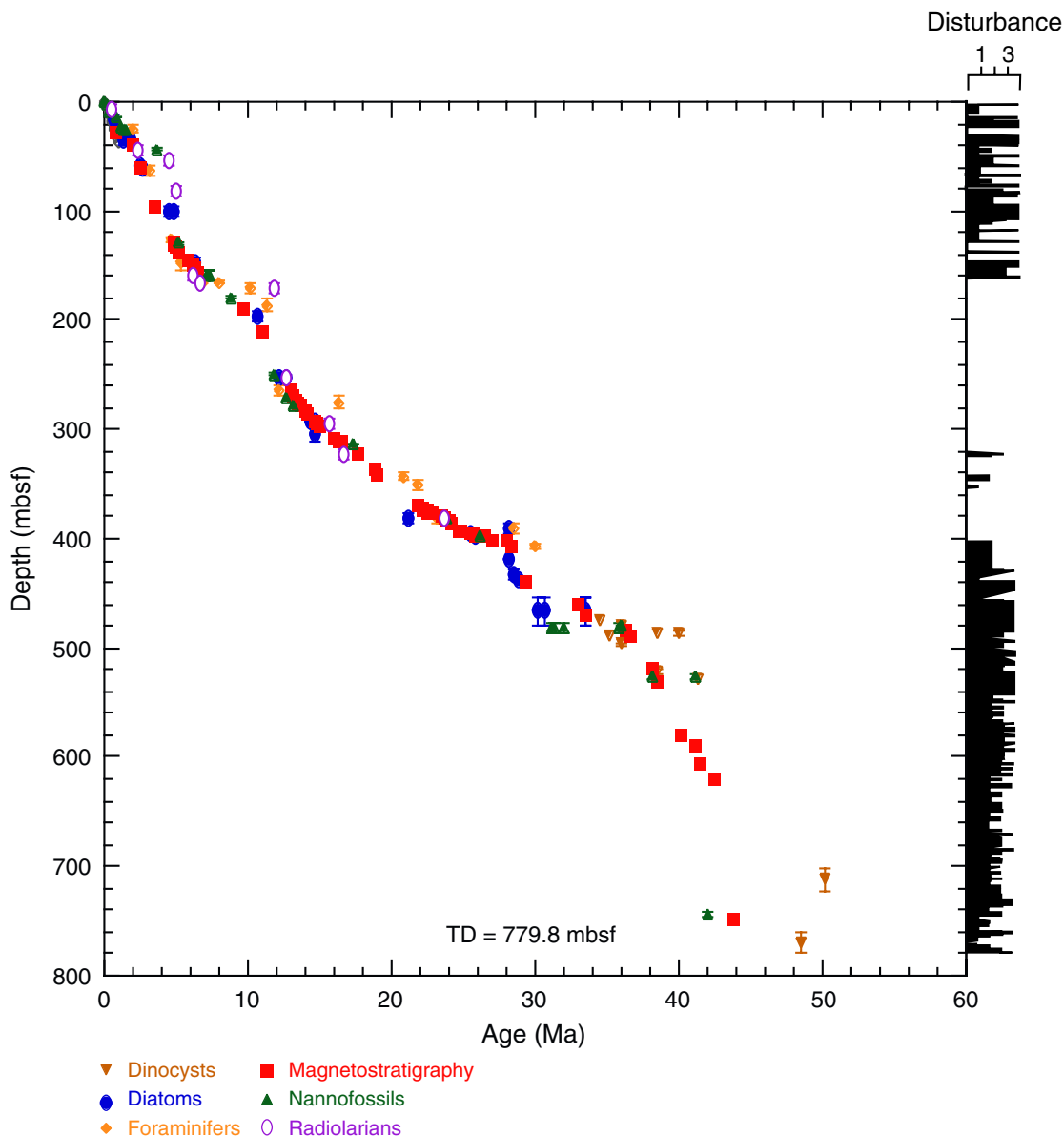


Figure F6. Age-depth plot, Site 1170, Paleogene. Core disturbance is shown in the right-hand column on an arbitrary scale of 1–4 (4 being the most disturbed intervals). All datums indicated in Table T1, p. 39, Table T2, p. 44, Table T3, p. 49, and Table T4, p. 57, (including alternative datums) are plotted to show scatter.

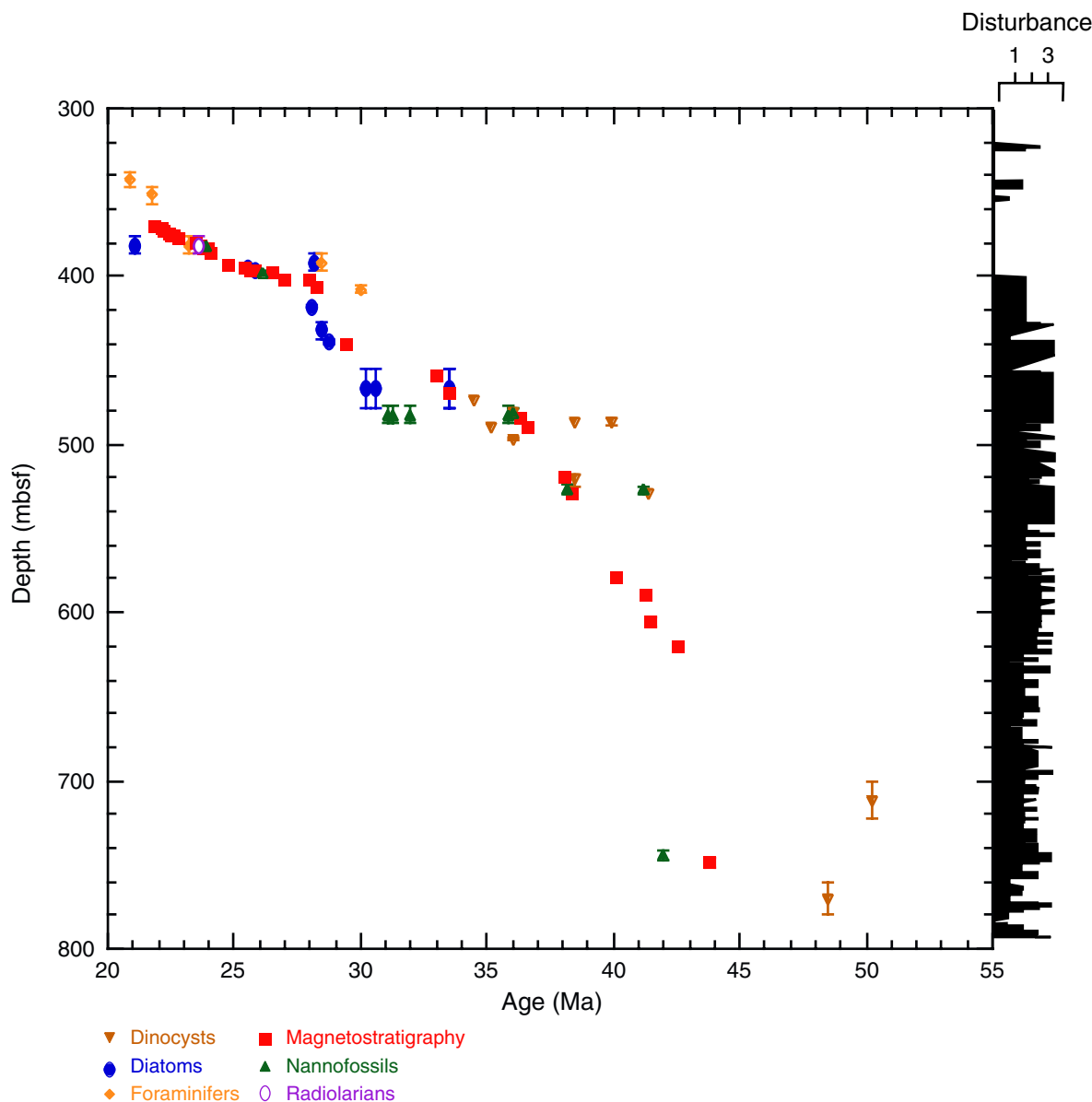


Figure F7. Age-depth plot, Site 1170, Neogene and Quaternary. Core disturbance is shown in the right-hand column on an arbitrary scale of 1–4 (4 being the most disturbed intervals). All datums indicated in Table T1, p. 39, Table T2, p. 44, Table T3, p. 49, and Table T4, p. 57, (including alternative datums) are plotted to show scatter.

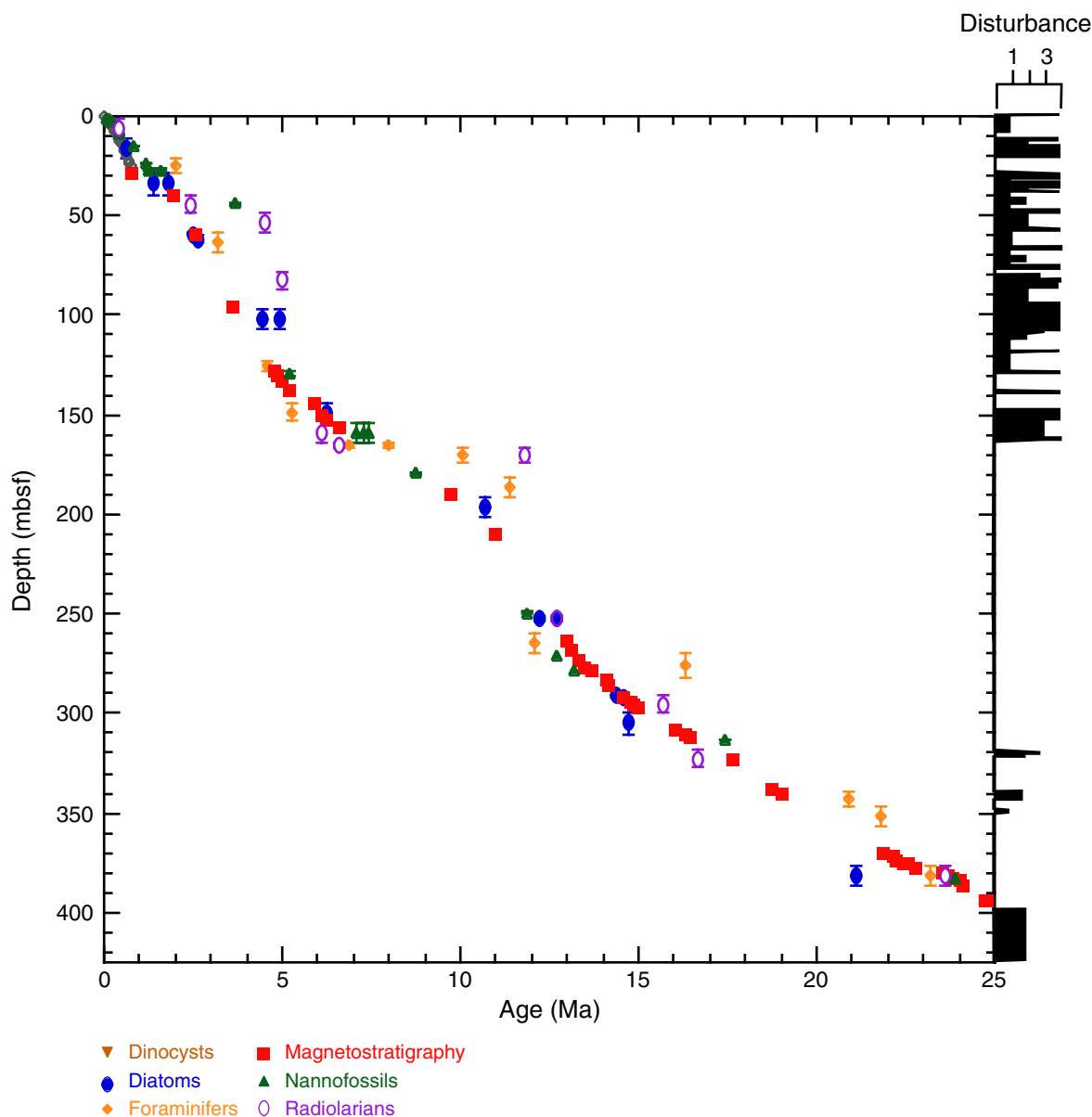


Figure F8. Age-depth plot, Site 1171. Core disturbance is shown in the right-hand column on an arbitrary scale of 1–4 (4 being the most disturbed intervals). All datums indicated in Table T1, p. 39, Table T2, p. 44, Table T3, p. 49, and Table T4, p. 57, (including alternative datums) are plotted to show scatter. TD = total depth.

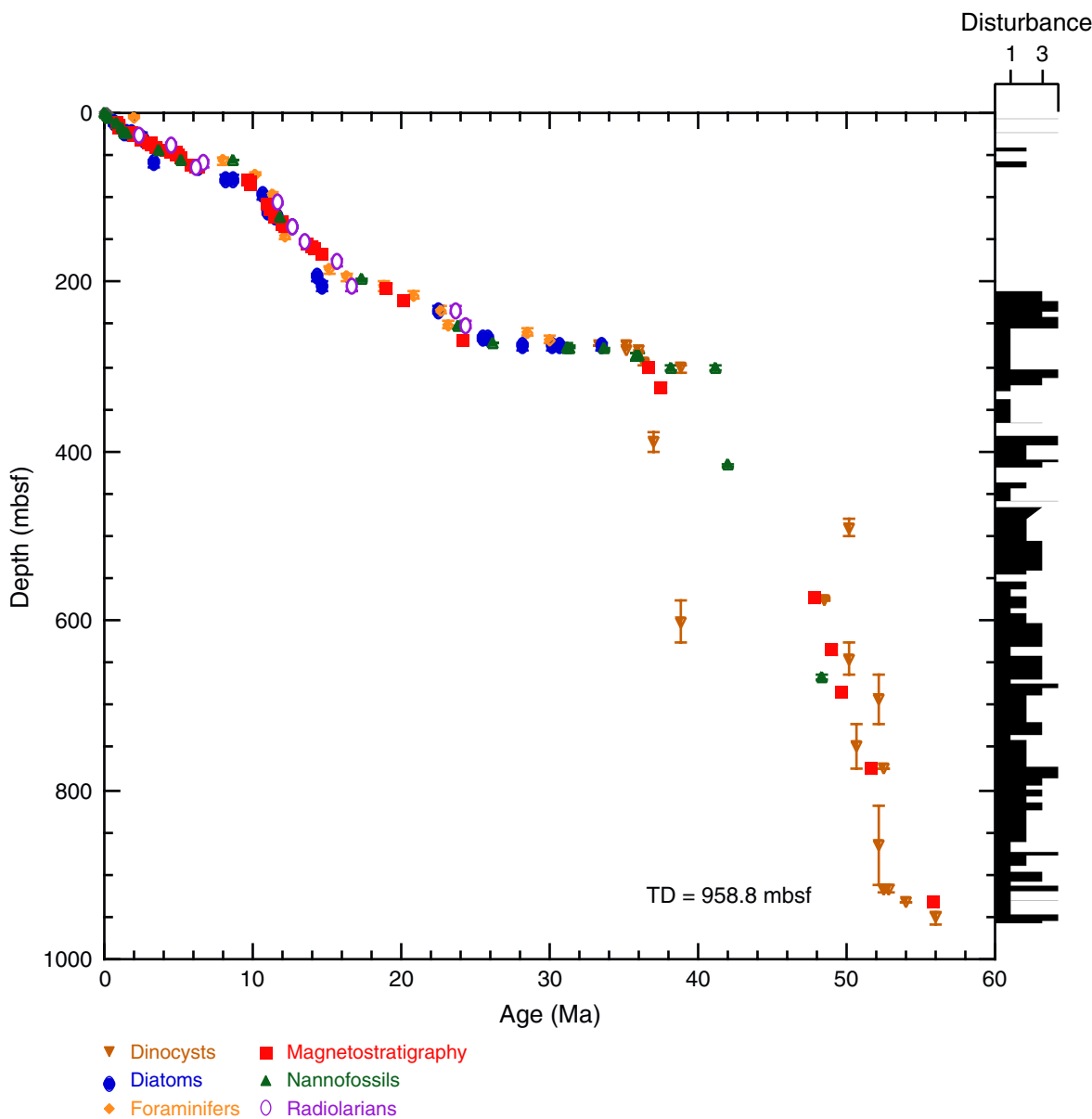


Figure F9. Age-depth plot, Site 1171, Paleogene. Core disturbance is shown in the right-hand column on an arbitrary scale of 1–4 (4 being the most disturbed intervals). All datums indicated in Table T1, p. 39, Table T2, p. 44, Table T3, p. 49, and Table T4, p. 57, (including alternative datums) are plotted to show scatter.

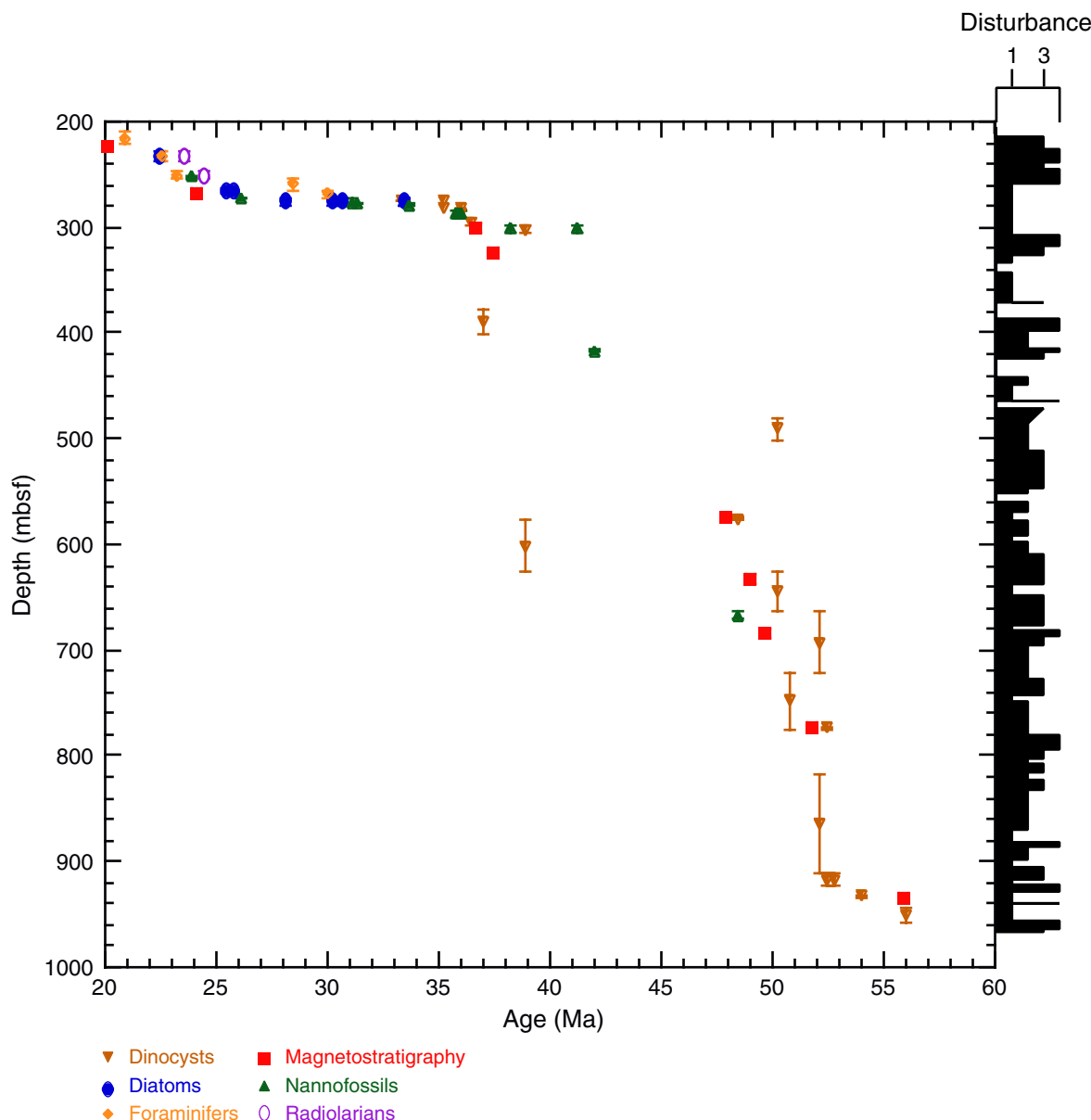


Figure F10. Age-depth plot, Site 1171, Neogene and Quaternary. Core disturbance is shown in the right-hand column on an arbitrary scale of 1–4 (4 being the most disturbed intervals). All datums indicated in Table T1, p. 39, Table T2, p. 44, Table T3, p. 49, and Table T4, p. 57, (including alternative datums) are plotted to show scatter.

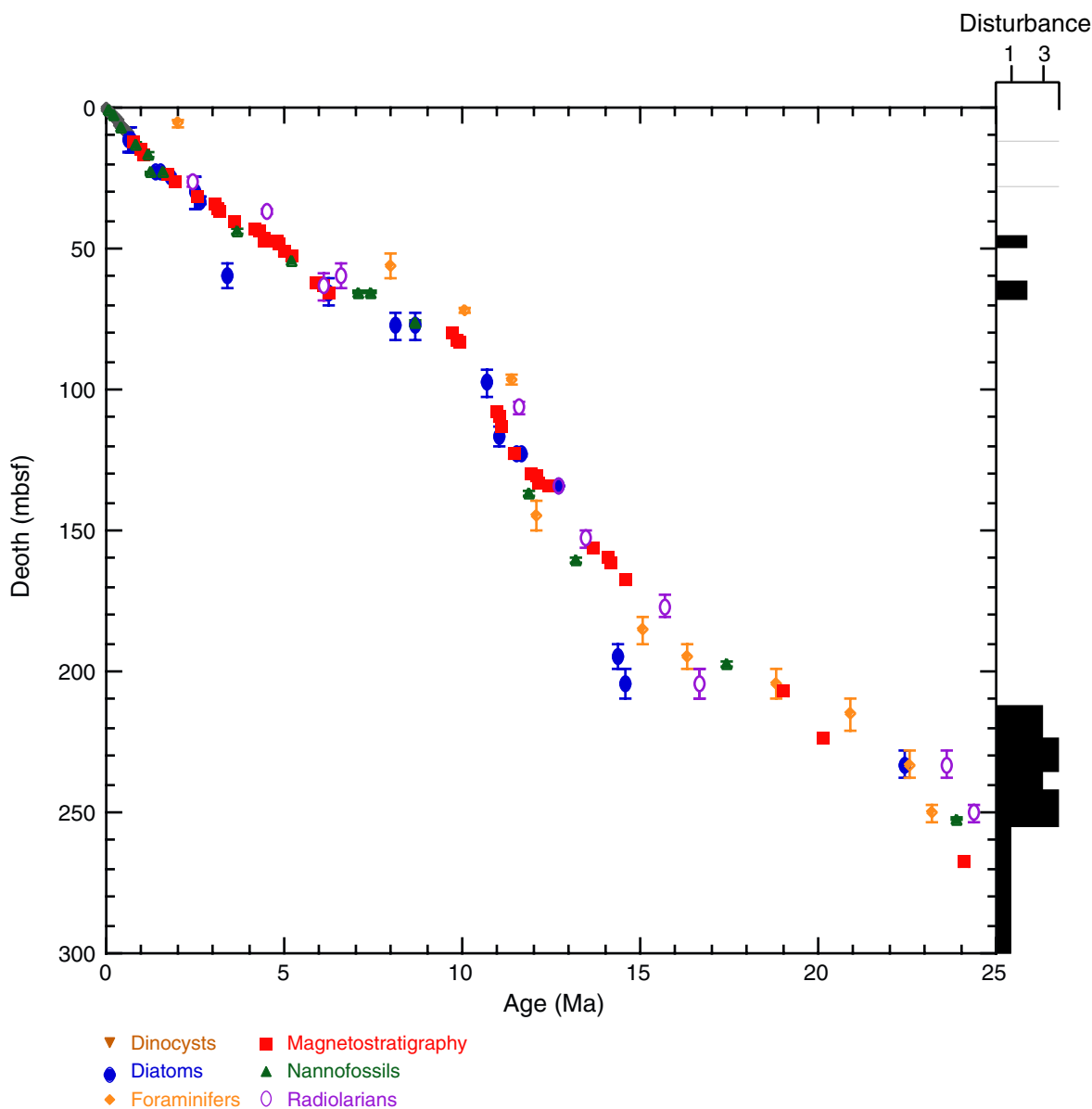


Figure F11. Age-depth plot, Site 1172. Core disturbance is shown in the right-hand column on an arbitrary scale of 1–4 (4 being the most disturbed intervals). All datums indicated in Table T1, p. 39, Table T2, p. 44, Table T3, p. 49, and Table T4, p. 57, (including alternative datums) are plotted to show scatter. TD = total depth.

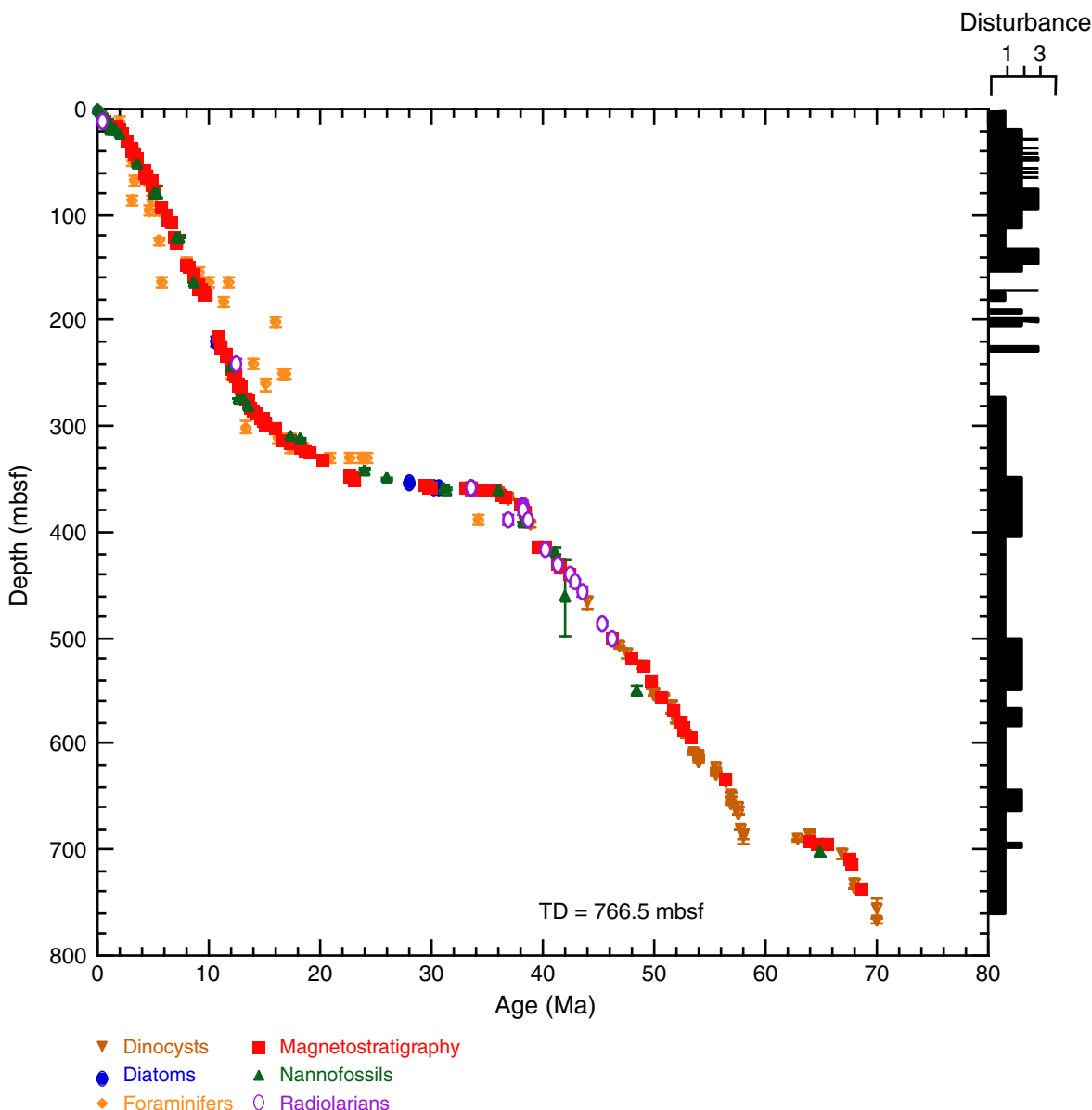


Figure F12. Age-depth plot, Site 1172, Maastrichtian and Paleogene. Core disturbance is shown in the right-hand column on an arbitrary scale of 1–4 (4 being the most disturbed intervals). All datums indicated in Table T1, p. 39, Table T2, p. 44, Table T3, p. 49, and Table T4, p. 57, (including alternative datums) are plotted to show scatter.

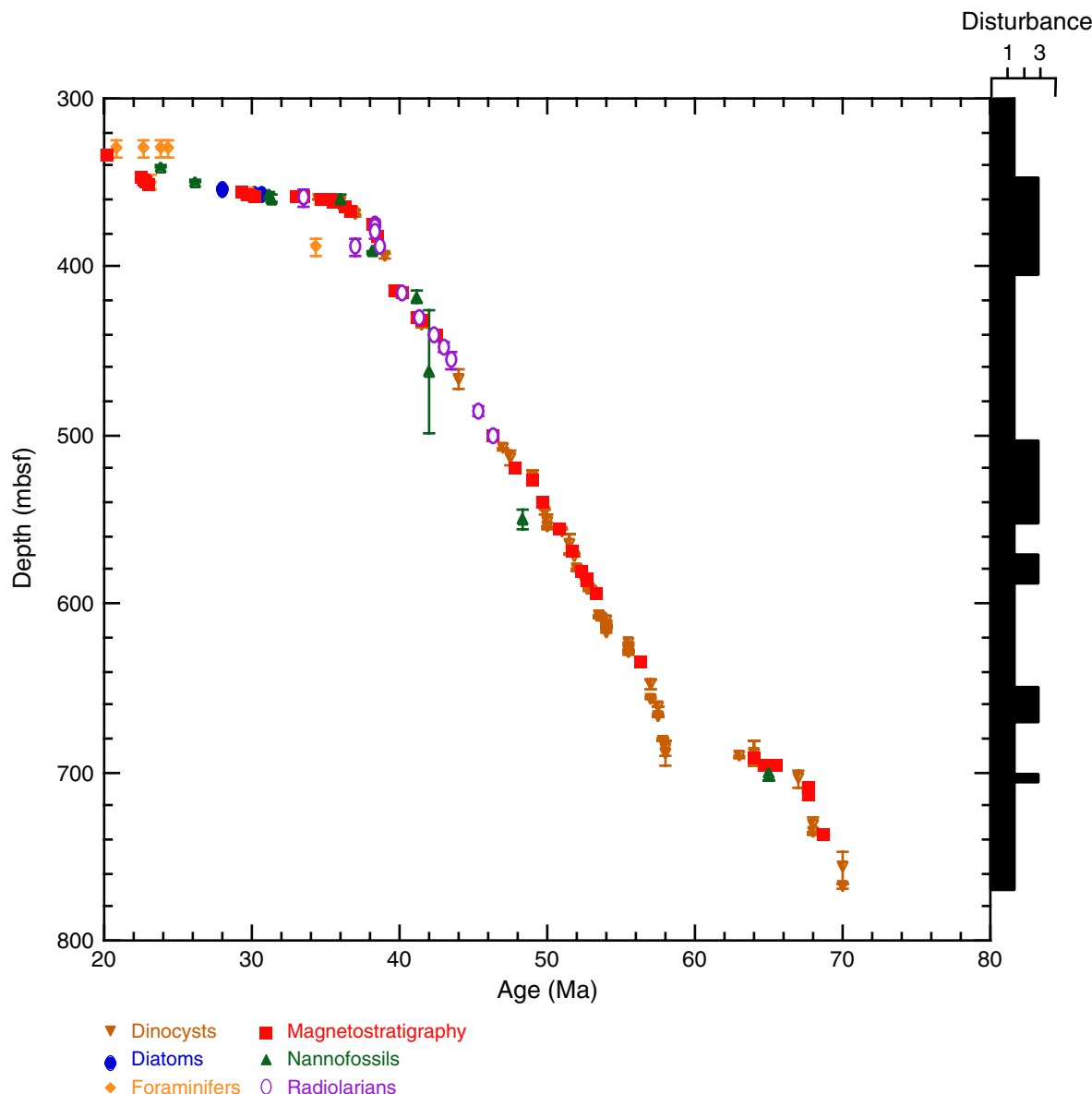


Figure F13. Age-depth plot, Site 1172, Neogene and Quaternary. Core disturbance is shown in the right-hand column on an arbitrary scale of 1–4 (4 being the most disturbed intervals). All datums indicated in Table T1, p. 39, Table T2, p. 44, Table T3, p. 49, and Table T4, p. 57, (including alternative datums) are plotted to show scatter.

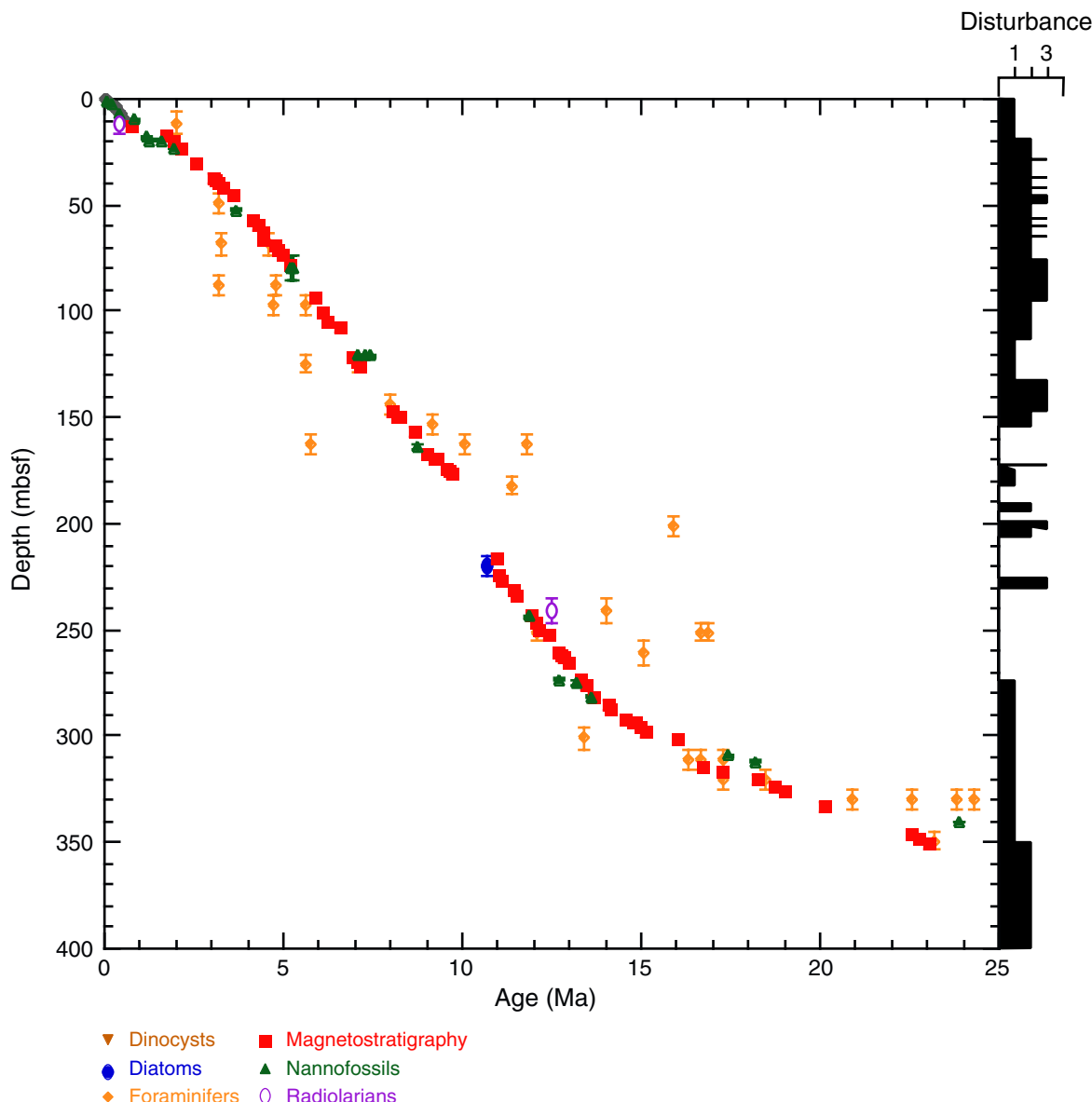


Table T1. Age-depth data, Site 1168. (See table notes. Continued on next four pages.)

Source	Hole	Event	Age (Ma)	Alternate Age (Ma)	Core, section, interval (cm)		Depth (mbsf)			Depth error (m)
					Top	Bottom	Top	Bottom	Mean	
189-1168A-										
BOI	1168A	Base Holocene plateau	0.0097						0.050	0.000
BOI		MIS 2.2	0.018						0.300	0.000
N		FO <i>Emiliania huxleyi</i> acme	0.085		1H-1, 15–16	1H-1, 90–91			0.530	0.375
BOI		Maximum close to 2.2	0.0219						0.550	0.000
BOI		MIS 3.3	0.0502						0.950	0.000
BOI		MIS 4.22	0.0641						1.100	0.000
BOI		MIS 5.3	0.0964						1.300	0.000
BOI		MIS 5.51	0.1226						1.550	0.000
BOI		MIS 6.2	0.1351						1.700	0.000
BOI		MIS 6.5	0.1751						1.800	0.000
BOI		MIS 7.1	0.1931						1.900	0.000
N		FO <i>Emiliania huxleyi</i>	0.24		1H-2, 15–16	1H-2, 90–91			2.030	0.375
BOI		MIS 7.3	0.2155						2.050	0.000
BOI		MIS 7.5	0.2402						2.150	0.000
BOI		MIS 8.4	0.2657						2.350	0.000
BOI		MIS 8.5	0.2885						2.550	0.000
M	1168B	Onset C1n	XXX	0.7800					2.580	
BOI	1168A	MIS 9.1	0.31						2.800	0.000
BOI		MIS 9.3	0.331						3.050	0.000
BOI		MIS 10.2	0.341						3.250	0.000
N		LO <i>Pseudoemiliania lacunosa</i>	0.42		1H-3, 15–16	1H-3, 90–91			3.530	0.375
M	1168B	Termination C1r.1n	XXX	0.99					4.200	
BOI	1168A	MIS 11.3	0.405						4.250	0.000
BOI		MIS 12.2	0.434						4.900	0.000
BOI		MIS 12.4	0.471						5.350	0.000
M	1168B	Onset C1r.1n	XXX	1.070					5.800	
BOI	1168A	MIS 13.2	0.512						5.950	0.000
BOI		MIS 16.2	0.625						6.900	0.000
BOI		MIS 18.2	0.722						8.000	0.000
N		LO <i>Reticulofenestra asanoi</i>	0.83		2H-1, 90–91	2H-2, 15–16			8.575	0.375
BOI		MIS 20.2	0.796						8.800	0.000
BOI		MIS 22	0.872						9.650	0.000
M	1168B	Termination C2n	XXX	1.770					10.000	
BOI	1168A	MIS 24	0.920						10.150	0.000
N		FO <i>Reticulofenestra asanoi</i>	1.16		2H-3, 15–16	2H-3, 90–91			10.830	0.375
N		LO <i>Helicosphaera sellii</i>	1.26		2H-3, 15–16	2H-3, 90–91			10.830	0.375
N		LO <i>Calcidiscus macintyrei</i>	1.59		2H-3, 15–16	2H-3, 90–91			10.830	0.375
M	1168B	Onset C2n	XXX	1.95					12.200	
N	1168A	FO <i>Gephyrocapsa oceanica</i>	1.65		2H-5, 15–16	2H-5, 90–91			13.830	0.375
F		FO <i>Globorotalia truncatulinoides</i>	XXX	2.0	2H-3, 78–83	2H-CC			14.035	2.930
M	1168B	Termination C2r.1n	XXX	2.14					14.300	
N	1168A	FO <i>Gephyrocapsa caribbeanica</i>	1.72		2H-5, 90–91	2H-6, 15–16			14.955	0.750
Pliocene/Pleistocene boundary 1.77 Ma										
M	1168B	Onset C2r.1n	XXX	2.15					15.900	
M		Termination C2An.1n	XXX	2.581					18.500	
N	1168A	LO <i>Discoaster surculus</i>	2.51		3H-3, 15–16	3H-3, 90–91			20.330	0.375
M	1168B	Onset C2An.1n	XXX	3.04					24.200	

Table T1 (continued).

Source	Hole	Event	Age (Ma)	Alternate Age (Ma)	Core, section, interval (cm)		Depth (mbsf)			Depth error (m)
					Top	Bottom	Top	Bottom	Mean	
D	1168A	LO <i>Invertocysta</i> spp.	XXX	2.5	189-1168A-3H-CC	189-1168A-4H-3, 60-62	26.580	29.860	28.220	1.640
F		FO <i>Globorotalia inflata</i>	3.2		4H-1, 79-83	4H-3, 79-83	27.110	30.060	28.585	1.475
M	1168B	Termination C2An.2n	3.11						29.600	
M		Onset C2An.2n	3.22						31.100	
M		Termination C2An.3n	3.33						33.600	
M		Onset C2An.3n	3.58						42.700	
lower/upper Pliocene boundary 3.58 Ma										
F	1168A	LO <i>Globorotalia conomicoza</i>	XXX	???	5H-CC	6H-1, 80-84	45.785	46.120	45.953	0.168
N		LO <i>Reticulofenestra pseudoumbilica</i>	3.65		6H-2, 15-16	6H-2, 90-91	46.955	47.705	47.330	0.375
F		LO <i>Globorotalia phiozea</i>	4.6		6H-1, 80-84	6H-3, 80-84	46.120	49.120	47.620	1.500
M	1168B	Termination C3n.1n	XXX	4.18					48.000	
M		Onset C3n.1n	XXX	4.29					50.700	
M		Onset C3n.2n	XXX	4.48					61.500	
M		Termination C3n.4n	XXX	4.98					71.100	
F	1168A	FO <i>Globorotalia crassaformis</i>	4.7		9H-1, 80-84	9H-3, 80-84	74.620	77.620	76.120	1.500
F		FO <i>Globorotalia puncticulata</i>	4.8		9H-1, 80-84	9H-3, 80-84	74.620	77.620	76.120	1.500
M	1168B	Onset C3n.4n	XXX	5.23					79.800	
F	1168A	FO <i>Globorotalia phiozea</i>	5.6		9H-CC	10H-1, 80-84	82.870	84.120	83.495	0.625
N		LO <i>Triquetrorhabdulus rugosus</i>	5.23		10H-1, 15-16	10H-2, 15-16	83.455	84.955	84.205	0.750
D		LO <i>Reticulatosphaera actinocoronata</i>	5.2		9H-CC	10H-7, 60-62	82.870	92.910	87.890	5.020
Miocene/Pliocene boundary 5.3 Ma										
M	1168B	Termination C3An.1n	5.894						89.900	
M		Onset C3An.2n	XXX	6.567					98.970	
F	1168A	FO <i>Globorotalia sphericomicoza</i>	5.6		11H-3, 80-84	11H-CC	96.620	102.525	99.573	2.953
N		LO <i>Reticulofenestra pseudoumbilica</i> paracme top	7.1		12H-1, 15-16	12H-2, 15-16	102.45	103.95	103.200	0.750
M	1168B	Termination C3Bn	XXX	6.935	12H-3, 15-16	12H-4, 15-16			104.000	
N	1168A	FO <i>Amaurolithus delicatus</i>	7.3				105.455	106.955	106.205	0.750
M	1168B	Onset C3Bn	XXX	7.091					107.300	
N	1168A	FO <i>Amaurolithus primus</i>	7.4		12H-6, 15-16	12H-7, 15-16	109.955	111.455	110.705	0.750
F		LO <i>Globorotalia panda</i>	XXX	11.8	13X-1, 80-84	13X-3, 80-84	112.620	115.620	114.120	1.500
Dm		FO <i>Fragilariopsis reinholdii</i>	XXX	8.1	13X-CC	14X-CC	115.900	125.710	120.805	4.905
F		FO <i>Globorotalia conomicoza</i>	7.12		14X-1, 80-84	14X-3, 80-84	119.320	122.320	120.820	1.500
N		LO <i>Minylitha convallis</i>	7.8		15X-1, 15-16	15X-2, 15-16	128.255	129.755	129.005	0.750
R		FO <i>Stylacantharium aquilonarium</i>	XXX	7.0	14X-CC	15X-CC	125.710	132.855	129.283	3.573
Dm		FO <i>Actinocyclus ingens</i> var. <i>ovalis</i>	8.68		14X-CC	15X-CC	125.710	132.855	129.283	3.573
F		LO <i>Globoquadrina dehiscens</i>	XXX	5.8	15X-1, 80-84	15X-3, 80-84	128.920	131.920	130.420	1.500
F		LO <i>Paragloborotalia continuosa</i>	8.0		15X-1, 80-84	15X-3, 80-84	128.920	131.920	130.420	1.500
N		LO <i>Reticulofenestra pseudoumbilica</i> paracme bottom	8.78		15X-2, 15-16	15X-3, 15-16	129.75	131.25	130.500	0.750
F		FO <i>Globorotalia cibaoensis</i>	XXX	7.8	15X-3, 80-84	15X-CC	131.920	132.855	132.388	0.468
F		FO <i>Globorotalia juanai</i>	XXX	8.1	16X-1, 80-84	16X-3, 80-84	138.520	141.520	140.020	1.500
R		LO <i>Cyrtocapsella japonica</i>	9.9			17X-CC	144.810	154.250	149.530	4.720
N		FO <i>Mirylitha convallis</i>	9.4		17X-4, 15-16	17X-5, 15-16	151.95	153.45	152.700	0.750
R		LAO <i>Cyrtocapsella japonica</i>	XXX	10.1	17X-CC	18X-CC	154.250	164.760	159.505	5.255
F		LO <i>Paragloborotalia nympha</i>	10.1		19X-3, 80-84	19X-CC	170.320	175.175	172.748	2.427
F		LO <i>Globorotalia miozea</i>	XXX	15.9	19X-CC	20X-1, 80-84	175.175	176.920	176.048	0.873
F		LO <i>Praeorbulina glomerosa</i>	XXX	14.8	20X-CC	21X-1, 80-84	184.100	186.520	185.310	1.210
F		FO <i>Neogloboquadrina pachyderma</i>	XXX	9.2	21X-1, 80-84	21X-3, 80-84	186.520	189.520	188.020	1.500
F		LO <i>Paragloborotalia mayeri</i>	11.4		22X-1, 80-84	22X-3, 80-84	186.520	189.520	188.020	1.500

Table T1 (continued).

Source	Hole	Event	Age (Ma)	Alternate Age (Ma)	Core, section, interval (cm)		Depth (mbsf)			Depth error (m)	
					Top	Bottom	Top	Bottom	Mean		
					189-1168A-		189-1168A-				
		middle/upper Miocene boundary 11.2 Ma									
N	1168A	LO <i>Cyclicargolithus floridanus</i>	11.9		22X-2, 15–16	22X-3, 15–16	197.055	198.555	197.805	0.750	
N		LO <i>Calcidiscus premacintyrei</i>	12.7		24X-5, 15–16	24X-6, 15–16	220.755	222.255	221.505	0.750	
F		LO <i>Globorotalia peripheroronta</i>	XXX	14.0	24X-CC	25X-1, 80–84	224.185	225.020	224.603	0.417	
F		FO <i>Paragloborotalia mayeri</i>	XXX	12.1	24X-CC	25X-3, 80–84	224.185	228.020	226.103	1.917	
F		LO <i>Globorotalia praescitula</i>	XXX	16.9	24X-CC	25X-3, 80–84	224.185	228.020	226.103	1.917	
N		LCO <i>Cyclicargolithus floridanus</i>	13.2		26X-2, 15–16	26X-3, 15–16	235.455	236.955	236.205	0.750	
F		FO <i>Paragloborotalia nympha</i>	13.4		26X-3, 80–84	26X-CC	237.620	243.420	240.520	2.900	
N		LO <i>Sphenolithus heteromorphus</i>	13.52		26X-6, 15–16	26X-7, 15–16	241.455	242.955	242.205	0.750	
F		FO <i>Orbulina suturalis</i>	15.1		28X-1, 80–82	28X-3, 80–82	253.810	256.730	255.270	1.460	
F		LO <i>Globorotalia zealandica</i>	16.7		28X-CC	29X-1, 80–82	260.090	263.410	261.750	1.660	
F		FO <i>Praeorbulina curva</i>	16.3		29X-1, 80–82	29X-3, 80–82	263.410	266.410	264.910	1.500	
		lower/middle Miocene boundary 16.4 Ma									
M	1168A	Onset C5Cn.1n	XXX	16.293					272.200		
M		Termination C5Cn.2n	XXX	16.327					276.700		
M		Onset C5Cn.2n	XXX	16.488					279.000		
N		FO <i>Calcidiscus premacintyrei</i>	17.4		30X-6, 15–16	30X-7, 15–16	279.855	280.855	280.355	0.500	
M		Termination C5Cn.3n	XXX	16.556					282.100		
M		Onset C5Cn.3n	XXX	16.726					287.400		
F		LO <i>Catapsydrax dissimilis</i>	XXX	17.3	31X-3, 80–82	31X-CC	285.610	291.465	288.538	2.928	
M		Termination C5Dn	XXX	17.277					292.200		
F		FO <i>Globorotalia miozea</i>	XXX	17.3	32X-1, 80–82	32X-3, 80–82	292.210	295.210	293.710	1.500	
N		FO <i>Sphenolithus heteromorphus</i>	18.2		32X-2, 15–16	32X-3, 15–16	293.055	294.555	293.805	0.750	
M		Onset C5Dn	XXX	17.615					296.500		
F		FO <i>Globorotalia zealandica</i>	XXX	17.3	32X-3, 80–82	32X-CC	295.210	300.805	298.008	2.798	
N		LO <i>Sphenolithus belemnos</i>	18.3		32X-6, 15–16	32X-7, 15–16	299.055	300.055	299.555	0.500	
F		FO <i>Globigerinoides trilobus</i>	18.8		32X-CC	33X-1, 80–82	300.805	301.510	301.158	0.352	
M		Termination C5En	XXX	18.281					307.000		
F		FO <i>Globorotalia praescitula</i>	XXX	18.5	33X-3, 80–82	33X-CC	304.510	309.835	307.173	2.662	
F		FO <i>Globoturborotalita connecta</i>	20.9		33X-CC	34X-4, 2–4	309.835	314.530	312.183	2.348	
N		FO <i>Sphenolithus belemnos</i>	19.2		34X-3, 15–16	34X-4, 15–16	313.155	314.655	313.905	0.750	
M		Onset C5En	XXX	18.781					315.000		
F		FO <i>Globorotalia incognita</i>	21.6		34X-6, 4–6	34X-CC	317.550	319.675	318.613	1.063	
M		Termination C6n	XXX	19.048					321.200		
M		Onset C6n	XXX	20.131					334.600		
F		LO <i>Turborotalia euapertura</i>	XXX	23.8	36X-CC	37X-1, 80–82	338.870	339.610	339.240	0.370	
M		Termination C6An.1n	XXX	20.518					339.500		
F		LO <i>Tenuitella munda</i>	XXX	21.4	37X-1, 80–82	37X-3, 80–82	339.610	342.610	341.110	1.500	
M		Onset C6An.1n	XXX	20.725					341.500		
M		Termination C6An.2n	XXX	20.996					343.700		
M		Onset C6An.2n	XXX	21.320					346.700		
M		Termination C6AAn	XXX	21.768					349.800		
M		Onset C6AAn	XXX	21.859					351.100		
M		Termination C6AAr.1n	XXX	22.151					351.800		
M		Onset C6AAr.1n	XXX	22.248					353.500		
M		Termination C6AAr.2n	XXX	22.459					358.400		
M		Onset C6AAr.2n	XXX	22.493					359.000		

Table T1 (continued).

Source	Hole	Event	Age (Ma)	Alternate Age (Ma)	Core, section, interval (cm)		Depth (mbsf)			Depth error (m)	
					Top	Bottom	Top	Bottom	Mean		
					189-1168A-		189-1168A-				
M		Termination C6Bn.1n	XXX	22.588					359.900		
M		Onset C6Bn.1n	XXX	22.75					366.000		
M		Termination C6Bn.2n	XXX	22.804					371.300		
F		FO <i>Globoturborotalita woodi</i>	22.6	21.8	40X-3, 80-82	40X-CC	371.410	376.335	373.873	2.462	
F		LO <i>Dentoglobigerina globularis</i>	22.8		41X-1, 80-82	41X-3, 80-82	378.110	381.110	379.610	1.500	
M		Onset C6Bn.2n	23.069						386.200		
F		FO <i>Globoquadrina dehiscens</i>	23.2		44X-2, 4-6	44X-4, 71-72	407.650	411.315	409.483	1.832	
D		LO <i>Chiropteridium</i> spp.	23.4		46X-1, 61-64	46X-4, 65-68	425.925	430.465	428.195	2.270	
N		LO <i>Sphenolithus capricornutus</i>	23.7		47X-2, 120-121	47X-2, 140-141	437.605	437.805	437.705	0.100	
Oligocene/Miocene boundary 23.8 Ma											
N	1168A	LO <i>Reticulofenestra bisecta bisecta</i>	23.9		47X-4, 68-69	47X-4, 80-81	440.085	440.205	440.145	0.060	
M		Onset C6Cn.3n?	24.118						462.600	0.000	
D		FO <i>Chiropteridium</i> spp.	24.5		50X-3, 60-62	50X-CC	467.310	472.510	469.910	2.600	
M		Termination C7n.1n?	24.730						472.000	0.000	
F		LO <i>Globigerina labiacrassata</i>	XXX	27.1	51X-1, 80-84	51X-3, 80-84	474.120	477.120	475.620	1.500	
D		FO <i>Ectosphaeropsis burdigalensis</i>	25.5		51X-4, 60-62	52X-5, 60-62	478.410	489.510	483.960	5.550	
M		Onset C7An?	25.648						500.000	0.000	
M		Termination C8n.1n?	25.823						509.350	0.000	
N		LO <i>Chiasmolithus altus</i>	26.1		55X-5, 125-126	55X-CC	518.940	521.020	519.980	1.040	
F		LO <i>Guembelitria triseriata</i>	27.0		56X-CC	57X-1, 80-84	529.420	531.920	530.670	1.250	
D		LO <i>Hystrichokolpoma</i> sp. cf. <i>Homotryblium oceanicum</i>	27.6		57X-2, 60-62	57X-7, 60-62	533.210	540.210	536.710	3.500	
D		LO <i>Svalbardella</i> spp.	27.7		57X-7, 60-62	58X-3, 60-62	540.210	544.310	542.260	2.050	
D		FO <i>Distatodinium bifffii</i>	27.7		57X-7, 60-62	58X-3, 60-62	540.210	544.310	542.260	2.050	
M		Onset C9n	27.972						546.200	0.000	
D		FO <i>Svalbardella</i> spp.	28.0		58X-3, 60-62	58X-CC	544.310	550.390	547.350	3.040	
D		LO <i>Wetzelia gochtii</i>	28.1		59X-6, 60-62	60X-2, 60-62	558.510	562.110	560.310	1.800	
D		LO <i>Hystrichokolpoma pusilla</i>	28.1		60X-2, 60-62	60X-4, 60-62	562.110	565.110	563.610	1.500	
F		LCO <i>Chiloguembelina cubensis</i>	28.5		60X-3, 84-88	60X-CC	563.860	569.190	566.525	2.665	
D		LO <i>Areoligera? semicirculata</i>	28.2		60X-4, 60-62	61X-3, 60-62	565.110	573.210	569.160	4.050	
M		Termination C10n.1n	28.283						572.900	0.000	
lower/upper Oligocene boundary 28.5 Ma											
M	1168A	Onset C10n.2n	28.745						592.000	0.000	
M		Onset C11n.1n	29.401						600.000	0.000	
D		FO <i>Hystrichokolpoma pusilla</i>	29.7		67X-4, 60-62	68X-3, 60-62	632.310	640.410	636.360	4.050	
D		FO <i>Invertocysta</i> spp.	29.9		70X-2, 60-62	70X-3, 60-62	658.210	659.710	658.960	0.750	
D		FO <i>Hystrichokolpoma</i> sp. cf. <i>Homotryblium oceanicum</i>	29.9		72X-2, 63-65	72X-4, 46-48	658.240	680.370	669.305	11.065	
D		LO <i>Corrudinium incompositum</i>	30.0		73X-3, 57-59	74X-2, 63-65	688.580	696.840	692.710	4.130	
F		LO <i>Subbotina angiporoides</i>	30.0		73X-CC	74X-CC	691.475	702.205	696.840	5.365	
F		FO <i>Guembelitria triseriata</i>	XXX	32.5	73X-CC	74X-CC	691.475	702.205	696.840	5.365	
D		FO <i>Areoligera? semicirculata</i>	30.4		74X-2, 63-65	74X-5, 60-62	696.840	701.310	699.075	2.235	
D		FO <i>Wetzelia gochtii</i>	30.4		74X-CC	75X-3, 60-62	702.205	707.910	705.058	2.853	
D		FO <i>Aptoeodinium australiense</i>	30.4		74X-CC	75X-3, 60-62	702.205	707.910	705.058	2.853	
M		Termination C12n	30.479						706.100	0.000	
D		FO <i>Cooksonidium capricornum</i>	XXX	36.0	75X-2, 56-58	75X-CC	706.370	713.880	710.125	3.755	
N		FO <i>Cyclicargolithus abisectus</i>	XXX	31.1	75X-4, 128-129	75X-5, 125-126	710.085	711.540	710.813	0.728	
M		Onset C12n	30.939						729.900	0.000	

Table T1 (continued).

Source	Hole	Event	Age (Ma)	Alternate Age (Ma)	Core, section, interval (cm)		Depth (mbsf)			Depth error (m)
					Top	Bottom	Top	Bottom	Mean	
D		LO <i>Enneadocysta partridgei</i>	32.5		189-1168A-77X-4, 60-62	189-1168A-78X-4, 60-62	728.710	737.260	732.985	4.275
N		LO <i>Reticulofenestra umbilicus</i>	31.3		77X-CC	78X-1, 38-39	733.255	733.585	733.420	0.165
N		LO <i>Isthmolithus recurvus</i>	32.3		77X-CC	78X-1, 38-39	733.255	733.585	733.420	0.165
M		Termination C13n	33.058						733.950	0.000
F		FO <i>Chiloguembelina cubensis</i>	XXX	41.2	77X-CC	78X-CC	733.255	742.990	738.123	4.868
M		Onset C13n	33.545						740.700	0.000
Eocene/Oligocene boundary 33.7 Ma										
D		LO <i>Stoveracysta ornata</i>	33.9		78X-CC	79X-3, 60-62	742.990	746.410	744.700	1.710
F		LO <i>Globigerapsis index</i>	34.3		78X-CC	79X-CC	742.990	752.385	747.688	4.698
D		LO <i>Stoveracysta kakanuiensis</i>	34.1		79X-3, 60-62	79X-5, 60-62	746.410	749.410	747.910	1.500
D		FO <i>Stoveracysta kakanuiensis</i>	34.5		79X-5, 60-62	79X-CC	749.410	752.385	750.898	1.488
M		Termination C15n	34.655						752.500	0.000
D		LO <i>Cooksonidium capricornum</i>	34.7		79X-CC, 34-39	80X-2, 60-62	752.385	754.510	753.448	1.062
M		Onset C15n	34.94						759.815	0.000
M		Termination C16n.1n	35.343						776.100	0.000
M		Onset C16n.1n	35.526						788.600	
M		Termination C16n.2n	35.685						794.000	
D		FO <i>Stoveracysta ornata</i>	36.0		84X-3, 60-62	84X-6, 60-62	794.410	798.910	796.660	2.250
D		LO <i>Hemiplacophora semilunifera</i>	36.0		84X-3, 60-62	84X-6, 60-62	794.410	798.910	796.660	2.250
D		FO <i>Reticulatospheara actinocoronata</i>	36.1		84X-6, 60-62	84X-CC	798.910	799.390	799.150	0.240
D		FO <i>Spiniferites mirabilis</i>	36.1		84X-6, 60-62	84X-CC	798.910	799.390	799.150	0.240
M		Onset C16n.2n	36.341						800.000	
M		Termination C17n.1n	36.618						812.850	0.000
N		LO <i>Reticulofenestra reticulata</i>	35.9		86X-4, 125-126	86X-CC	815.640	818.170	816.905	1.265
D		LO <i>Schematophora speciosa</i>	35.35		86X-CC	87X-2, 60-62	818.170	821.610	819.890	1.720
D		LO <i>Aireana verrucosa</i>	35.5		88X-1, 60-62	88X-6, 60-62	829.710	837.210	833.460	3.750
D		FO <i>Aireana verrucosa</i>	35.6		88X-6, 60-62	89X-3, 60-62	837.210	842.310	839.760	2.550
F		FO <i>Globigerapsis index</i>	XXX	42.9	88X-CC	89X-CC	837.550	847.600	842.575	5.025
D		LO <i>Deflandrea convexa</i>	35.8		92X-2, 60-62	92X-7, 55-57	863.510	870.660	867.085	3.575
D		FO <i>Schematophora speciosa</i>	36.0		94X-3, 64-66	94X-CC	876.980	880.305	878.643	1.662

Notes: BOI = benthic oxygen isotope data, D = dinocyst, Dm = diatom, F = planktonic foraminifer, M = magnetostratigraphic event, N = nannofossil, R = radiolarian. FO = first occurrence, LO = last occurrence, LAO = last abundant occurrence, LCO = last common occurrence. MIS = marine isotope stage. Top sample = last downhole occurrence of marker (FO); next sample up in case of LO. Bottom sample = first downhole occurrence of marker (LO); next sample down in case of FO. Error = half depth of top-bottom sample range. Tables are arranged by depth (mbsf). The primary age model comprises the most robust data available. XXX = alternate data provided. Alternative datums remain less robust until further work can resolve them. We include these data in the tables to highlight problem areas. See text for datum references.

Table T2. Age-depth data, Site 1170. (See table notes. Continued on next four pages.)

Source	Hole	Event	Age (Ma)	Alternate Age (Ma)	Core, section, interval (cm)		Depth (mbsf)			Depth error (m)	
					Top	Bottom	Top	Bottom	Mean		
					189-1170A-		189-1170A-				
BOI	1170A	Core top	0.0002						0.000	0.000	
BOI		Base Holocene plateau	0.0097						0.200	0.000	
BOI		MIS 2.2	0.0179						0.300	0.000	
BOI		MIS 3.1	0.0254						0.600	0.000	
N		FO <i>Emiliana huxleyi</i> acme	0.085		1H-1, 60-61		1H-1, 110-111		0.605	1.105	0.855
BOI		MIS 3.3	0.0502						0.900	0.000	
BOI		MIS 4.2	0.0652						1.100	0.000	
BOI		MIS 5.1	0.0793						1.400	0.000	
BOI		MIS 5.2	0.0910						1.510	0.000	
BOI		MIS 5.4	0.1108						1.900	0.000	
BOI		MIS 5.51	0.1226						1.950	0.000	
BOI		MIS 6.2	0.1351						2.150	0.000	
BOI		MIS 6.3	0.1423						2.550	0.000	
N		FO <i>Emiliana huxleyi</i>	0.24		2H-1, 60-61		2H-1, 110-111		2.305	2.805	2.555
BOI		MIS 6.4	0.1526						2.700	0.000	
BOI		MIS 6.5	0.1751						3.300	0.000	
BOI		MIS 6.6	0.1833						3.450	0.000	
BOI		MIS 7.1	0.1931						3.650	0.000	
BOI		MIS 7.3	0.2155						4.050	0.000	
BOI		MIS 7.4	0.2249						4.500	0.000	
BOI		MIS 7.5	0.2402						5.050	0.000	
BOI		MIS 8.02	0.2476						5.300	0.000	
BOI		Maximum close to 8.4	0.2675						6.100	0.000	
R		LO <i>Stylatractus universus</i>	0.45		1H-CC		2H-CC		1.570	11.635	6.603
BOI		MIS 8.5	0.287						6.550	0.000	
BOI		MIS 9.1	0.310						7.500	0.000	
BOI		MIS 9.3	0.331						7.800	0.000	
BOI		MIS 10.2	0.341						8.800	0.000	
BOI		MIS 11.3	0.405						10.700	0.000	
N		LO <i>Pseudoemiliana lacunosa</i>	0.42		2H-7, 60-61		3H-1, 60-61		11.300	11.800	11.550
BOI		MIS 12.2	0.434						11.900	0.000	
BOI		MIS 12.3	0.46						13.000	0.000	
BOI		MIS 12.4	0.471						13.500	0.000	
BOI		MIS 13.1	0.481						14.000	0.000	
N		LO <i>Reticulofenestra asanoi</i>	0.83		3H-3, 60-61		3H-3, 110-111		14.805	15.305	15.055
BOI		MIS 13.3	0.524						16.000	0.000	
Dm		LO <i>Actinocyclus ingens</i>	0.64		2H-CC		3H-CC		11.635	20.710	16.173
BOI		MIS 15.1	0.571						17.970	0.000	
BOI		MIS 15.3	0.610						19.220	0.000	
BOI		MIS 16.2	0.625						19.720	0.000	
BOI		MIS 17.1	0.691						22.650	0.000	
N		FO <i>Reticulofenestra asanoi</i>	1.16		4H-3, 60-61		4H-3, 110-111		23.635	24.135	23.885
BOI		MIS 18.2	0.722						24.080	0.000	
F		FO <i>Globorotalia truncatulinoides</i>	XXX	2.0	3H-CC		4H-CC		20.710	29.005	24.858
N		LO <i>Helicosphaera sellii</i>	1.26		4H-4, 110-111		4H-5, 60-61		25.590	26.550	26.070
N		LO <i>Calcidiscus macintyrei</i>	1.59		4H-5, 60-61		4H-5, 110-110		26.555	27.055	26.805
Dm		LO <i>Fragilariopsis barronii</i>	XXX	1.40	4H-CC		5H-CC		29.005	39.385	34.195

Table T2 (continued).

Source	Hole	Event	Age (Ma)	Alternate Age (Ma)	Core, section, interval (cm)		Depth (mbsf)			Depth error (m)	
					Top	Bottom	Top	Bottom	Mean		
Pliocene/Pleistocene boundary 1.77 Ma					189-1170A-	189-1170A-					
Dm		LO <i>Proboscia barboi</i>	1.80		4H-CC	5H-CC	29.005	39.385	34.195	5.190	
M		Onset C2n	1.95						39.700	0.000	
N		LO <i>Reticulofenestra pseudoumbilica</i>	XXX	3.65	6H-3, 60-61	6H-4, 60-61	43.305	44.805	44.055	0.750	
R		LO <i>Pseudocubus vema</i>	2.4		5H-CC	6H-CC	39.385	49.015	44.200	4.815	
R		FO <i>Pseudocubus vema</i>	XXX	4.5	6H-CC	7H-CC	49.015	58.225	53.620	4.605	
Dm		LO <i>Thalassiosira complicata</i>	2.5		7H-CC	Top C2An.1n	58.225	60.300	59.263	1.038	
Dm		LO <i>Thalassiosira inura</i>	2.5		7H-CC	Top C2An.1n	58.225	60.300	59.263	1.038	
M		Termination C2An.1n	2.581						60.300	0.000	
Dm		LO <i>Fragilariopsis weaveri</i>	2.65		Top C2An.1n	Median 7H-CC to 8H-CC	60.300	63.120	61.710	1.410	
F		FO <i>Globorotalia inflata</i>	3.2		7H-CC	8H-CC	58.225	68.015	63.120	4.895	
R		LO <i>Lychnocanoma grande</i>	XXX	5.0	9H-CC	10H-CC	77.810	87.445	82.628	4.818	
M		Onset C2An.3n	3.58						96.200	0.000	
lower/upper Pliocene boundary 3.58 Ma											
Dm	1170A	FO <i>Thalassiosira complicata</i>	4.44		11H-CC	12H-CC	96.845	106.425	101.635	4.790	
Dm		FO <i>Thalassiosira inura</i>	4.9		11H-CC	12H-CC	96.845	106.425	101.635	4.790	
M	1170B	Termination C3n.3n	XXX	4.8					128.500	0.000	
F	1170A	LO <i>Globorotalia piozea</i>	XXX	4.6	14H-CC	15H-CC	123.700	133.905	128.803	5.103	
N		LO <i>Triquetrorhabdulus rugosus</i>	5.23		15H-3, 60-61	15H-4, 60-61	128.320	130.320	129.320	1.000	
Miocene/Pliocene boundary 5.3 Ma											
M	1170B	Onset C3n.3n	XXX	4.89					130.500	0.000	
M		Termination C3n.4n	XXX	4.98					133.500	0.000	
M		Onset C3n.4n	XXX	5.23					138.000	0.000	
M		Termination C3An.1n	XXX	5.894					144.200	0.000	
F	1170A	FO <i>Globorotalia puncticulata</i>	XXX	5.3	16H-CC	17H-CC	143.715	153.485	148.600	4.885	
Dm		LO <i>Actinocyclus ingens</i> var. <i>ovalis</i>	XXX	6.269	16H-CC	17H-CC	143.715	153.485	148.600	4.885	
M	1170B	Onset C3An.1n	XXX	6.137					150.300	0.000	
M		Termination C3An.2n	XXX	6.269					152.900	0.000	
M		Onset C3An.2n	XXX	6.567					157.250	0.000	
R	1170A	LO <i>Amphymenium challengerae</i>	6.137		17H-CC	18H-CC	153.485	163.610	158.548	5.062	
N		<i>Reticulofenestra pseudoumbilica</i> paracme top	7.1		17H-CC	19X-1, 60-61	153.570	163.800	158.685	5.115	
N		FO <i>Amaurolithus delicatus</i>	7.3		17H-CC	19X-1, 60-61	153.570	163.800	158.685	5.115	
N		FO <i>Amaurolithus primus</i>	7.4		17H-CC	19X-1, 60-61	153.570	163.800	158.685	5.115	
R		FO <i>Amphymenium challengerae</i>	6.6	?	18H-CC	19X-CC	163.610	167.145	165.378	1.768	
F		FO <i>Globorotalia conomiozea</i>	6.9	?	18H-CC	19X-CC	163.610	167.145	165.378	1.768	
F		LO <i>Paragloborotalia continua</i>	8.0	?	18H-CC	19X-CC	163.610	167.145	165.378	1.768	
F		LO <i>Paragloborotalia nympha</i>	XXX	10.1	19X-CC	20X-CC	167.145	174.460	170.803	3.658	
R		FO <i>Dictyophimus splendens</i>	XXX	11.8	19X-CC	20X-CC	167.145	174.460	170.803	3.658	
N		<i>Reticulofenestra pseudoumbilica</i> paracme bottom	8.78		21X-2, 60-61	21X-3, 60-61	178.400	179.900	179.150	0.750	
F		LO <i>Paragloborotalia mayeri</i>	XXX	11.4	21X-CC	22X-CC	180.880	192.015	186.448	5.568	
M	1170B	Termination C5n.1n	9.74						190.000	0.000	
Dm	1170A	LO <i>Denticulopsis dimorpha</i>	10.7		22X-CC	23X-CC	192.015	201.095	196.555	4.540	
M	1170B	Onset C5n.2n	10.949						210.000	0.000	

Table T2 (continued).

Source	Hole	Event	Age (Ma)	Alternate Age (Ma)	Core, section, interval (cm)		Depth (mbsf)			Depth error (m)
					Top	Bottom	Top	Bottom	Mean	
middle/upper Miocene boundary 11.2 Ma										
					189-1170A-	189-1170A-				
N	1170A	LO <i>Cyclicargolithus floridanus</i>	11.9		28X-4, 60-61	28X-5, 60-61	248.605	250.105	249.355	0.750
Dm		FO <i>Denticulopsis dimorpha</i>	12.2		Top 28X-CC	Base 28X-CC	250.500	253.100	251.800	1.300
R		LAO <i>Cyrtocapsella tetraptera</i>	12.71		Top 28X-CC	Base 28X-CC	250.500	253.100	251.800	1.300
Dm		LO <i>Actinocyclus ingens</i> var. <i>nodus</i>	12.71		Top 28X-CC	Base 28X-CC	250.500	253.100	251.800	1.300
M		Termination C5AAn	12.991						264.000	0.000
F		FO <i>Paragloborotalia mayeri</i>	XXX	12.1	29X-CC	30X-CC	259.415	270.200	264.808	5.393
M		Onset C5AAn	13.139						268.500	0.000
N		LO <i>Calcidiscus premacintyrei</i>	12.700		30X-5, 60-61	31X-1, 60-61	269.300	272.900	271.100	1.800
M		Termination C5ABn	13.302						273.000	0.000
F		FO <i>Praeorbulina curva</i>	XXX	16.3	30X-CC	31X-CC	270.200	281.705	275.953	5.753
M		Onset C5ABn	13.51						277.000	0.000
M		Termination CSACn	13.703						278.000	0.000
N		LCO <i>Cyclicargolithus floridanus</i>	13.200		31X-4, 60-61	31X-5, 60-61	277.400	278.900	278.150	0.750
M		Onset CSACn	14.076						283.500	0.000
M		Termination C5ADn	14.178						286.000	0.000
Dm		FO <i>Actinocyclus ingens</i> var. <i>nodus</i>	14.38		32X-CC	Onset C5ADn	290.840	292.000	291.420	0.580
Dm		LO <i>Cavatatus jouseanus</i>	14.612		Onset C5ADn	Onset C5ADn	292.000	292.000	292.000	0.000
M		Onset C5ADn	14.612						292.000	0.000
M		Termination C5Bn.1n	14.8						294.000	0.000
R		FO <i>Lychnocanoma nipponica</i> s. str.	XXX	15.7	32X-CC	33X-CC	290.840	299.570	295.205	4.365
M		Onset C5Bn.1n	14.888						296.000	0.000
M		Termination C5Bn.2n	15.034						297.500	0.000
Dm		LO <i>Denticulopsis maccollumii</i>	XXX	14.7	33X-CC	34X-CC	299.570	310.310	304.940	5.370
M		Termination C5Cn.1n	16.014						308.000	0.000
M		Onset C5Cn.1n	16.293						310.500	0.000
lower/middle Miocene boundary 16.4 Ma										
N	1170A	FO <i>Calcidiscus premacintyrei</i>	17.4		35X-2, 60-61	35X-3, 60-61	312.200	313.700	312.950	0.750
M		Termination C5Cn.2n	XXX	16.327					311.000	0.000
M		Onset C5Cn.2n	XXX	16.488					312.000	0.000
R		LO <i>Cenospaera coronata</i>	XXX	16.7	35X-CC	36X-CC	318.360	327.465	322.913	4.553
M		Onset C5Dn	XXX	17.615					323.000	0.000
M		Onset C5En	18.781						338.000	0.000
F		FO <i>Globigerinoides trilobus</i>	18.8		Base C5En	37X-CC	338.000	338.745	338.373	0.373
M		Termination C6n	19.048						341.000	0.000
F		FO <i>Globoturborotalita connecta</i>	20.9		37X-CC	38X-CC	338.745	347.140	342.943	4.197
F		FO <i>Globoturborotalita woodi</i>	21.8	22.60	38X-CC	39X-CC	347.140	356.460	351.800	4.660
M		Onset C6AAn	21.859						370.500	0.000
M		Termination C6AAr.1n	22.151						372.200	0.000
M		Onset C6AAr.1n	22.248						373.600	0.000
M		Termination C6AAr.2n	22.459						374.900	0.000
M		Onset C6AAr.2n	22.493						375.4	0.000
M		Termination C6Bn.1n	22.588						375.800	0.000
M		Termination C6Bn.2n	22.804						377.400	0.000
M		Onset C6Cn.1n	23.535						380.000	0.000

Table T2 (continued).

Source	Hole	Event	Age (Ma)	Alternate Age (Ma)	Core, section, interval (cm)		Depth (mbsf)			Depth error (m)
					Top	Bottom	Top	Bottom	Mean	
Dm		LO <i>Azpeitia gombosi</i>	XXX	21.1	189-1170A-	189-1170A-				
F		FO <i>Globoquadrina dehiscens</i>	23.2		41X-CC	42X-CC	376.410	387.050	381.730	5.320
R		FO <i>Cyrtocapsella tetrapera</i>	23.62		41X-CC	42X-CC	376.410	387.050	381.730	5.320
M		Termination C6Cn.2n	23.677		41X-CC	42X-CC	376.410	387.050	381.730	5.320
N		LO <i>Reticulofenestra bisecta</i> s. str.	23.9		42X-3, 110-111	42X-4, 60-61	381.500	382.505	382.003	0.502
M		Onset C6Cn.2n	23.8						382.900	0.000
Oligocene/Miocene boundary 23.8 Ma										
M	1170A	Termination C6Cn.3n	23.999						383.5	0.000
M		Onset C6Cn.3n	24.118						386	0.000
Dm		LO <i>Coscinodiscus lewisianus</i> var. <i>levis</i>	XXX	28.2	42X-CC	43X-CC	387.050	396.585	391.818	4.768
F		FO <i>Chiloguembelina cubensis</i>	XXX	28.5	42X-CC	43X-CC	387.050	396.585	391.818	4.768
M		Termination C7n.1n	24.73						393.400	0.000
M		Onset C7n.1n	24.781						394.000	0.000
M		Termination C7An	25.496						395.000	0.000
Dm		LO <i>Roccella vigilans</i> var. B	25.0		43X-6, 28-30	3X-7, 41-43	394.790	396.420	395.605	0.815
M		Onset C7An	25.648						396.200	0.000
Dm		FO <i>Roccella gelida</i>	25.823		43X-7, 41-43	44X-1, 40-42	396.420	397.010	396.715	0.295
M		Termination C8n.1n	25.823						397.000	0.000
N		LO <i>Chiasmolithus altus</i>	26.1		44X-1, 10-11	44X-2, 10-11	396.705	398.205	397.455	0.750
M		Onset C8n.2n	26.554						398.600	0.000
M		Termination C9n	27.027						402.000	0.000
M		Onset C9n	27.972						403.000	0.000
M		Termination C10n.1n	XXX	28.283					406.500	0.000
F		LO <i>Subbotina angiporoidea</i>	XXX	30.0	44X-CC	45X-CC	405.700	409.925	407.813	2.113
Dm		FO <i>Roccella vigilans</i> var. B	28.0		46X-2, 40-42	46X-3, 40-42	417.710	419.210	418.460	0.750
Dm	1170D	FO <i>Coscinodiscus lewisianus</i> var. <i>levis</i>	28.5		1R-CC	2R-CC	427.240	437.465	432.353	5.113
lower/upper Oligocene boundary 28.5 Ma										
Dm	1170D	LO <i>Roccella vigilans</i> var. A	29.0		2R-3, 40-42	Top C11n.1n	436.910	440.000	438.455	1.545
M		Termination C11n.1n	29.401						440.000	0.000
M		Termination C13n	33.058						460.000	0.000
Dm		FO <i>Roccella vigilans</i> var. A	30.24		4R-2, 40-42	7R-2, 39-41	454.610	478.500	466.555	11.945
Dm		FO <i>Cavitatus jouseanus</i>	30.62		4R-2, 40-42	7R-2, 39-41	454.610	478.500	466.555	11.945
Dm		LO <i>Hemiaulus characteristicus</i>	33.5		4R-2, 40-42	7R-2, 39-41	454.610	478.500	466.555	11.945
Dm		LO <i>Distephanosira architecturalis</i>	33.5		4R-2, 40-42	7R-2, 39-41	454.610	478.500	466.555	11.945
M		Onset C11n	30.098						470.000	0.000
Eocene/Oligocene boundary 33.7 Ma										
D	1170D	FO <i>Stoveracysta kakanuiensis</i>	34.5		6R-CC	7R-1, 0-2	472.600	476.620	474.610	2.010
N		FO <i>Isthmolithus recurvus</i>	36.0		8R-5, 50-51	9R-CC	478.970	482.370	480.670	1.700
D		LAO <i>Spinidinium</i> spp.	36.0		7R-2, 85-87	8R-1, 85-87	478.970	482.370	480.670	1.700
N		FO <i>Cyclicargolithus abisectus</i>	XXX	31.1	7R-1, 90-91	8R-5, 10-11	477.505	487.605	482.555	5.050
N		LO <i>Reticulofenestra umbilicus</i>	XXX	31.3	7R-1, 90-91	8R-5, 10-11	477.505	487.605	482.555	5.050
N		LO <i>Isthmolithus recurvus</i>	XXX	32.0	7R-1, 90-91	8R-5, 10-11	477.505	487.605	482.555	5.050
N		LO <i>Reticulofenestra reticulata</i>	35.9		7R-1, 90-91	8R-5, 10-11	477.505	487.605	482.555	5.050
M		Onset C16n.1n	35.526						485.000	0.000
D		FO <i>Stoveracysta ornata</i>	39.95		Base C16n.2n	8R-CC	485.000	488.385	486.693	1.693
D		LO <i>Hystrichosphaeridium truswelliae</i>	38.5		8R-4, 85-87	8R-5, 82-84	486.870	488.340	487.605	0.735

Table T2 (continued).

Source	Hole	Event	Age (Ma)	Alternate Age (Ma)	Core, section, interval (cm)		Depth (mbsf)			Depth error (m)
					Top	Bottom	Top	Bottom	Mean	
M	Termination C16n.2n		35.685		189-1170A-	189-1170A-			490.000	0.000
D	FO <i>Deflandrea</i> sp. A		35.2		8R-5, 82-84	9R-1, 85-87	488.340	491.970	490.155	1.815
D	FCO <i>Alterbidinium distinctum</i>		36.0		9R-4, 85-87	9R-CC	496.470	497.635	497.053	0.582
M	Onset C17n.3n		38.113						520.000	0.000
D	LO <i>Arachnodinium antarcticum</i>		38.5		11R-CC	12R-CC	518.255	524.540	521.398	3.142
N	LO <i>Chiasmolithus solitus</i>		38.2		12R-4, 10-11	13R-1, 40-41	524.105	529.805	526.955	2.850
N	FO <i>Reticulofenestra reticulata</i>		XXX	41.2	12R-CC	13R-1, 40-41	524.540	529.805	527.173	2.632
D	FO <i>Hemiplacophora semilunifera</i>		XXX	41.4	12R-CC	13R-CC, 16-21	524.590	534.830	529.710	5.120
M	Termination C18n.1n		38.426						530.000	0.000
M	Onset C18n.2n		40.13						580.000	0.000
M	Termination C19n		41.257						590.000	0.000
M	Onset C19n		41.521						605.000	0.000
M	Termination C21n		42.536						620.000	0.000
D	FAO <i>Vozzhenikovia</i> spp.		XXX	50.24	30R-CC	32R-CC	701.350	722.085	711.718	10.368
N	FO <i>Reticulofenestra umbilicus</i>		XXX	42.0	34R-CC	35R-5, 10-11	741.400	747.305	744.353	2.953
M	Onset C21n		43.789						748.2	0.000
D	FAO <i>Enneadocysta partridgei</i>		48.5		36R-CC	38R-CC	760.490	779.590	770.125	9.550

Notes: BOI = benthic oxygen isotope data, D = dinocyst, Dm = diatom, F = planktonic foraminifer, M = magnetostratigraphic event, N = nannofossil, R = radiolarian. FO = first occurrence, FCO = first common occurrence, LO = last occurrence, LAO = last abundant occurrence, LCO = last common occurrence. MIS = marine isotope stage. Top sample = Last downhole occurrence of marker (FO); next sample up in case of LO. Bottom sample = first downhole occurrence of marker (LO); next sample down in case of FO. Error = half depth of top-bottom sample range. Tables are arranged by depth (mbsf). The primary age model comprises the most robust data available. XXX = alternate data provided. Alternative datums remain less robust until further work can resolve them. We include these data in the tables to highlight problem areas. See text for datum references.

Table T3. Age-depth data, Site 1171. (See table notes. Continued on next seven pages.)

Source	Hole	Event	Age (Ma)	Alternate age (Ma)	Core, section, interval (cm)		Depth (mbsf)			Depth error (m)
					Top	Bottom	Top	Bottom	Mean	
L*	1171A		0.0003		189-	189-			0.000	
L*			0.0023						0.050	
L*			0.0043						0.100	
L*			0.0062						0.150	
L*			0.0086						0.210	
L*			0.0101						0.250	
L*			0.0118						0.300	
L*			0.0135						0.350	
L*			0.0152						0.400	
L*			0.0163						0.450	
L*			0.0181						0.500	
N	FO <i>Emiliania huxleyi</i> acme		0.085		1171A-1H-1, 15–16	1171A-1H-1, 90–91	0.155	0.905	0.530	0.375
L*			0.0198						0.550	
L*			0.0215						0.600	
L*			0.026						0.650	
L*			0.0296						0.690	
L*			0.0363						0.750	
L*			0.0406						0.800	
L*			0.0447						0.850	
L*			0.0487						0.900	
L*			0.0527						0.950	
L*			0.0572						1.000	
L*			0.0619						1.050	
L*			0.0672						1.100	
L*			0.0728						1.150	
L*			0.078						1.200	
L*			0.0818						1.250	
L*			0.0855						1.300	
L*			0.0894						1.350	
L*			0.0934						1.400	
L*			0.1011						1.500	
L*			0.1037						1.550	
L*			0.1054						1.600	
L*			0.1144						1.650	
L*			0.1264						1.700	
L*			0.1293						1.750	
L*			0.1323						1.800	
L*			0.1351						1.850	
L*			0.1379						1.900	
L*			0.1406						1.950	
L*			0.1433						2.000	
L*			0.1466						2.050	
L*			0.1526						2.100	
L*			0.1594						2.150	
L*			0.1647						2.200	

Table T3 (continued).

Source	Hole	Event	Age (Ma)	Alternate age (Ma)	Core, section, interval (cm)		Depth (mbsf)			Depth error (m)
					Top	Bottom	Top	Bottom	Mean	
L*			0.1677		189-	189-				2.250
L*			0.1697							2.300
L*			0.1705							2.350
L*			0.1715							2.400
L*			0.1758							2.450
L*			0.1802							2.500
L*			0.1832							2.550
L*			0.1865							2.600
L*			0.1898							2.650
L*			0.1926							2.700
N	FO <i>Emiliania huxleyi</i>		0.24		1171A-1H-2, 90–91	1171A-1H-3, 15–16	2.405	3.155	2.780	0.375
L*			0.1955							2.750
L*			0.206							2.800
L*			0.2157							2.850
L*			0.2254							2.900
L*			0.2316							2.950
L*			0.2364							3.000
L*			0.239							3.050
L*			0.2417							3.100
L*			0.2451							3.150
L*			0.2516							3.200
L*			0.2567							3.250
L*			0.2601							3.300
L*			0.2633							3.350
L*			0.2661							3.400
L*			0.2687							3.450
L*			0.2713							3.500
L*			0.2764							3.550
L*			0.2804							3.600
L*			0.2843							3.650
L*			0.2882							3.700
L*			0.2911							3.750
L*			0.2935							3.800
L*			0.2961							3.850
L*			0.2987							3.900
L*			0.3013							3.950
L*			0.3039							4.000
L*			0.3053							4.050
L*			0.3068							4.100
L*			0.3083							4.150
L*			0.3097							4.200
L*			0.3107							4.250
L*			0.3114							4.300
L*			0.312							4.350
L*			0.3126							4.400
L*			0.3139							4.500
L*			0.3145							4.550
L*			0.316							4.600

Table T3 (continued).

Source	Hole	Event	Age (Ma)	Alternate age (Ma)	Core, section, interval (cm)		Depth (mbsf)			Depth error (m)
					Top	Bottom	Top	Bottom	Mean	
L*			0.3176		189-	189-				4.650
L*			0.3192							4.700
L*			0.3206							4.750
L*			0.3214							4.800
L*			0.3222							4.850
L*			0.323							4.900
L*			0.3238							4.950
L*			0.3247							5.000
L*			0.3255							5.050
L*			0.3264							5.100
L*			0.3272							5.150
L*			0.3283							5.200
L*			0.3301							5.250
L*			0.3318							5.300
L*			0.3342							5.350
L*			0.3367							5.400
L*			0.3396							5.450
L*			0.344							5.500
L*			0.3484							5.550
F	T 1171B; B 1171A	FO <i>Globorotalia truncatulinoides</i>	XXX	2.0	1171B-1H-CC	1171A-1H-CC	4.190	7.005	5.598	1.408
L*			0.3575							5.600
L*			0.3613							5.650
L*			0.3649							5.700
L*			0.368							5.750
L*			0.3725							5.800
L*			0.3792							5.850
L*			0.3844							5.900
L*			0.3871							5.950
L*			0.3882							6.000
L*			0.3894							6.050
L*			0.3906							6.100
L*			0.3922							6.150
L*			0.3957							6.200
L*			0.3967							6.250
L*			0.3977							6.300
L*			0.3987							6.350
L*			0.3998							6.400
L*			0.4008							6.450
L*			0.4035							6.500
L*			0.4066							6.550
L*			0.4093							6.600
L*			0.4141							6.650
L*			0.4175							6.700
L*			0.4184							6.750
L*			0.4192							6.800
L*			0.4201							6.850
L*			0.4212							6.900
L*			0.422							6.940

Table T3 (continued).

Source	Hole	Event	Age (Ma)	Alternate age (Ma)	Core, section, interval (cm)		Depth (mbsf)			Depth error (m)
					Top	Bottom	Top	Bottom	Mean	
N		LO <i>Pseudoemiliania lacunosa</i>	0.42	189-1171A-1H-5, 90-91	189-1171A-1H-CC		6.905	7.005	6.955	0.050
L*			0.423						6.990	
L*			0.4252						7.100	
L*			0.4262						7.150	
L*			0.4271						7.200	
L*			0.4281						7.250	
L*			0.4305						7.300	
L*			0.4411						7.350	
L*			0.4435						7.400	
L*			0.4555						7.450	
L*			0.4643						7.500	
L*			0.4715						7.550	
L*			0.4774						7.600	
L*			0.4827						7.650	
L*			0.4881						7.700	
L*			0.4902						7.750	
L*			0.4924						7.800	
L*			0.4945						7.850	
L*			0.4967						7.900	
L*			0.4988						7.950	
L*			0.501						8.000	
L*			0.5035						8.050	
L*			0.5077						8.100	
L*			0.5118						8.150	
L*			0.5154						8.200	
L*			0.5189						8.250	
L*			0.5223						8.300	
L*			0.5253						8.350	
L*			0.5284						8.400	
L*			0.5315						8.450	
L*			0.5345						8.500	
L*			0.5384						8.600	
L*			0.5395						8.650	
L*			0.5421						8.700	
L*			0.5451						8.750	
L*			0.548						8.800	
L*			0.5521						8.850	
L*			0.5562						8.900	
L*			0.5607						8.950	
L*			0.5663						9.000	
L*			0.5723						9.050	
L*			0.5784						9.100	
L*			0.5844						9.150	
L*			0.5915						9.200	
L*			0.5938						9.250	
L*			0.5963						9.300	
L*			0.5989						9.350	
L*			0.6015						9.400	

Table T3 (continued).

Source	Hole	Event	Age (Ma)	Alternate age (Ma)	Core, section, interval (cm)		Depth (mbsf)			Depth error (m)
					Top	Bottom	Top	Bottom	Mean	
L*			0.6034		189-	189-				9.450
L*			0.6049							9.500
L*			0.6063							9.550
L*			0.6087							9.600
L*			0.6115							9.650
L*			0.614							9.700
L*			0.6163							9.750
L*			0.6186							9.800
L*			0.6209							9.850
L*			0.6233							9.900
L*			0.6256							9.950
L*			0.628							10.000
L*			0.6309							10.050
Dm		LO <i>Actinocyclus ingens</i>	0.64		1171A-1H-CC	1171A-2H-CC	7.005	16.045	11.525	4.520
Dm		LO <i>Fragilaropsis reinholdii</i>	0.65		1171A-1H-CC	1171A-2H-CC	7.005	16.045	11.525	4.520
Dm		LO <i>Thalassiosira fasciculata</i>	0.7		1171A-1H-CC	1171A-2H-CC	7.005	16.045	11.525	4.520
M	1171C	Onset C1n	0.78							12.600
N	1171A	LO <i>Reticulofenestra asanoi</i>	0.83		1171A-2H-4, 90-91	1171A-2H-5, 15-16	12.505	13.255	12.880	0.375
M	1171C	Termination C1r.1n	0.99							14.900
M		Onset C1r.1n	1.07							16.500
N	1171A	FO <i>Reticulofenestra asanoi</i>	1.16		1171A-2H-4, 90-91	1171A-3H-1, 90-91	16.100	17.505	16.803	0.703
N		LO <i>Helicosphaera sellii</i>	1.26		1171A-3H-3, 90-91	1171A-3H-4, 15-16	20.500	21.250	20.875	0.375
Dm		LO <i>Fragilaropsis barronii</i>	1.4		Top LO <i>H. sellii/C. macintyreai</i>	Base LO <i>H. sellii/C. macintyreai</i>	22.755	23.505	23.130	0.375
Dm		LO <i>Thalassiosira tetraoestrupii</i> var. <i>reimeri</i>	1.5		Top LO <i>H. sellii/C. macintyreai</i>	Base LO <i>H. sellii/C. macintyreai</i>	22.755	23.505	23.130	0.375
N		LO <i>Calcidiscus macintyreai</i>	1.59		1171A-3H-5, 15-16	1171A-3H-5, 90-91	22.755	23.505	23.130	0.375
Pliocene/Pleistocene boundary 1.77 Ma										
M	1171C	Termination C2n	1.77							24.000
Dm	1171A	LO <i>Proboscia barboi</i>	1.8		Termination C2n	3H-CC	24.000	24.700	24.350	0.350
M	1171C	Onset C2n	1.95							26.000
R	T 1171A; B 1171C	LO <i>Pseudocubus vema</i>	2.4		1171A-3H-CC	1171C-3H-CC	24.700	28.500	26.600	1.900
Dm	1171A	LO <i>Thalassiosira complicata</i>	2.5		1171A-3H-CC	1171C-3H-CC	24.700	35.705	30.203	5.503
Dm		LO <i>Thalassiosira inura</i>	2.5		1171A-3H-CC	1171C-3H-CC	24.700	35.705	30.203	5.503
M	1171C	Termination C2An.1n	2.581							31.750
Dm	1171A	LO <i>Thalassiosira insignia</i>	2.63		Termination C2An.1n	Onset C2An.1n	31.750	34.500	33.125	1.375
Dm		LO <i>Fragilaropsis weaveri</i>	2.65		Termination C2An.1n	Onset C2An.1n	31.750	34.500	33.125	1.375
M	1171C	Onset C2An.1n	3.04							34.500
M		Termination C2An.2n	3.11							35.600
F	T 1171C; B 1171A	FO <i>Globorotalia inflata</i>	3.2		Termination C2An.2n	1171A-4H-CC	35.600	35.705	35.653	0.052
R	T 1171A; B 1171C	FO <i>Pseudocubus vema</i>	XXX	4.5	1171A-4H-CC	1171C-4H-CC	35.705	37.755	36.730	1.025
M	1171C	Onset C2An.2n	3.22							36.800
M		Onset C2An.3n	3.58							40.400
lower/upper Pliocene boundary 3.58 Ma										
M		Termination C3n.1n	XXX	4.18						42.700
N	1171A	LO <i>Reticulofenestra pseudoumbilica</i>	3.65		1171A-5H-6, 15	1171A-5H-7, 15	43.255	44.755	44.005	0.750

Table T3 (continued).

Source	Hole	Event	Age (Ma)	Alternate age (Ma)	Core, section, interval (cm)		Depth (mbsf)			Depth error (m)
					Top	Bottom	Top	Bottom	Mean	
189-										
M	1171C	Onset C3n.1n	XXX	4.29						44.300
M		Termination C3n.2n	4.462							46.500
M		Onset C3n.2n	4.48							47.000
M		Termination C3n.3n	4.8							47.600
M		Onset C3n.3n	4.89							48.500
M		Termination C3n.4n	4.98							50.600
M		Onset C3n.4n	5.23							52.400
N	1171A	LO <i>Triquetrorhabdulus rugosus</i>	5.23		1171A-6H-7, 15	1171A-7H-1, 15	54.255	54.755	54.505	0.250
Miocene/Pliocene boundary 5.3 Ma										
F	1171B	LO <i>Paragloborotalia continuosa</i>	XXX	8.0	1171A-6H-CC	1171A-7H-CC	52.000	60.690	56.345	4.345
Dm	1171A	FO <i>Fragilaropsis weaveri</i>	XXX	3.4	1171A-6H-CC	1171A-7H-CC	55.110	64.100	59.605	4.495
R		FO <i>Amphymenium challengerae</i>	XXX	6.6	1171A-6H-CC	1171A-7H-CC	55.110	64.100	59.605	4.495
M	1171C	Termination C3An.1n	5.894							62.300
R	1171A	LO <i>Amphymenium challengerae</i>	6.137		Onset C3An.1n (6H-CC)	C3An.1n (7H-CC)	55.110	64.100	63.600	4.495
M	1171C	Onset C3An.1n	6.137							63.600
M		Termination C3An.2n	6.269							65.500
Dm		LO <i>Actinocyclus ingens</i> var. <i>ovalis</i>	6.269		Termination C3An.2n (6H-CC)	Termination C3An.2n (7H-CC)	57.380	67.040	65.500	4.830
N	1171A	<i>Reticulofenestra pseudoumbilica</i> paracme top	7.1		1171A-8H-2, 15-16	1171A-8H-3, 15-16	65.25	65.89	65.89	0.320
N		FO <i>Amaurolithus primus</i>	7.4		1171A-8H-2, 15-16	1171A-8H-3, 15-16	65.25	65.89	65.89	0.320
N		LO <i>Minylitha convalis</i>	7.8		1171A-8H-2, 15-16	1171A-8H-3, 15-16	65.25	65.89	65.89	0.320
F	T 1171B; B 1171A	LO <i>Paragloborotalia nympha</i>	XXX	10.1	1171B-8H-CC	1171A-8H-CC	70.705	73.005	71.855	1.150
N	1171A	<i>Reticulofenestra pseudoumbilica</i> paracme bottom	8.78		1171B-9H-2, 15-16	1171A-9H-3, 15-16	75.25	76.75	76.75	0.750
Dm		FO <i>Fragilaropsis reinholdii</i>	8.1		1171B-8H-CC	1171A-9H-CC	73.005	82.330	77.668	4.663
Dm		FO <i>Actinocyclus ingens</i> var. <i>ovalis</i>	8.68		1171B-8H-CC	1171A-9H-CC	73.005	82.330	77.668	4.663
M	1171C	Termination C5n.1n	9.74							80.000
M		Onset C5n.1n	9.88							82.500
M		Termination C5n.2n	9.92							83.500
F	T 1171C; B 1171B	LO <i>Paragloborotalia mayeri</i>	XXX	11.4	1171C-10H-CC	1171B-11H-CC	94.370	97.890	96.130	1.760
Dm	1171A	LO <i>Denticulopsis dimorpha</i>	10.7		1171C-10H-CC	1171B-11H-CC	92.615	102.450	97.533	4.918
R	T 1171C; B 1171B	LAO <i>Cyrtocapsella japonica</i>	XXX	11.6	1171C-11H-CC	1171B-12H-CC	104.160	109.040	106.600	2.440
M	1171C	Onset C5n.2n	10.949							107.750
M		Termination C5r.1n	11.052							109.500
M		Onset C5r.1n	11.099							113.000
Dm	1171A	FO <i>Actinocyclus fryxellae</i>	XXX	11.05	1171C-13X-CC	1171B-14X-CC	113.585	120.480	117.033	3.448
middle/upper Miocene boundary 11.2 Ma										
M	1171C	Termination C5r.2n	11.476							123.000
Dm		LO <i>Denticulopsis praedimorpha</i>	11.53		Termination C5r.2n	1171B-14X-CC	123.000	123.450	123.225	0.225
Dm		LO <i>Nitzschia denticuloides</i>	11.7		Termination C5r.2n	1171B-14X-CC	123.000	123.450	123.225	0.225
M		Termination C5An.1n	11.935							129.750
M		Onset C5An.1n	12.078							130.600
M		Termination C5An.2n	12.184							133.400
M		Onset C5An.2n	12.401							134.500
R		LAO <i>Cyrtocapsella tetrapera</i>	12.71		Top 1171C-15X-CC	Base 1171B-15X-CC	134.320	134.500	134.410	0.090

Table T3 (continued).

Source	Hole	Event	Age (Ma)	Alternate age (Ma)	Core, section, interval (cm)		Depth (mbsf)			Depth error (m)
					Top	Bottom	Top	Bottom	Mean	
Dm		FO <i>Proboscia barboi</i>	12.71		189-	189-				
Dm		LO <i>Actinocyclus ingens</i> var. <i>nodus</i>	12.71		Top 1171C-15X-CC	Base 1171B-15X-CC	134.320	134.500	134.410	0.090
N		LO <i>Cyclicargolithus floridanus</i>	11.9		1171C-16X-2, 150-16	1171B-16X-3, 15-16	136.155	137.655	136.905	0.750
F		FO <i>Paragloborotalia mayeri</i>	XXX	12.1	1171C-16X-CC	1171B-17X-CC	139.600	150.150	144.875	5.275
N		LO <i>Calcidiscus premacintyrei</i>	12.7		1171C-17X-1, 15-16	1171B-17X-2, 15-16	144.26	145.76	145.005	0.750
R		LO <i>Lynchnocanoma conica</i>	13.5		1171C-17X-CC	1171B-18X-CC	150.150	162.875	156.513	6.363
M		Termination C5ACn	13.703						156.000	
M		Onset C5ACn	14.076						159.350	
N		LCO <i>Cyclicargolithus floridanus</i>	13.200		1171C-18X-5, 15-16	1171B-18X-6, 15-16	159.86	161.36	160.605	0.750
M		Termination C5ADn	14.178						161.300	
M		Onset C5ADn	14.612						167.200	
R		FO <i>Lynchnocanoma nipponica</i> s. str.	XXX	15.7	1171C-19X-CC	1171B-20X-CC	172.725	181.055	176.890	4.165
F		FO <i>Orbulina suturalis</i>	15.1		1171C-20X-CC	1171B-21X-CC	181.055	190.045	185.550	4.495
Dm		FO <i>Actinocyclus ingens</i> var. <i>nodus</i>	XXX	14.38	1171C-21X-CC	1171B-22X-CC	190.045	198.875	194.460	4.415
F		FO <i>Praeorbolina curva</i>	16.3		1171C-21X-CC	1171B-22X-CC	190.045	198.875	194.460	4.415
lower/middle Miocene boundary 16.4 Ma										
N	1171C	FO <i>Calcidiscus premacintyrei</i>	17.4		1171C-22X-4, 15-16	1171B-22X-5, 15-16	196.455	197.955	197.205	0.750
Dm		LO <i>Cavitätus jouseanus</i>	XXX	14.612	1171C-22X-CC	1171B-23X-CC	198.875	210.055	204.465	5.590
R		LO <i>Cenosphaera coronata</i>	XXX	16.7	1171C-22X-CC	1171B-23X-CC	198.875	210.055	204.465	5.590
R		FO <i>Eucyrtidium cienkowskii</i> gr.	XXX	16.7	1171C-22X-CC	1171B-23X-CC	198.875	210.055	204.465	5.590
F		FO <i>Globigerinoides trilobus</i>	18.8		1171C-22X-CC	1171B-23X-CC	198.875	210.055	204.465	5.590
M		Termination C6n	19.048						207.200	
F		FO <i>Globoturborotalita connecta</i>	XXX	20.9	1171C-23X-CC	Base 171B-24X-CC	210.055	220.700	215.378	5.322
M		Onset C6n	20.131						223.500	
Dm		LO <i>Roccella gelida</i>	22.46		1171C-25X-CC	1171B-26X-CC	228.410	237.515	232.963	4.552
F		FO <i>Globoturborotalita woodi</i>	22.6	21.80	1171C-25X-CC	1171B-26X-CC	228.410	237.515	232.963	4.552
R		FO <i>Cyrtocapsella tetrapera</i>	XXX	23.6	1171C-25X-CC	1171B-26X-CC	228.410	237.515	232.963	4.552
F		FO <i>Globoquadrina dehiscens</i>	23.2		1171C-27X-CC	1171B-28X-CC	247.175	253.670	250.423	3.247
R		FO <i>Cenosphaera coronataformis</i>	24.4		1171C-27X-CC	1171B-28X-CC	247.175	253.670	250.423	3.247
Oligocene/Miocene boundary 23.8 Ma										
N	1171C	LO <i>Reticulofenestra bisecta</i> s. str.	23.9		1171C-28X-4, 15-16	1171B-28X-CC	253.16	253.67	253.413	0.257
F		LO <i>Chiloguembelina cubensis</i>	XXX	28.5	1171C-28X-CC	1171B-29X-CC	253.670	264.680	259.175	5.505
Dm		LO <i>Roccella vigilans</i> var. B	25.0		1171C-29X-4, 10-12	1171B-30X-1, 10-12	263.110	268.210	265.660	2.550
lower/upper Oligocene boundary 28.5 Ma										
Dm	1171C	FO <i>Roccella gelida</i>	25.823		1171C-29X-CC	1171B-30X-1, 10-13	264.680	268.210	266.445	1.765
M		Onset C6Cn.3n	XXX	24.118					268.000	
F		LO <i>Subbotina angiporoidea</i>	XXX	30.0	1171C-29X-CC	1171B-30X-CC	264.680	272.740	268.710	4.030
N	1171D	LO <i>Chiasmolithus altus</i>	26.1		1171C-3R-3, 2-3	1171B-3R-3, 20-21	273.225	273.405	273.315	0.090
D		FAO <i>Briantidinium?</i> sp.	XXX	35.2	1171C-3R-3, 105-107	1171B-3R-4, 13-15	274.260	274.500	274.380	0.120
D	1171C	LO <i>Enneadocysta</i> sp. A	33.3		Top 1171C-31X-CC	Base 1171B-31X-CC	274.150	274.800	274.475	0.325
Dm	1171D	FO <i>Roccella vigilans</i> var. B	28.0		1171C-3R-2, 10-12	1171B-4R-1, 10-12	271.810	279.910	275.860	4.050
Dm		FO <i>Roccella vigilans</i> var. A	30.24		1171C-3R-2, 10-12	1171B-4R-1, 10-12	271.810	279.910	275.860	4.050
Dm		FO <i>Cavitätus jouseanus</i>	30.62		1171C-3R-2, 10-12	1171B-4R-1, 10-12	271.810	279.910	275.860	4.050
Dm		LO <i>Hemiaulus characteristicus</i>	33.5		1171C-3R-2, 10-12	1171B-4R-1, 10-12	271.810	279.910	275.860	4.050

Table T3 (continued).

Source	Hole	Event	Age (Ma)	Alternate age (Ma)	Core, section, interval (cm)		Depth (mbsf)			Depth error (m)
					Top	Bottom	Top	Bottom	Mean	
Dm N N		LO <i>Distephanosira architecturalis</i>	33.5	31.1	189-	189-	271.810	279.910	275.860	4.050
		FO <i>Cyclcargolithus abisectus</i>	XXX		1171C-3R-2, 10-12	1171B-4R-1, 10-12				
		LO <i>Reticulofenestra umbilicus</i>	31.3		1171C-3R-3, 20-21	1171B-3R-CC				
Eocene/Oligocene boundary 33.7 Ma					1171C-3R-3, 20-21	1171B-3R-CC	276.340	277.915	277.128	0.787
N	1171D	LO <i>Reticulofenestra oamaruensis</i>	33.7		Base 1171C-31X-CC (3R-3, 20-21)	1171B-3R-CC	278.400	279.800	279.100	0.700
D		LAO <i>Spinidinium</i> spp.	XXX	36	1171C-4R-1, 105-107	1171B-4R-2, 5-7	280.860	281.360	281.110	0.250
D		FO <i>Deflandrea</i> sp. A	35.2		1171C-4R-2, 5-7	1171B-4R-2, 55-57	281.360	281.800	281.580	0.220
D		FCO <i>Alterbininium distinctum</i>	36.0		1171C-4R-CC	1171B-5R-CC	284.140	291.110	287.625	3.485
N		FO <i>Reticulofenestra oamaruensis</i>	35.8		1171C-4R-CC	1171B-5R-CC	284.140	291.110	287.625	3.485
N		LO <i>Reticulofenestra reticulata</i>	35.9		1171C-4R-CC	1171B-5R-CC	284.140	291.110	287.625	3.485
N		FO <i>Isthmolithus recurvus</i>	36.0		1171C-4R-CC	1171B-5R-CC	284.140	291.110	287.625	3.485
D		FO <i>Stoveracysta ornata</i>	36.4		1171C-5R-CC	1171B-6R-CC	291.110	298.850	294.980	3.870
N		LO <i>Chiasmolithus solitus</i>	XXX	38.2	1171C-6R-CC	1171B-7R-1, 25-26	298.850	304.255	301.553	2.702
N		FO <i>Reticulofenestra reticulata</i>	XXX	41.2	1171C-6R-CC	1171B-7R-1, 25-26	298.850	304.255	301.553	2.702
M		Termination C17n.1n	36.618						301.600	
D		LO <i>Arachnodinium antarcticum</i>	XXX	38.9	1171C-6R-CC	1171B-7R-CC	298.850	305.850	302.350	3.500
M		Onset C17n.1n	37.473						323.600	
D		LAO <i>Enneadocysta partridgei</i>	XXX	37.0	1171C-15R-CC	1171B-17R-CC	377.875	401.855	389.865	11.990
N		FO <i>Reticulofenestra umbilicus</i>	42.0		1171C-19R-1, 59-60	1171B-19R-3, 59-60	414.995	417.995	416.495	1.500
D		FAO <i>Vozzhenikovia</i> spp.	XXX	50.24	1171C-25R-CC	1171B-27R-CC	480.435	501.040	490.738	10.303
M		Onset C21n	47.906						574.600	
D		FAO <i>Enneadocysta partridgei</i>	48.5		Base C21n	1171B-35R-CC	574.600	577.450	576.025	1.425
D		LO <i>Membranophoridium perforatum</i>	48.5		Base C21n	1171B-35R-CC	574.600	577.450	576.025	1.425
D		LO <i>Hystrichokolpoma spinosa</i>	XXX	38.9	1171C-35R-CC	1171B-40R-CC	577.450	626.230	601.840	24.390
lower/middle Eocene boundary 49 Ma										
M	1171D	Termination C22n	49.037						633.600	
D		LO <i>Charlesdowniea edwardsii</i>	XXX	50.24	1171C-40R-CC	1171B-44R-CC	626.230	664.250	645.240	19.010
N		LO <i>Discoaster kupperi</i>	XXX	48.4	1171C-44R-CC	1171B-45R-CC	664.250	669.405	666.828	2.578
M		Onset C22n	49.714						683.600	
D		FO <i>Charlesdowniea edwardsii</i>	XXX	52.1	1171C-44R-CC	1171B-50R-CC	664.250	721.990	693.120	28.870
D		FO <i>Enneadocysta</i> sp. A	50.73		1171C-50R-CC	1171B-56R-CC	721.990	774.940	748.465	26.475
M		Onset C23n.2n	51.743						773.600	
D		FO <i>Membranophoridium perforatum</i>	52.5		Base C23n.2n	1171B-56R-CC	773.600	774.940	774.270	0.670
D		LO <i>Dracodinium waipawaense</i>	XXX	52.1	1171C-60R-CC	1171B-70R-CC	818.175	911.610	864.893	46.718
D		FO <i>Hystrichokolpoma spinosa</i>	XXX	52.5	1171C-70R-CC	1171B-71R-CC	911.610	922.575	917.093	5.483
D		FO <i>Dracodinium waipawaense</i>	52.8		1171C-70R-CC	1171B-71R-CC	911.610	922.575	917.093	5.483
M		Termination C24n	52.364						933.600	
D		FO <i>Deflandrea phosphoritica</i> complex	54.0		1171C-73R-CC	1171B-75R-CC	943.135	958.450	950.793	7.658

Notes: D = dinocyst, Dm = diatom, F = planktonic foraminifer, L* = reflectivity, M = magnetostratigraphic event, N = nannofossil, R = radiolarian. FO = first occurrence, LO = last occurrence, LAO = last abundant occurrence, LCÖ = last common occurrence. MIS = marine isotope stage. T = top, B = base. Top sample = last downhole occurrence of marker (FO); next sample up in case of LO. Bottom sample = first downhole occurrence of marker (LO); next sample down in case of FO. Error = half depth of top-bottom sample range. Tables are arranged by depth (mbsf). The primary age model comprises the most robust data available. XXX = alternate data provided. Alternative datums remain less robust until further work can resolve them. We include these data in the tables to highlight problem areas. See text for datum references.

Table T4. Age-depth data, Site 1172. (This table is available in an [oversized format](#).)